Geosci. Model Dev., 18, 5143–5204, 2025
https://doi.org/10.5194/gmd-18-5143-2025

Geoscientific Model Development
Open Access
EGU

TROLL 4.0: representing water and carbon fluxes, leaf phenology, and intraspecific trait variation in a mixed-species individual-based forest dynamics model – Part 1: Model description

Isabelle Maréchaux[1], Fabian Jörg Fischer[2,3], Sylvain Schmitt[1,4,5], and Jérôme Chave[2]

[1]AMAP, Univ Montpellier, CIRAD, CNRS, INRAE, IRD, 34000 Montpellier, France
[2]CRBE, Université de Toulouse, CNRS, IRD, Toulouse INP, 118 route de Narbonne, 31062 Toulouse, France
[3]School of Biological Sciences, University of Bristol, Bristol, BS8 1TQ, United Kingdom
[4]CIRAD, UPR Forêts et Sociétés, 34398 Montpellier, France
[5]Forêts et Sociétés, Univ Montpellier, CIRAD, Montpellier, France

Correspondence: Isabelle Maréchaux (isabelle.marechaux@inrae.fr)

Received: 4 October 2024 – Discussion started: 17 October 2024
Revised: 11 April 2025 – Accepted: 12 May 2025 – Published: 25 August 2025

Abstract. TROLL 4.0 is an individual-based forest dynamics model that is capable of jointly simulating forest structure, diversity, and ecosystem functioning, including the ecosystem water balance and productivity, leaf area dynamics, and the tree community functional and taxonomic composition. It represents ecosystem flux processes in a manner similar to dynamic global vegetation models, while adopting a representation of plant community structure and diversity at a resolution consistent with that used by field ecologists. Specifically, trees are modelled as three-dimensional individuals with a metric-scale spatial representation, providing a detailed description of ecological processes such as competition for resources and tree demography. Carbon assimilation and plant water loss are explicitly represented at tree level using coupled photosynthesis and stomatal conductance models, depending on the micro-environmental conditions experienced by trees. Soil water uptake by trees is also modelled. Physiological and demographic processes are parameterized using plant functional traits measured in the field. Here we provide a detailed description and discussion of the implementation of TROLL 4.0. An evaluation of the model at two tropical forest sites is provided in a companion paper (Schmitt et al., 2025). TROLL 4.0's representation of processes reflects the state of the art, and we discuss possible developments to improve its predictive capability and its capacity to address challenges in forest monitoring, forest dynamics, and carbon cycle research.

1 Introduction

Modelling vegetation dynamics remains a major challenge (Prentice et al., 2015; Song et al., 2021; Mahnken et al., 2022), and the wide variety of modelling concepts that coexist depend on models' initial objectives. Early versions of global vegetation models were developed to provide boundary conditions for energy, carbon, and water budgets in global atmospheric models (Sellers et al., 1986, 1997). With the refinement of modelling concepts and computer power, feedback loops between the atmosphere and vegetation have gradually been taken into account (Charney, 1975; Cox et al., 2000; Meir et al., 2006), leading to an improved representation of fluxes of energy, carbon, and water across the vegetation layer (Fisher et al., 2015; Moorcroft, 2003; Pitman, 2003). However, dynamic global vegetation models (DGVMs) typically adopt a simplified representation of floristic composition and vegetation structure (Fisher et al., 2014; Prentice et al., 2007). In many of these models, fluxes between vegetation and the atmosphere are still calculated in an average environment per grid cell (e.g. $1° \times 1°$) for an average leaf of an individual drawn from a dozen plant functional types (PFTs). The diversity of plant strategies is therefore typically represented by a small number of PFTs even in highly diverse tropical forests (Fisher et al., 2014; Poulter et al., 2011).

In parallel, stand-scale process-based models have been developed to better understand the exchanges between vege-

tation and the atmosphere through an up-scaling of fine-scale ecophysiological processes and to account for within-stand micro-environmental heterogeneity (Wang and Jarvis, 1990; Gu et al., 1999; Williams et al., 1996; Ogée et al., 2003; Duursma and Medlyn, 2012; Fyllas et al., 2014). These process-based models are conceptually close to DGVMs, but they implement a more detailed representation of plant structure at the stand scale, and they have nurtured some important advances in DGVM development over the past decades (e.g. Chen et al., 2016). Typically used to assimilate eddy flux data, they do not include demographic processes, however.

Forest growth models have a different history as they were initially developed to predict successional dynamics and inform forest management (Watt, 1947; Botkin et al., 1972; Vanclay, 1994; Porté and Bartelink, 2002; Liang and Picard, 2013). A key innovation is gap models that represent recruitment, growth, mortality, and competition between individual trees within forest patches. Forest patches are typically the size of a canopy opening created by the fall of a dominant tree (gap or chablis; Bugmann, 2001) and modelled as horizontally homogeneous, with a spatially implicit representation of tree positions. Through the simulation of a large number of patches, gap models can represent spatial heterogeneity due to gap dynamics within stands, and larger-scale applications have been enabled by the increase in computing power and the combination with remote sensing products (Shugart et al., 2015, 2018, 2020). Overall, these models adopt a finer representation of vegetation structure than classic DGVMs, but biogeochemical processes are generally modelled more coarsely, using ideal yield curves for tree growth rates combined with limiting factors imposed by the patch environment. Since these empirical relationships can only be parameterized on the basis of a large amount of data – readily available in plantations but difficult to obtain elsewhere – gap models typically also use plant functional types to simulate diverse forest stands. The number and definition of these groups have been much discussed in the literature, with no clear consensus (Swaine and Whitmore, 1988; Vanclay, 1991; Köhler and Huth, 1998; Köhler et al., 2000; Gourlet-Fleury et al., 2005; Kazmierczak et al., 2014), and these plant functional types are difficult to transfer from one site to another (Picard and Franc, 2003; Picard et al., 2012).

Modelling vegetation from a completely different perspective and building upon flora distribution maps and biogeographic concepts (von Humboldt, 1849; Grisebach, 1872), plant species distribution models have long been developed (SDMs; Guisan et al., 2017). Generally, SDMs first estimate the envelope of environmental conditions for a species based on species occurrence data (Guisan and Thuiller, 2005; Hutchinson, 1957; Soberón, 2007), which is used to infer a probability distribution in space (Elith and Leathwick, 2009). These models require little knowledge on the processes underlying species distribution, which explains their widespread use. However, because these models are statistical in nature, their ability to project future states is unclear, and a great deal of research has been devoted to implementing process-based versions of these SDMs (Chuine and Beaubien, 2001; Ferrier and Guisan, 2006; Morin and Lechowicz, 2008; Morin and Thuiller, 2009; Kearney and Porter, 2009; Dormann et al., 2012; Journé et al., 2020).

From this brief and non-exhaustive overview it emerges that each research community in vegetation modelling emphasizes one representation of vegetation dimension – functioning, structure, or diversity – to the detriment of the others (Maréchaux et al., 2021). Data availability and computing power partly explain such trade-offs, and increasing model complexity does not necessarily translate into an increase in reliability and robustness (Mahnken et al., 2022; Prentice et al., 2015). However, a consensus has emerged in the literature that a better integration of plant species diversity, structure, and functioning should improve the predictive power of vegetation models (Purves and Pacala, 2008; Thuiller et al., 2008; McMahon et al., 2011; Evans, 2012; Dormann et al., 2012; Mokany et al., 2016; Fisher et al., 2018). For example, tree species diversity influences the productivity and resilience of forest ecosystems (Schnabel et al., 2019), and these biodiversity–ecosystem functioning relationships result from local interactions where competition for resources is a key process (Fichtner et al., 2018; Guillemot et al., 2020; Jourdan et al., 2020; Yu et al., 2024; Nemetschek et al., 2025). Similarly, the fine details of stand structure control the uptake of resources by vegetation (Braghiere et al., 2019, 2021; Brum et al., 2019; Ivanov et al., 2012; De Deurwaerder et al., 2018), and they also determine the response to environmental stresses and disturbances (Blanchard et al., 2023; Jucker et al., 2018; Seidl et al., 2014; De Frenne et al., 2019). More generally, the contribution of vegetation in biogeochemical cycles, albeit typically quantified from stand to global scales (e.g. biomass, productivity), ultimately depends on individual processes (e.g. mortality, Johnson et al., 2016) controlled by fine-scale heterogeneity and the various ecological strategies of species (Poorter et al., 2015).

Therefore, recent developments in DGVMs have sought to better represent plant community structure and diversity. Several cohort-based DGVMs have been developed to refine the representation of vegetation heterogeneity (Moorcroft et al., 2001; Fisher et al., 2015; Longo et al., 2019; Smith et al., 2001; Koven et al., 2020). Continuous representations of functional diversity have also been proposed using the distribution and covariation of traits at the individual level or trait–climate relationships (Sakschewski et al., 2015; Verheijen et al., 2015; Scheiter et al., 2013; Pavlick et al., 2013; Berzaghi et al., 2020; Van Bodegom et al., 2014). These developments represent major advances in vegetation modelling, but scale mismatches between field data and model representations limit the ability to assimilate data of various nature and resolution. While inverse modelling approaches can partially alleviate these constraints (Hartig et al., 2012; Dietze et al., 2013; LeBauer et al., 2013; Fer et al., 2018; Lagarrigues et al., 2015), they rely heavily on confidence in the model struc-

ture and can therefore raise equifinality issues (Medlyn et al., 2005) and increase rapidly in computational complexity in high-dimensional parameter sets.

Finally, most of these challenges are exacerbated for tropical forests, as they are structurally complex (Doughty et al., 2023), support a large number of tree species per hectare (up to several hundred; Wilson et al., 2012), and are more difficult to access for evaluation in the field (Schimel et al., 2015). Given that they provide a range of ecosystem services and play a major role in regional and global biogeochemical cycles (Beer et al., 2010; Bonan, 2008; Pan et al., 2011; Harper et al., 2013), tropical forests and their responses to changing environmental factors have been identified as one of the greatest sources of uncertainty in Earth system models (Koch et al., 2021; Powell et al., 2013; Restrepo-Coupe et al., 2017; Huntingford et al., 2013). Thus, many advances in vegetation modelling have been, and still are, motivated by the challenge of tropical forests.

Here we describe a major upgrade of the TROLL forest dynamics model (Chave, 1999; Maréchaux and Chave, 2017; Fischer, 2019), referred to here as TROLL 4.0. TROLL 4.0 brings together various modelling traditions, including elements of DGVMs, stand-scale process-based models, and forest gap models while adopting a species-level representation of plant diversity to jointly simulate the functioning, structure, and diversity of forest ecosystems, in particular tropical forests. TROLL is a spatially explicit forest dynamics model, with an individual- and trait-based representation (Fig. 1). Individual trees from 1 cm diameter at breast height (dbh) are explicitly represented in a three-dimensional space discretized at a resolution of 1 m, allowing a fine representation of stand structure and local interactions via explicit competition for resources. Each tree belongs to a species, with a list of mean traits per species provided as input. These traits control the physiological and demographic processes of the tree's functioning and life cycle, from recruitment and growth to seed dispersal and death. This type of trait-based parameterization is based on recent advances in plant physiology and functional ecology and has been facilitated by the expansion of large databases of functional traits (Díaz et al., 2016, 2022; Kattge et al., 2011, 2020), in particular for tropical trees (Baraloto et al., 2010a; Vleminckx et al., 2021).

In TROLL 4.0, as opposed to previous versions, a water cycle is explicitly simulated, with the state and dynamics of soil water explicitly represented and coupled with the vegetation dynamics. Carbon assimilation and water loss by transpiration are represented explicitly using a photosynthesis model coupled with a stomatal conductance model. Both take into account variation in micro-environmental conditions between and within tree crowns, as well as the newly represented tree's access to soil water. The influence of water availability on leaf-level gas exchanges, leaf phenology, tree recruitment, and death is now simulated by means of a parameterization using the leaf water potential at turgor loss point (Bartlett et al., 2012b) and mechanistic-based coordination with other hydraulic traits (Bartlett et al., 2016b). Carbon that is not consumed by the respiration of living tissues is then allocated to leaf production, carbon storage, and tree growth through allometric relationships. Compared to TROLL version 2.3.2 (Maréchaux and Chave, 2017), TROLL 4.0 includes other improvements: plant functional traits can vary among trees of the same species, tree crown shapes can be more realistic than cylinders, and leaf density can vary within the tree crowns. Altogether, the new developments made for this new TROLL version allow us to further bridge the gap between existing forest modelling approaches through a better integration of forest structure, diversity, and ecosystem functioning in the model representation.

In this contribution, we provide a detailed description of the structure and objectives of the TROLL 4.0 model, discussing how new modelling representations are an outcome of the state of knowledge and the availability of data. Finally, we discuss the limitations of the model and future developments. An evaluation of the model's ability to simulate forest structure, diversity, and functioning for two Amazonian forest sites is reported in a companion paper (Schmitt et al., 2025). The model is written in C++ and wrapped in the R environment through a dedicated package named *rcontroll* (Schmitt et al., 2023).

2 Model description

2.1 Environmental conditions

TROLL 4.0 simulates an idealized forest stand with a typical size of 1 to 100 ha. Parallel computing may be used to simulate several times the same stand or to simulate several forest stands with different environmental conditions. Climatic drivers are similar to those represented in many DGVMs (air temperature, vapour pressure deficit, wind speed, and light intensity above the canopy, as well as precipitation). The forest ecosystem is divided into an aboveground and belowground part. Soil is explicitly represented as a water reservoir, but soil nutrients are not modelled. The topography within a stand is assumed to be flat.

2.2 Light availability and aboveground variation in micro-climate

Above ground, the simulated forest stand is represented as a discrete grid of $1\,m^3$ cubic voxels. Light diffuses vertically through the forest's leaf layers from the top of the canopy to the ground, with one recalculation each day. Variation in the solar zenith angle is thus neglected here, a first assumption made for the model application to tropical regions which could be reconsidered in the future. In a given voxel, light availability is the photosynthetic photon flux density in $\mu mol\ photons\ m^{-2}\ s^{-1}$ and is computed as a function of the incident light intensity at canopy top ($PPFD_{top}$, see Table A1 for a list of symbols), the cumulated leaf density of voxels

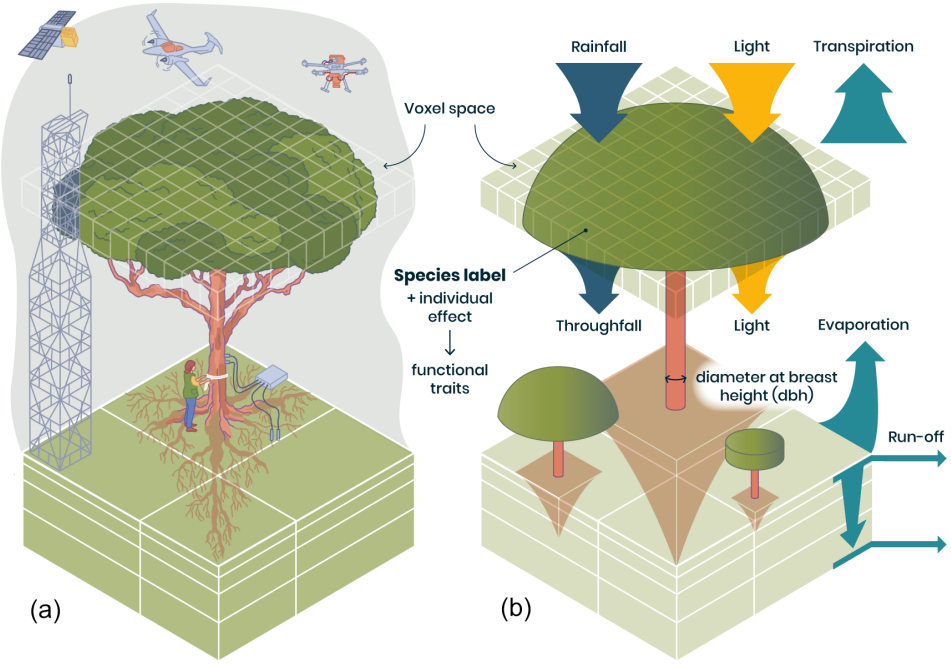

Figure 1. Representation of individual trees in a spatially explicit environment in TROLL 4.0 **(b)**, allowing direct comparison with data of various nature **(a)**. In TROLL 4.0, each tree is composed of a trunk, a crown whose shape evolves from a cylinder to an umbrella as the tree grows, and root biomass that decreases exponentially with soil depth. Tree dimensions are updated at each time step, depending on the net assimilated carbon that is allocated to growth and following allometric relationships depending on tree diameter at breast height (dbh). Each tree has a species label associated with plant functional traits, which, together with an individual effect randomly attributed at tree birth, determine the tree's functional traits. These traits are used to parameterize physiological and demographic processes that govern tree functioning throughout its life cycle. Light diffusion is computed explicitly at each time step and within each voxel from the canopy top to the ground. Water balance is also computed at each time step, and the resulting water availability across soil voxels influences tree functioning. With this representation of forest structure, composition, and functioning, model outputs can be directly compared with a wide range of data, including carbon and water fluxes provided by eddy flux towers, field inventories, and 3D structure estimates from remote sensing **(a)**. In TROLL 4.0, aboveground voxels typically have a finer horizontal resolution than belowground voxels, but the latter are vertically finer and increase in thickness with depth **(b)**. This resolution matches that of fine-scale remote sensing products or soil water content monitoring **(a)**.

above, and the (constant) leaf density within the voxel itself. The Beer–Lambert extinction of light within the canopy allows calculating the incident PPFD (per unit ground area) above any layer at vertical extent v as

$$\mathrm{PPFD}(v) = \mathrm{PPFD}_{\mathrm{top}} \times \exp[-k \times \mathrm{LAI}(v)], \quad (1)$$

where $\mathrm{LAI}(v)$ is the cumulated leaf area above height v, and k is the extinction coefficient. We define $k = k_{\mathrm{geom}} \times \mathrm{absorptance}_{\mathrm{leaves}}$, where k_{geom} reflects the geometric arrangement of leaves in the voxel (a value of 0.5 reflecting spherical leaf distribution; Ross, 1981) and $\mathrm{absorptance}_{\mathrm{leaves}}$, the fraction of absorbed light within a single leaf (Long et al., 1993; Poorter et al., 1995). In the absence of sufficient relevant species-specific data, both k_{geom} and $\mathrm{absorptance}_{\mathrm{leaves}}$ are assumed to be constant across species here.

The absorbed light in a layer a of thickness Δa is then

$$\mathrm{PPFD}_{\mathrm{abs}}(a) = \mathrm{PPFD}_{\mathrm{top}} \times \exp[-k \times \mathrm{LAI}(a)] - \mathrm{PPFD}_{\mathrm{top}} \times \exp[-k \times \mathrm{LAI}(a + \Delta a)]. \quad (2)$$

Assuming that leaf area per unit ground area ($\mathrm{m}^2\,\mathrm{m}^{-2}$), or $\mathrm{dens}(a)$, is constant within the layer, this simplifies to

$$\mathrm{PPFD}_{\mathrm{abs}}(a) = \mathrm{PPFD}_{\mathrm{top}} \times \exp[-k \times \mathrm{LAI}(a)] \times (1 - \exp[-k \times \mathrm{dens}(a)]). \quad (3)$$

For photosynthesis calculations, absorbed PPFD per unit ground area is converted into absorbed PPFD per unit leaf area by dividing $\mathrm{PPFD}_{\mathrm{abs}}(a)$ by $\mathrm{dens}(a)$.

Air micro-environmental variation within the canopy is represented as follows. Nighttime temperature (T_{night}) is assumed to be constant throughout the night and within the canopy, while temperature (T) and vapour pressure deficit (VPD) vary across voxels depending on the variable $\lambda(v) = \frac{\mathrm{LAI}(v)}{\mathrm{LAI}_{\mathrm{sat}}}$ with $\mathrm{LAI}_{\mathrm{sat}}$ a threshold LAI and $\mathrm{LAI}(v)$ the LAI above voxel v. At height v above ground, we calculate temperature and VPD as follows:

$$T(v) = T_{\text{top}} - \Delta T \times \lambda(v) \tag{4}$$

$$\text{VPD}(v) = \text{VPD}_{\text{top}} \times \left[C_{\text{VPD0}} + (1 - C_{\text{VPD0}})\sqrt{(1 - \lambda(v))}\right], \tag{5}$$

where ΔT and C_{VPD0} are set parameters and T_{top} and VPD_{top} are values at the top of the canopy. For any given layer a of depth Δa, temperatures and VPDs are then calculated by averaging both functions from a to $a + \Delta a$.

$$T_{\text{mean}}(a) = \frac{1}{\Delta a}\int_{a}^{a+\Delta a}\left(T_{\text{top}} - \frac{\Delta T}{\text{LAI}_{\text{sat}}} \times \text{LAI}(v)\right)\mathrm{d}v \tag{6}$$

$$\text{VPD}_{\text{mean}}(a) = \frac{1}{\Delta a}\int_{a}^{a+\Delta a}\text{VPD}_{\text{top}} \times \left[C_{\text{VPD0}} + \frac{(1 - C_{\text{VPD0}})}{\sqrt{\text{LAI}_{\text{sat}}}}\sqrt{(\text{LAI}_{\text{sat}} - \text{LAI}(v))}\right]\mathrm{d}v \tag{7}$$

Equations (6) and (7) can then be simplified using the assumption of constant leaf density within a layer and redefining v with respect to the current layer a so that $\text{LAI}(v) = \text{LAI}(a) + \text{dens}(a) \times v$.

This empirical representation of variation of T and VPD within the canopy is in qualitative agreement with empirical observations of micro-climate gradients within tropical forest canopies (Camargo and Kapos, 1995; Shuttleworth, 1985; Shuttleworth et al., 1989; Tymen et al., 2017), with a consistent buffering effect of forest canopies on understorey micro-environment (De Frenne et al., 2019) and a strong control by forest structure (Gril et al., 2023b, a; Tymen et al., 2017; Zellweger et al., 2019). Alternative empirical or process-based representations of micro-environmental variations (e.g. Maclean and Klinges, 2021; Ogée et al., 2003) may be tested in the future, especially for more in-depth explorations of understorey biodiversity and functioning under climate change (De Frenne et al., 2021; Haesen et al., 2023).

Wind speed attenuation inside the canopy is simulated as described in Rau et al. (2022b), who explored the effect of wind speed on forest structure in a forest exposed to cyclones using TROLL. Wind speed is usually measured above the canopy and decreases as one approaches the canopy top layer, so wind speed at the top of the canopy is (Monteith and Unsworth 2008)

$$u(z) = \frac{u_*}{\kappa}\ln\left(\frac{z-d}{z_0}\right), \quad \text{if } z \geq H, \tag{8}$$

where $u(z)$ is the horizontal wind speed in m s^{-1} at a height z (m) above ground, H is the height of the top of the canopy (m), u_* is the friction velocity, κ is the von Kármán constant ($\kappa = 0.40$), d is the zero-plane displacement height, here assumed to be equal to $0.8H$, and z_0 is the aerodynamic roughness, here assumed to be equal to $0.06H$ (Rau et al., 2022b). Within the canopy, wind speed decreases as (Inoue 1963)

$$u(z) = u(H)\exp\left(-\alpha\left(1 - \frac{z}{H}\right)\right), \quad \text{if } z < H, \tag{9}$$

with $\alpha \approx 3$ (Raupach et al., 1996). Wind speed was not computed at the voxel scale but using the coarser horizontal resolution of the belowground field (see Sect. 2.3 below, e.g. 25×25 m), and a mean top canopy height H was computed as input to Eqs. (8) and (9).

Finally, air CO_2 concentration is assumed to be constant across the canopy, in agreement with observations within a tropical forest site (Buchmann et al., 1997).

2.3 Soil water availability

In TROLL 4.0, the belowground part of the ecosystem is explicitly represented, and its discretization is specified by the user, including the number and depth of layers and horizontal dimensions of the cells. Belowground voxels are typically coarser horizontally (e.g. $25\,\text{m} \times 25\,\text{m}$, as commonly implemented in gap models; Bugmann, 2001), but finer vertically, than aboveground $1\,\text{m}^3$ voxels. Metric-scale lateral water fluxes are difficult to parameterize and evaluate, and neglecting them here limits the computational burden. Soil layers typically increase in thickness with depth, as in most DGVMs or forest physiological models (Prentice et al., 2015) and in standard soil assessments (e.g. Hengl et al., 2017). In this representation, contrasting root depth and access to water can be represented across individual trees together with potential variation in soil properties and hydraulic state. This approach contrasts with some forest dynamics models that use a single-layer belowground representation (e.g. Gutiérrez et al., 2014; Christoffersen et al., 2016; Fyllas et al., 2014).

The water content in each belowground voxel is simulated using a bucket model, which relies on the vertical water balance for each voxel. Neglecting horizontal lateral fluxes, the water balance for a given soil column amounts to

$$\Delta\text{SWC} = P - I - Q - E - T - L, \tag{10}$$

where SWC is the soil water content, P the incident rainfall, I the canopy interception, Q the run-off, E the evaporation from the soil, T the transpiration, i.e. the plant water uptake, and L the leakage. This water balance is established for each soil layer, with inputs from upwards and outputs downwards starting from the top layer ($l = 1$): outputs of layer l are inputs for layer $l+1$, with L corresponding to the output of the deepest layer and $P - I - Q$ to the input of the top layer. The water balance for the topsoil layer thus reads

$$\Delta\text{SWC} = \text{SWC}(t+1) - \text{SWC}(t) = P - I - Q - E - T - L_{1\to 2}, \tag{10a}$$

with $L_{1\to 2}$ the water flow from the first topsoil layer to the next one, and the water balance of the other layers reads

$$\Delta\text{SWC} = \text{SWC}(t+1) - \text{SWC}(t) = L_{l-1\to l} - L_{l\to l+1}, \tag{10b}$$

with $L_{l\to l+1}$ the water flow from the soil layer l to soil layer $l+1$ that equals L if layer l is the deepest one. Note that this downward iteration neglects (i) potential hydraulic lift (upward water redistribution; see e.g. Dawson, 1993; Burgess et al., 1998; Oliveira et al., 2005) and (ii) potential interaction with the water table (Costa et al., 2023; Sousa et al., 2022). Further developments could account for these two mechanisms where they are expected to play a significant role. In particular, flooded areas could be easily represented, with a shallower soil depth and a prescribed boundary condition, i.e. a shallower water table. We now describe and discuss each term of the water balance and the corresponding modelling choices.

2.3.1 Rainfall

Rainfall (P, mm) is a model input. It is assumed that the total daily rainfall corresponds to a single event of rain per day (one storm, as in e.g. Rodriguez-Iturbe et al., 1999; Laio et al., 2001; Fischer et al., 2014; Gutiérrez et al., 2014).

2.3.2 Interception

Rainfall interception by the canopy is simulated using a model where interception depends on LAI, as proposed by Liang et al. (1994):

$$I = \min\left(P,\ K \times \mathrm{LAI}\right), \tag{11}$$

where $K = 0.2\,\mathrm{mm}$ and LAI corresponds to the leaf area index at ground level, averaged across the ground-level aboveground voxels that contribute to a single belowground voxel (typically $625 = 25^2$ aboveground voxels contribute to one belowground voxel). Similar simple formulations of canopy interception have been used elsewhere (e.g. Liu et al., 2017), and this choice is justified by the lack of relevant data to properly parameterize more complex formulations at most field sites. More complex models of rainfall interception also exist, however (Rutter and Morton, 1977; Gash, 1979; Gash et al., 1995).

2.3.3 Run-off and infiltration

As in most bucket models coupled with a forest dynamics model, the temporal propagation of the wetting front into the soil is not explicitly simulated here because of the daily time step and the vertically lumped representation of soil moisture dynamics (e.g. Laio et al., 2001; Guimberteau et al., 2014). When the soil top layer has enough available storage to absorb the totality of the throughfall (i.e. when throughfall is smaller than the layer water content at field capacity minus the current soil water content), it is assumed that the increment in soil water content of that top layer is equal to the throughfall. Otherwise, the excess water percolates to the next layer below ($L_{1\to 2}$ in Eq. 10a). In the absence of an explicit wetting front, run-off occurs only when the superficial layer is already saturated, which is similar to Dunne run-off (Dunne and Black, 1970). More complex formulations of run-off exist (d'Orgeval et al., 2008; Guimberteau et al., 2014; Horton, 1933), but because of the high porosity of many tropical forest soils (Hodnett and Tomasella, 2002; Sander, 2002) and the lack of explicit topography in this version, our choice is parsimonious.

2.3.4 Soil evaporation

We assumed that water evaporates from the topsoil layer only, a reasonable assumption if the topsoil layer is not too thin. We followed Sellers et al. (1992) under which evaporation from the soil is expressed as (see Merlin et al., 2016 for a review of alternatives)

$$E = \frac{M_\mathrm{w}}{RT_\mathrm{s}} \times \frac{e_\mathrm{s} - e_\mathrm{a}}{r_\mathrm{soil} + r_\mathrm{aero}}, \tag{12}$$

where E is in $\mathrm{kg\,m^{-2}\,s^{-1}}$, M_w is the molar mass of water vapour ($M_\mathrm{w} = 18\,\mathrm{kg\,mol^{-1}}$), R is the ideal gas constant ($R = 8.31\,\mathrm{J\,mol^{-1}\,K^{-1}}$), T_s is the temperature at the soil surface in Kelvin computed using Eq. (4) at ground level, e_s is the vapour pressure of the soil surface in Pa, e_a is the vapour pressure of air above the soil surface in Pa, r_soil is the soil surface resistance in $\mathrm{s\,m^{-1}}$, and r_aero is the aerodynamic resistance to heat transfer in $\mathrm{s\,m^{-1}}$. Soil water pressure e_s is a function of the water potential of the topsoil belowground voxel ($\psi_\mathrm{soil,\,top}$ – MPa; Jones, 2013, Eq. 5.14 therein):

$$\begin{aligned} e_\mathrm{s} &= e_\mathrm{sat}\left(T_\mathrm{s}\right) \times \exp\left(\frac{V_\mathrm{w}}{RT_\mathrm{s}} \times \psi_\mathrm{soil,top}\right) \\ &= e_\mathrm{sat}\left(T_\mathrm{s}\right) \times \exp\left(2.17 \times \frac{\psi_\mathrm{soil,\,top}}{T_\mathrm{s}}\right), \end{aligned} \tag{13}$$

where V_w is the partial molal volume of water ($V_\mathrm{w} = 18 \times 10^{-6}\,\mathrm{m^3\,mol^{-1}}$), and $e_\mathrm{sat}\left(T_\mathrm{s}\right)$ is the saturated vapour pressure at T_s computed following the Buck equation (Jones, 2013, Appendix 4 therein). e_a is by definition equal to $e_\mathrm{sat}\left(T_\mathrm{s}\right) - \mathrm{VPD_{ground}}$, where the latter is the VPD at ground level in Pa. r_soil is computed following Sellers et al. (1992, Eq. 19 therein, see also Merlin et al., 2016, Eq. 12):

$$r_\mathrm{soil} = \exp\left(8.206 - 4.255 \times \frac{\theta_\mathrm{top}}{\theta_\mathrm{fc,\,top}}\right), \tag{14}$$

where θ_top is the water content of the topsoil belowground voxel and $\theta_\mathrm{fc,\,top}$ is its water content at field capacity (in $\mathrm{m^3}$). Aerodynamic resistance r_aero is computed as follows (Merlin et al., 2016, Eq. B10 therein):

$$r_\mathrm{aero} = \frac{1}{\kappa^2 \times u\left(Z\right)} \ln\left(\frac{Z}{Z_\mathrm{m}}\right)^2, \tag{15}$$

with κ again being the von Kármán constant ($\kappa = 0.40$), $u\left(Z\right)$ the wind seed (in $\mathrm{m\,s^{-1}}$) at reference height Z, here taken at 1 m above ground, and Z_m the momentum soil roughness in metres, set to 0.001 m.

2.3.5 Transpiration

Trees transpire soil water from the belowground voxel they are rooted in (see Sect. 2.4.3). For a given tree, the total daily soil water uptake is the sum of the water transpired by leaves across its crown and across daytime half-hours (see Sect. 2.5.2). Soil layers contribute to water uptake as a function of tree-dependent weights, w_l (see Eq. 21, Sect. 2.4.3), which depend on root biomass and on the soil hydraulic state in each layer.

For each belowground voxel in layer l, the soil water potential (ψ_l) and the soil hydraulic conductivity (K_l) are computed at each time step from the soil water content in the focal voxel using the van Genuchten–Mualem soil characteristic and hydraulic conductivity curves (Mualem, 1976; van Genuchten, 1980; see Table 1 in Marthews et al., 2014). Parameters of these curves are estimated using regression models (pedotransfer functions) for tropical soils (Hodnett and Tomasella, 2002), except the saturated hydraulic conductivity, which is computed following Cosby et al. (1984; see Table 2 in Marthews et al., 2014). In practice, when only soil texture data are available, TROLL 4.0 contains a default option to apply the texture-based-only pedotransfer function provided by Tomasella and Hodnett (1998), coupled to the soil characteristic and hydraulic conductivity curves of Brooks and Corey (1964) (see Tables 1 and 2 in Marthews et al., 2014).

2.4 Representation of trees in the model

2.4.1 Species affiliation and intraspecific trait variability

In TROLL 4.0, each tree (and seed) is attributed a botanical species defined by a taxonomic binomial. It is assumed that the user has sufficiently good knowledge of the tree species growing in the study area so that a list of species-specific mean plant functional trait values can be provided as input. These are the leaf mass per area (LMA, in $\mathrm{g\,m^{-2}}$), the leaf area (LA, $\mathrm{cm^2}$), the leaf nitrogen content per dry mass (N, in $\mathrm{mg\,g^{-1}}$), the leaf phosphorous content per dry mass (P, in $\mathrm{mg\,g^{-1}}$), the wood specific gravity (wsg, in $\mathrm{g\,cm^{-3}}$), the leaf water potential at turgor loss point (π_{tlp}, in MPa), and three allometric parameters ($\mathrm{dbh_{thres}}$, h_{lim}, a_h, all in metres; see Sect. 2.4.2). The number of species provided as input is not limited. In addition to mean plant functional trait values, it is possible to input individual trait values from which a trait variance–covariance matrix is computed (alternatively the trait variance–covariance matrix can be prescribed). With this option, for each recruited tree, the trait values are drawn from a distribution rather than attributed the species-specific mean value. For each trait i and tree j, the species-specific mean value is multiplied by a factor $e^{\varepsilon_{i,j}}$, where $\varepsilon_{i,j} \sim N(0, \sigma_i)$ and σ_i is the trait-specific standard deviation on a logarithmic scale (lognormal variation). The sole exception is wood specific gravity, which we assume to be normally distributed around the mean with $\varepsilon_{\mathrm{wsg},\,j} \sim N(0, \sigma_{\mathrm{wsg}})$. Trait covariance is only considered for leaf N, leaf P, and LMA, and other traits are assumed to be decoupled (Baraloto et al., 2010b). Note that with this implementation, intraspecific variation is not heritable or structured in space or time, and it is thus a surrogate for variability emerging from genetic variation or plasticity (Girard-Tercieux et al., 2023, 2024). A more realistic representation of the latter, especially light-driven trait plasticity along the vertical canopy gradient (Lamour et al., 2023b; Lloyd et al., 2010), is left for a future version.

2.4.2 Aboveground structure

Above ground, the tree geometry is represented as a three-dimensional object within the voxelized space and consists of a trunk and a crown filled with leaves. The trunk is assumed to be a cylinder characterized by its total height and its diameter (dbh, for diameter at breast height, by analogy with forest inventories). The aboveground dimensions of trees are predicted from their dbh via scaling rules. For tree j with dbh_j, we calculate its height h_j, its crown radius cr_j, and its crown depth cd_j as follows.

$$h_j = \frac{h_{\mathrm{lim}} \times \mathrm{dbh}_j}{\left(a_h + \mathrm{dbh}_j\right)} \times e^{\varepsilon_{h,\,j}} \tag{16}$$

$$\mathrm{cr}_j = e^{a_{\mathrm{cr}}} \times \mathrm{dbh}^{b_{\mathrm{cr}}} \times e^{\varepsilon_{\mathrm{cr},\,j}} \tag{17}$$

$$\mathrm{cd}_j = \min\left(\frac{h_j}{2}, (a_{\mathrm{cd}} + b_{\mathrm{cd}} \times h_j) \times e^{\varepsilon_{\mathrm{cd},\,j}}\right) \tag{18}$$

Here, h_{lim} and a_h are species-specific coefficients of the Michaelis–Menten function, and a_{cr}, b_{cr}, a_{cd}, and b_{cd} are allometric coefficients that are species-independent. $\varepsilon_{h,\,j}$, $\varepsilon_{\mathrm{cr},\,j}$, and $\varepsilon_{\mathrm{cd},\,j}$ are tree-level variance terms to simulate intraspecific variation that are randomly drawn at tree birth with $\varepsilon_{h,\,j} \sim N(0, \sigma_h)$, $\varepsilon_{\mathrm{cr},\,j} \sim N(0, \sigma_{\mathrm{cr}})$, and $\varepsilon_{\mathrm{cd},\,j} \sim N(0, \sigma_{\mathrm{cd}})$. Tree crown architecture is known to depend on species ecological strategies (Bohlman and O'Brien, 2006; Iida et al., 2012; Poorter et al., 2006; Laurans et al., 2024), but given that crown extents are difficult to measure reliably in the dense canopies of tropical forests, we used a single set of parameters for all the species.

In the previously published version (Maréchaux and Chave, 2017), tree crowns were represented as cylinders with homogeneous leaf densities. Since v.3.0, TROLL has also been able to model tree crowns as flexible, umbrella-like shapes with heterogeneous leaf density distributions. Small tree crowns are simulated as cylinders but consist of up to three separate 1 m layers of leaves (top, intermediate, and bottom layer). Each layer can be assigned a percentage of the total leaf area (which results from the processes of carbon allocation to leaf production and leaf shedding, see Sect. 2.6.2) to reflect gradients in leaf densities from the upmost to lower crown layers (e.g. 50 %, 30 %, 20 %; Kitajima et al., 2005),

but the default is an equal distribution (33 %, 33 %, 33 %) across all layers. Once a tree surpasses 3 m in crown depth, no new layers are added. In this case, tree height directly above the tree stem (tree top height) and crown extent are derived using the same allometric equations (Eqs. 16–18), but, instead of the flat tops of small trees, it is now possible to prescribe a change in height from the centre of the crown to the crown's edges. Different geometric forms are available to describe this variation, but here we chose a simple linear decrease between the radius at the top of the crown and the radius at the bottom of the crown. The ratio between the two radii is controlled through the global parameter *shape_crown*, which varies between 0 (conical shape) and 1 (cylinder) and thus allows for various "conifer-like" and "broadleaf-like" shapes in between. Within the first 3 m of the resulting crown shape, leaves are allocated as before and folded around the tree trunk like an umbrella at various stages of opening (see Fig. 1b in Schmitt et al., 2023, and similar tree representations in Strigul et al., 2008). The crown shape only affects the geometry of the crown, not the amount of total leaf area allocated to it (see Sect. 2.6.2).

We also relax the assumption that tree crowns are homogeneously filled across their horizontal extent. In TROLL 4.0, crowns have small 1 m^2 openings (or gaps) in their crowns, parameterized as a percentage of total crown area that is not filled with leaves, f_{gap}. This allows for the modelling of a spatially heterogeneous light environment in the understorey (Tymen et al., 2017), with a theoretical range from $f_{\text{gap}} = 0\,\%$ (full crown cover, no openings) to $f_{\text{gap}} = 100\,\%$ (a hypothetical crown with no leaf area). When calibrating TROLL for tropical forests with airborne laser scanning (Fischer et al., 2019), we found a value of $f_{\text{gap}} = 15\,\%$ to be a good approximation for this within-crown gap fraction. If intraspecific variation in crown extent is explicitly modelled, the fraction of crown gaps is rescaled so that the absolute crown cover stays constant (i.e. the fraction of crown gaps is divided by $e^{2\varepsilon_{\text{cr},\,j}}$). Within species and for trees with the same stem size (i.e. similar total sapwood area), crown extent is thus assumed to be decoupled from variation in leaf area, i.e. reflecting variation in branch angles and directions, but not branch number or biomass.

2.4.3 Belowground structure

As in other models (e.g. Xu et al., 2016), TROLL 4.0 makes the assumption that total fine root biomass is equal to leaf biomass. Future developments should endeavour to represent a more explicit belowground allocation scheme (Merganičová et al., 2019; Huaraca Huasco et al., 2021). Direct estimates of individual tree root depth and root distribution are rare in moist tropical forests (Canadell et al., 1996; Jackson et al., 1996, 1999; Nepstad et al., 1994; Cusack et al., 2024; Guerrero-Ramírez et al., 2021). Some studies have quantified the depth of tree water uptake using indirect methods, such as pre-dawn leaf water potential, or isotope labelling (Brum et al., 2019; Stahl et al., 2013a), but this does not give access to the actual rooting depth. Tree root depth was assumed here to increase with tree size and was computed as a function of tree dbh as follows (Kenzo et al., 2009, Fig. 4 therein):

$$\text{RD} = 0.35 \times \text{dbh}^{0.54}, \tag{19}$$

with root depth (RD, m) and diameter at breast height (dbh, cm). As in Xu et al. (2016), the exponent was based on Kenzo et al. (2009), who reported on data from excavated trees in secondary forests in Malaysia. The first parameter (0.35, root depth at dbh = 1 cm) was adjusted to avoid unrealistic water depletion of the topsoil layer. In the absence of relevant species-specific data, this allometric equation was assumed to hold for all species, even if root depth is known to be highly plastic (e.g. Rowland et al., 2023). Correlations between rooting depth and leaf phenological habit have been reported, but in drier or more seasonal sites than Amazonian rainforests (Brum et al., 2019; Hasselquist et al., 2010; Smith-Martin et al., 2020), and trait coordinations are known to be typically stronger under harsher environmental conditions (Dwyer and Laughlin, 2017; Delhaye et al., 2020).

We assumed that vertical tree root distribution follows an exponential profile, as observed empirically at the stand scale (Fisher et al., 2007; Humbel, 1978; Jackson et al., 1996). The fine root biomass in layer l, at depths ranging from z_l to z_{l+1} ($> z_l$), is computed as

$$\text{RB}_l = \text{RB}_t \times \left(\exp\left(-3\frac{z_l}{\text{RD}}\right) - \exp\left(-3\frac{z_{l+1}}{\text{RD}}\right)\right), \tag{20}$$

where RB_t is the total tree fine root biomass (g), RB_l the fine root biomass in layer l (g), and RD the tree rooting depth (m). The factor 3 was determined so that about 95 % of the root biomass is contained between the soil surface and RD (note that $-\log(0.05) \approx 3$) (Arora and Boer, 2003). Tree roots are distributed across vertical layers but do not spread across belowground voxels horizontally. This assumption was considered a first parsimonious representation given the size of belowground voxels and the scarcity of data on root horizontal distribution worldwide, particularly in tropical biomes (see Cusack et al., 2024, where root horizontal distribution is not mentioned, but see Schenk and Jackson, 2002, for data on water-limited systems). As a result, trees only deplete the water content of the belowground voxels located below their trunk position and thus compete for water with trees sharing the same belowground voxels only (see Sect. 2.3), but this could easily be revisited in the future.

The soil water potential in the root zone, ψ_{root} (in MPa), captures how the plant equilibrates with the soil water state across its root profile. It is computed as the weighted mean of the belowground voxel water potentials across layers. We used the weighting scheme proposed by Williams et al. (2001; see also Bonan et al., 2014; Duursma and Medlyn, 2012), which accounts for the variation of soil water avail-

ability and conductance across layers as follows:

$$\psi_{\text{root}} = \sum_l w_l \times \psi_l \quad \text{with}$$
$$w_l = \frac{\left(\psi_l - \psi_{\text{R,min}}\right) \times G_l}{\sum_{ll}\left(\psi_{ll} - \psi_{\text{R,min}}\right) \times G_{ll}}, \tag{21}$$

where ψ_l is the soil water potential in layer l, and $\psi_{\text{R,min}}$ is the root water potential below which there is no water uptake within the layer (minimal root water potential, assumed to be -3 MPa as in Duursma and Medlyn, 2012). G_l, the soil-to-root water conductance in layer l, in mmol H_2O m^{-2} s^{-1} MPa^{-1}, is computed as follows (Gardner, 1964).

$$G_l = \frac{2\pi L_{\text{a},l} K_l}{\log\left(\frac{r_s}{r_r}\right)} \tag{22}$$

In Eq. (22), $L_{\text{a},l}$ is the total root length per unit area in the layer (in $m\,m^{-2}$), with the total root length in the layer computed as $RB_l \times SRL$ where SRL is the specific root length, here assumed to be constant ($10\,m\,g^{-1}$, Bonan et al., 2014; Metcalfe et al., 2008; Weemstra et al., 2016). K_l is the soil hydraulic conductivity of layer l (in mmol H_2O m^{-1} s^{-1} MPa^{-1}, see Sect. 2.3), r_r is the mean fine root radius, here set at 1 mm, and r_s is half the mean distance between roots, calculated with the assumption of uniform root spacing in a given layer (Newman, 1969):

$$r_s = \frac{1}{\sqrt{\pi L_{\text{v},l}}}, \tag{23}$$

where $L_{\text{v},l}$ is the total root length per unit soil volume in the layer (in $m\,m^{-3}$), computed in the same way as $L_{\text{a},l}$, but also divided by layer depth.

A range of other models have been used to infer ψ_{root} using the relative tree root biomass in each layer directly as weights (De Kauwe et al., 2015a; Naudts et al., 2015; Powell et al., 2013; Schaphoff et al., 2018; Sakschewski et al., 2021; Verbeeck et al., 2011). However, trees do not take up water simply as a proportion of root density but can equilibrate with the wettest soil layers (Schmidhalter, 1997; Duursma and Medlyn, 2012): the contrasting temporal variations in water availability across layers result in seasonal changes in the depth of active water withdrawal (Bruno et al., 2006; Joetzjer et al., 2022). For instance, cavitation in the driest part of the soil disconnects roots from the soil (Sperry et al., 2002; see also Fisher et al., 2006). This is likely why deeper roots, although often very rare, disproportionately contribute to sustaining forest productivity during dry seasons.

2.5 Leaf physiology

The carbon assimilated and the water transpired by a tree within a day are the sum of the leaf-level carbon and water fluxes across daytime half-hours. Leaf-level carbon assimilation is computed per crown layer of each tree, using the Farquhar–von Caemmerer–Berry model of C_3 photosynthesis (Farquhar et al., 1980, see Sect. 2.5.1), coupled to the model of stomatal conductance of Medlyn et al. (2011; see Sect. 2.5.2) as in Maréchaux and Chave (2017). In TROLL 4.0 the dependences on leaf temperature (T_l), vapour pressure deficit at the leaf surface (VPD_s), and CO_2 concentration at the leaf surface (c_s) are now determined iteratively at the leaf surface, starting from air temperature (T), air vapour pressure deficit (VPD_a), and air CO_2 concentration (c_a) averaged across the tree crown layer (see Sect. 2.2 and 2.4.2) and with transpiration computed using the Penman–Monteith equation (see Sect. 2.5.4).

2.5.1 Photosynthesis

In Farquhar et al. (1980), the leaf-level net carbon assimilation rate (A_n, μmol CO_2 m^{-2} s^{-1}) is limited by either Rubisco activity (A_v, μmol CO_2 m^{-2} s^{-1}) or RuBP regeneration (A_j, μmol CO_2 m^{-2} s^{-1}):

$$A_n = \min\left\{A_v,\, A_j\right\} - R_p\left(T_l\right)\ ;$$
$$A_v = V_{\text{cmax}}\left(T_l,\, \psi_{\text{pd}}\right) \times \frac{c_i\,\Gamma^*}{c_i + K_m\left(T_l\right)};$$
$$A_j = \frac{J}{4}\,\frac{c_i - \Gamma^*\left(T_l\right)}{c_i + 2\Gamma^*\left(T_l\right)}, \tag{24}$$

where R_p is the photorespiration rate (μmol C m^{-2} s^{-1}), V_{cmax} the maximum rate of carboxylation (μmol CO_2 m^{-2} s^{-1}), c_i the CO_2 partial pressure at carboxylation sites, Γ^* the CO_2 compensation point in the absence of dark respiration, K_m the apparent kinetic constant of the Rubisco (von Caemmerer, 2000), and J the electron transport rate (μmol e^- m^{-2} s^{-1}), which depends on PPFD through

$$J = \frac{1}{2\theta}\left[\alpha \times \text{PPFD} + J_{\text{max}}\left(T_l,\, \psi_{\text{pd}}\right)\right.$$
$$\left. - \sqrt{\begin{array}{l}\left(\alpha \times \text{PPFD} + J_{\text{max}}\left(T_l,\, \psi_{\text{pd}}\right)\right)^2 \\ -4\theta \times \alpha \times \text{PPFD} \times J_{\text{max}}\left(T_l,\, \psi_{\text{pd}}\right)\end{array}}\right]. \tag{25}$$

J_{max} is the maximal electron transport capacity (μmol e^- m^{-2} s^{-1}), θ the curvature factor (unitless), and α the apparent quantum yield to electron transport (mol e^- mol photons^{-1}), computed following von Caemmerer (2000) as $\alpha = (1 - \text{LSQ}) \times 0.5$, with LSQ the effective spectral quality of light, fixed at 0.15, and the factor 0.5 accounting for the fact that each photosystem absorbs half of the photons.

The V_{cmax} and J_{max} parameters depend on leaf properties, leaf temperature (T_l), and water state (through the leaf pre-dawn water potential, ψ_{pd}; see Eq. 37) and represent a large source of uncertainty in vegetation models (Zaehle et

al., 2005; Mercado et al., 2009; Rogers et al., 2017). In tropical forest environments, Domingues et al. (2010) suggested that V_{cmax} and J_{max} are co-limited by the leaf concentration of nitrogen and phosphorus as follows (see also Walker et al., 2014):

$$V_{\text{cmax-M}}\,(25\,^{\circ}\text{C}) = \min\{-1.56 + 0.43 \times N - 0.37 \times \text{LMA}; \\ -0.80 + 0.45 \times P - 0.25 \times \text{LMA}\}, \quad (26)$$

$$J_{\text{max-M}}\,(25\,^{\circ}\text{C}) = \min\{-1.50 + 0.41 \times N - 0.45 \times \text{LMA}; \\ -0.74 + 0.44 \times P - 0.32 \times \text{LMA}\}, \quad (27)$$

with $V_{\text{cmax-M}}$ and $J_{\text{max-M}}$ the photosynthetic capacities at 25 °C of unstressed mature leaves on a leaf dry mass basis, in $\mu\text{mol}\,CO_2\,g^{-1}\,s^{-1}$ and $\mu\text{mol}\,e^{-}\,g^{-1}\,s^{-1}$, respectively. N and P are leaf nitrogen and phosphorus concentrations in $\text{mg}\,g^{-1}$, and LMA is the leaf mass per area in $\text{g}\,\text{cm}^{-2}$. $V_{\text{cmax-M}}$ and $J_{\text{max-M}}$ can be converted into area-based V_{cmax} and J_{max} by multiplying by LMA. We used this leaf-trait-based parameterization of $V_{cmax}\,(25\,^{\circ}\text{C})$ and $J_{max}\,(25\,^{\circ}\text{C})$ in the absence of water stress (as in Fyllas et al., 2014; Mercado et al., 2011). The dependence of V_{cmax} and J_{max} on temperature was given by equations in Bernacchi et al. (2003), and the dependence on water availability was modelled by a function of ψ_{pd} (WSF_{ns}, see Sect. 2.5.3, Eq. 40).

$$V_{cmax}\left(T_l, \psi_{pd}\right) = V_{cmax}\,(25\,^{\circ}\text{C}) \times e^{\left(26.35 - \frac{65.33}{R \times (T_l + 273.15)}\right)} \\ \times \text{WSF}_{ns}\left(\psi_{pd}\right) \quad (28)$$

$$J_{max}\left(T_l, \psi_{pd}\right) = J_{max}\,(25\,^{\circ}\text{C}) \times e^{\left(17.57 - \frac{43.54}{R \times (T_l + 273.15)}\right)} \\ \times \text{WSF}_{ns}\left(\psi_{pd}\right) \quad (29)$$

R is the molar gas constant ($0.008314\,\text{kJ}\,\text{K}^{-1}\,\text{mol}^{-1}$), and T_l is the leaf temperature in degrees Celsius. The temperature dependence of Γ^* and K_m followed von Caemmerer (2000).

$$\Gamma^*\,(T_l) = 37 \times e^{23.4 \times \frac{(T_l - 25)}{298 \times R \times (273 + T_l)}} \quad (30)$$

$$K_m\,(T_l) = 404 \times e^{59.36 \times \frac{(T_l - 25)}{298 \times R \times (273 + T_l)}} \\ \times \left(1 + \frac{210}{248 \times e^{35.94 \times \frac{T_l - 25}{298 \times R \times (273 + T_l)}}}\right) \quad (31)$$

Temperature dependencies in Eqs. (28)–(31) are consistent with Domingues et al. (2010), following recommendations from Rogers et al. (2017).

The leaf photorespiration rate R_p (Eq. 24) was assumed to be a fixed fraction (40 %) of the leaf dark respiration rate (Eqs. 32–33; Atkin et al., 2000). We used the Atkin et al. (2015) "broadleaved trees" empirical model to estimate mature leaf dark respiration rates as a function of plant functional traits:

$$R_{d-M}\,(25\,^{\circ}\text{C}) = 8.5341 - 0.1306 \times N \\ - 0.5670 \times P - 0.0137 \times \text{LMA} + 11.1 \times V_{\text{cmax-M}} \\ + 0.1876 \times N \times P, \quad (32)$$

with R_{d-M} the leaf dark respiration rate on a dry mass basis and at a reference temperature of 25 °C (in $\text{nmol}\,CO_2\,g^{-1}\,s^{-1}$). Multiplying R_{d-M} by LMA gives the area-based leaf dark respiration R_d (in $\mu\text{mol}\,C\,m^{-2}\,s^{-1}$). The temperature dependence of mature leaf dark respiration rates was calculated as (Atkin et al., 2015, Eq. 1 therein; see also Heskel et al., 2016)

$$R_d(T_l) = R_d\,(25\,^{\circ}\text{C}) \\ \times \left[3.09 - 0.043 \times \frac{(T_l + 25)}{2}\right]^{\frac{(T_l - 25)}{10}}. \quad (33)$$

Long-term acclimation to temperature is not considered in TROLL 4.0 (Kattge and Knorr, 2007; Smith and Dukes, 2013).

2.5.2 Stomatal conductance

Carbon assimilation by photosynthesis is limited by the CO_2 partial pressure at carboxylation sites, which is controlled by stomatal transport as modelled by the diffusion equation:

$$A_n = g_s\,(c_s - c_i), \quad (34)$$

with g_s the stomatal conductance to CO_2 ($\text{mol}\,CO_2\,m^{-2}\,s^{-1}$). The representation of stomatal conductance varies greatly across vegetation models (Damour et al., 2010; Bonan et al., 2014; Rogers et al., 2017; see Appendix B, Table B1) and remains an active research topic (Anderegg et al., 2018; Dewar et al., 2018; Lamour et al., 2022; Sperry et al., 2017; Wolf et al., 2016; Sabot et al., 2022). In TROLL 4.0, stomatal conductance to water vapour is simulated as (Medlyn et al., 2011)

$$g_{sw} = g_0 + 1.6 \times \left(1 + \frac{g_1}{\sqrt{\text{VPD}_s}}\right) \times \frac{A_n}{c_s}, \quad (35)$$

where g_{sw} is the stomatal conductance to water vapour in $\text{mol}\,H_2O\,m^{-2}\,s^{-1}$, 1.6 is the ratio of the diffusivities of H_2O to CO_2 (Massman, 1998), VPD_s is the vapour pressure deficit at the leaf surface in kPa, A_n is the assimilation rate in $\mu\text{mol}\,CO_2\,m^{-2}\,s^{-1}$ (Eq. 24 above), c_s is the CO_2 concentration at the leaf surface in ppm, g_0 is the minimum conductance for water vapour in $\text{mol}\,H_2O\,m^{-2}\,s^{-1}$ (Duursma et al., 2019), and g_1 is a model parameter in $\text{kPa}^{1/2}$. Equations (24), (34), and (35) taken together lead to two quadratic equations for c_i, one when Rubisco activity is limiting and one when RuBP regeneration is limiting, and the solution is the highest root.

The parameter g_1 varies with species ecological strategies and carbon cost of water use (Domingues et al., 2014; Franks et al., 2018; Héroult et al., 2013; Lin et al., 2015; Wolz et al., 2017). Consequently, it is expected that g_1 should differ across plant functional types (e.g. Xu et al., 2016). Here we assumed a dependence of g_1 on wood density (wsg, in

$g\,cm^{-3}$) as in Lin et al. (2015). We also assumed a dependence on water availability, modelled by a function of ψ_{pd} (WSF_s; see Sect. 2.5.3).

$$g_1 = (-3.97 \times wsg + 6.53) \times WSF_s\left(\psi_{pd}\right) \quad (36)$$

This parameterization of g_1 based on wood density is a matter of debate, however, and alternatives have been proposed (Wu et al., 2020; Lamour et al., 2023a).

The parameter g_0 quantifies water fluxes through the leaf cuticle (cuticular conductance) and from stomatal leaks. Although it is increasingly recognized as a key parameter explaining tree water loss in drought conditions (Cochard, 2021; Martin-StPaul et al., 2017), its values and variation with other functional traits are poorly documented (Duursma et al., 2019; Slot et al., 2021; Nemetschek et al., 2024), and here we assumed a fixed value. Note that some previous studies have defined g_0 as cuticular conductance only, ignoring stomatal leak effects and thus underestimating g_0.

Both g_0 and g_1 were assumed not to depend on temperature in the absence of clear empirical evidence for tropical forest trees (Duursma et al., 2019; Slot et al., 2021; Rogers et al., 2017), but this may be further explored in the future through measurements and experiments (Cochard, 2021).

2.5.3 Effect of water availability on leaf-level gas exchange

Under water stress, leaf-level gas exchanges and photosynthesis are impaired, but how this is represented varies greatly across models (Appendix B, Table B1; Powell et al., 2013; Trugman et al., 2018; Verhoef and Egea, 2014). A common approach is to define a single integrative water stress factor cumulating all effects along the soil–plant–atmosphere pathway, some of which are difficult to evaluate empirically (e.g. Fischer et al., 2014; Gutiérrez et al., 2014; Krinner et al., 2005; Clark et al., 2011). This factor is then used to modify the parameters of the stomatal conductance and/or photosynthesis models (Egea et al., 2011; Verhoef and Egea, 2014). Depending on models, water stress factors have been assumed to depend on soil water content or on soil water potential in the root zone (De Kauwe et al., 2015a; Drake et al., 2017; Joetzjer et al., 2014; Powell et al., 2013; Trugman et al., 2018). Alternatively, some models have implemented a water stress factor as a function of leaf water potential (ψ_{leaf}; Anderegg et al., 2017; Christoffersen et al., 2016; Duursma and Medlyn, 2012; Kennedy et al., 2019; Xu et al., 2016; see also the pioneer work of Tuzet et al., 2003) or used optimization approaches (Williams et al., 1996; Anderegg et al., 2018; Sabot et al., 2020; Sperry et al., 2017; Wolf et al., 2016) to account for the cost of water uptake and transportation in the plant water column. The shape of such functions remains contentious, however (Table B1), resulting in substantial differences in model predictions.

Also, there is no consensus on the relative role of stomatal and non-stomatal limitations in leaf CO_2 assimilation under drying conditions, reflecting contrasting experimental results (Drake et al., 2017; Zhou et al., 2014; Keenan et al., 2010; Appendix B, Table B2). Under stomatal limitation, stomatal closure reduces leaf gas exchanges, and the water stress factor is applied to stomatal conductance or stomatal conductance model parameters (e.g. g_1). Under non-stomatal limitations, drought (leading to increased leaf temperature and/or decreased leaf water potential) impairs the biochemical photosynthesis apparatus, which results in a reduction of photosynthetic capacities and/or mesophyll conductance (Flexas et al., 2004, 2012). In this latter case, the water stress factor is applied to V_{cmax} and J_{max} (Drake et al., 2017; Keenan et al., 2010). Some models consider only one limitation and others both (Appendix B, Table B1).

In TROLL 4.0, two water stress factors are used, one for stomatal limitation, modifying the g_1 parameter (WSF_s; Eq. 36), and one for non-stomatal limitations, modifying the V_{cmax} and J_{max} parameters of the photosynthesis model (WSF_{ns}; Eqs. 28 and 29). Both water stress factors are assumed to depend on the leaf pre-dawn water potential (ψ_{pd}; De Kauwe et al., 2015a; Verhoef and Egea, 2014), which is a function of the soil water potential in the root zone (ψ_{root}, Eq. 21) (Stahl et al., 2013a, but see Bucci et al., 2004; Donovan et al., 2003) as follows (Jones, 2013; Eq. 4.9 therein):

$$\psi_{pd} = \psi_{root} - \rho g h \simeq \psi_{root} - 0.01 \times h, \quad (37)$$

where ρ is the density of water, g the gravitational force ($g = 9.81\,m\,s^{-2}$), and h total tree height in metres. Here, WSF_s was computed as (Zhou et al., 2013; De Kauwe et al., 2015a)

$$WSF_s = \exp\left(b \times \psi_{pd}\right), \quad (38)$$

where b is a parameter. To parameterize b, we used the relationship between the leaf water potential at turgor loss point (π_{tlp} in MPa) and the water potential causing 90 % of stomatal closure (ψ_{gs90}, in MPa): $\pi_{tlp} = 0.97 \times \psi_{gs90}$ ($P < 0.01$, $R^2 = 0.4$; Fig. 1 in Martin-StPaul et al., 2017) and assumed that $WSF_s \approx 0.1$ at ψ_{gs90} (an approximation given the shape of Eq. 35), leading to

$$WSF_s = \exp\left(-2.23 \times \frac{\psi_{pd}}{\pi_{tlp}}\right). \quad (39)$$

The link between the leaf water potential at stomatal closure and the leaf water potential at turgor loss point is supported by several studies (Bartlett et al., 2016b; Brodribb et al., 2003; Farrell et al., 2017; Martin-StPaul et al., 2017; Meinzer et al., 2016; Rodriguez-Dominguez et al., 2016; Trueba et al., 2019). The formulation of WSF_s in Eq. (39) was preferred over alternatives, such as a linear relationship between WSF_s and ψ_{pd} (Oleson et al., 2008; Powell et al., 2013; Verhoef and Egea, 2014). The latter is less supported by data and leads to threshold responses as soil water content declines and similar responses across species, in contrast with empirical evidence (Kursar et al., 2009; Zhou et al., 2013).

The water stress factor for non-stomatal limitation (WSF_{ns}) was computed following Xu et al. (2016):

$$WSF_{ns} = \left(1 + \left(\frac{\psi_{pd}}{\pi_{tlp}}\right)^{a}\right)^{-1}, \quad (40)$$

with $a = 6$ estimated from data reported in Brodribb et al. (2003). In this formula, $WSF_{ns} = 1/2$ when $\psi_{pd} = \pi_{tlp}$, in agreement with empirical findings (Brodribb et al., 2002; Manzoni, 2014).

The parameterization of WSF_s and WSF_{ns} based on π_{tlp} is supported by the fact that leaf cells need to maintain turgor to sustain functioning (Hsiao, 1973). These functions do not depend on π_{tlp} when $\psi_{pd} = \pi_{tlp}$, so there is a simple link between the leaf drought tolerance, as informed by π_{tlp}, and the response of leaf-level gas exchange to water availability. Also, these equations predict that the decline of stomatal conductance as water availability decreases precedes that of photochemistry, consistent with observations (Fig. 2; Fatichi et al., 2016; Trueba et al., 2019).

Note that, since mesophyll conductance is not explicitly represented here, the effect of water stress on photosynthetic capacities (WSF_{ns}) includes both direct effects on the photosynthetic machinery and indirect effects from the reduction of mesophyll conductance (Drake et al., 2017; Keenan et al., 2010). Alternative shapes of water stress factors could be explored in the future, and a more explicit representation of the water flow through the plant water column could be implemented (Paschalis et al., 2024). In the absence of a clear consensus on the effect of water stress on respiration, TROLL 4.0 does not assume that respiration depends on water availability (Flexas et al., 2006, 2005; Rowland et al., 2018, 2015; Santos et al., 2018; Stahl et al., 2013b).

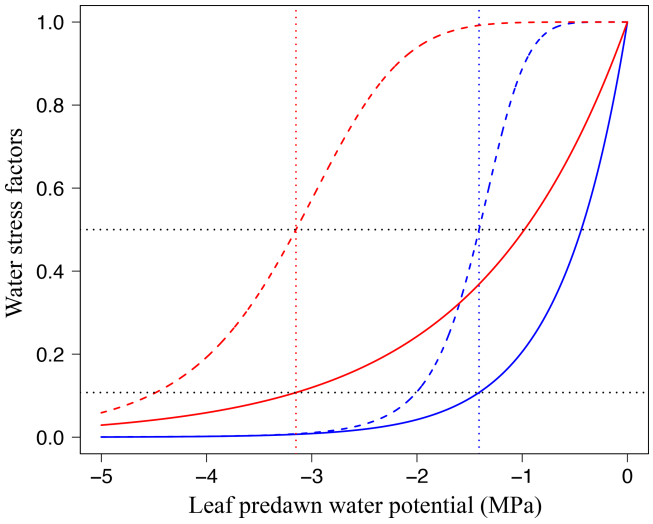

Figure 2. Responses of leaf-level gas exchange to water stress, depending on the leaf drought tolerance. Water stress factors are shown for the stomatal conductance parameter g_1 (stomatal limitation, WSF_s, Eq. 39; solid lines) and for the photosynthetic capacities J_{max} and V_{cmax} (non-stomatal limitation, WSF_{ns}, Eq. 40; dashed lines) as a function of leaf pre-dawn water potential (ψ_{pd}, MPa). WSFs are shown for a drought-vulnerable species ($\pi_{tlp} = -1.41$ MPa, the least negative value reported in Maréchaux et al., 2015; blue lines) and for a drought-tolerant species ($\pi_{tlp} = -3.15$ MPa, the most negative value reported in Maréchaux et al., 2015). Vertical dotted lines: π_{tlp}, horizontal dotted black lines: WSF_s and WSF_{ns} at π_{tlp}.

2.5.4 Leaf energy balance

In TROLL 4.0, the leaf temperature (T_l), vapour pressure deficit (VPD_s), and CO_2 concentration (c_s) at the leaf surface are computed through an iterative scheme that solves the leaf energy balance (Medlyn et al., 2007; Wang and Leuning, 1998; Duursma, 2015; Vezy et al., 2018). This is an important step because the leaf boundary layer plays a key role in gas exchanges, especially in dense tropical moist forests, given the large size of tropical tree leaves and the low wind speeds within canopies (De Kauwe et al., 2017; Jarvis and McNaughton, 1986; Meinzer et al., 1997). The iterative scheme is as follows. Initially, T_l, VPD_s, and c_s are set equal to surrounding air values (T, VPD, and c_a). Leaf photosynthesis (A_n) and stomatal conductance (g_{sw}) are computed using Eqs. (24), (34), and (35). Next, the boundary layer conductance and radiation conductance are computed, and finally the leaf-level transpiration rate is deduced from the Penman–Monteith equation (Eq. 41 below). After these steps, new values for T_l, VPD_s, and c_s are computed, and the above steps are repeated until leaf temperature converges, i.e. when the absolute difference between the T_l values of two consecutive iterations is lower than 0.01 °C.

The leaf-level transpiration rate E_l (in mol H_2O m^{-2} s^{-1}) is calculated as

$$E_l = \frac{1}{\lambda} \times \frac{s R_{ni} + VPD_a g_H C_p M_a}{s + \gamma \frac{g_H}{g_w}}, \quad (41)$$

where λ is the latent heat of water vapour (in J mol^{-1}), s is the slope of the (locally linearized) relationship between saturated vapour pressure and temperature (in Pa K^{-1}, see Jones, 2013, Eq. 5.15 therein), R_{ni} is the isothermal net radiation (in J m^{-2} s^{-1}), g_H is the total leaf conductance to heat (in mol m^{-2} s^{-1}), C_p is the heat capacity of air (1010 J kg^{-1} K^{-1}), M_a is the molecular mass of air (28.96×10^{-3} kg mol^{-1}), γ the psychrometric constant (in Pa K^{-1}), and g_w the total conductance to water vapour (mol H_2O m^{-2} s^{-1}). The latent heat of water vapour λ depends on air temperature as follows.

$$\lambda = \left(2.501 \times 10^{3} - 2.365 \times T\right) \times 18 \quad (42)$$

The isothermal net radiation R_{ni} has two components, the absorbed solar radiation (S_{abs}), including both PAR and NIR wavebands, and the net longwave radiation (Leuning et al.,

1995; Appendix D therein):

$$R_{\mathrm{ni}} = S_{\mathrm{abs}} - B_{\mathrm{n},0} \times k_{\mathrm{d}} \exp(-k_{\mathrm{d}}\mathrm{LAI}), \quad (43)$$

where $B_{\mathrm{n},0}$ is the net longwave radiation at the top of the canopy, and $k_{\mathrm{d}} \exp(-k_{\mathrm{d}}\mathrm{LAI})$ accounts for its extinction within the canopy, with k_{d} set equal to 0.8. To account for the absorbed NIR radiation at a given height within the canopy in S_{abs}, we used the relationship reported by Kume et al. (2011; Fig. 4 therein) that links the transmitted NIR to the transmitted and incident PAR and assumed a leaf absorptance in the NIR equal to 0.1. $B_{\mathrm{n},0}$ is then computed as the absorbed minus the emitted longwave radiation:

$$B_{\mathrm{n},0} = \varepsilon_{\mathrm{l}}(1-\varepsilon_{\mathrm{a}})\sigma T_{\mathrm{top}}^4, \quad (44)$$

where T_{top} is the top canopy air temperature in Kelvin, σ is the Stefan–Boltzmann constant ($\sigma = 5.67 \times 10^{-8}\,\mathrm{W\,m^{-2}\,K^{-4}}$), ε_{l} is the emissivity of the canopy leaves, here assumed to be 1, and ε_{a} is the emissivity of the atmosphere. Several models exist for ε_{a}, with varying performance depending on the sky conditions (Marthews et al., 2012). We used Dilley and O'Brien (1998) here, which compromises between parsimony and performance across sky conditions (Marthews et al., 2012; Tables 2 and 5 therein).

g_{H}, the total leaf conductance to heat, has three components, the boundary layer conductance for free convection g_{bHf}, the boundary layer for forced convection g_{bHu}, and the radiation conductance g_{r} (Leuning et al., 1995; Jones, 2013):

$$g_{\mathrm{H}} = 2 \times (g_{\mathrm{bHf}} + g_{\mathrm{bHu}} + g_{\mathrm{r}}), \quad (45)$$

where the factor 2 accounts for the two sides of the leaves' g_{bHf}. The boundary layer conductance for free convection is given by

$$g_{\mathrm{bHf}} = 0.5 \times D_{\mathrm{H}} \times \left(\frac{1.6 \times 10^8 \times |T_{\mathrm{l}} - T|}{w_{\mathrm{l}}}\right)^{0.25} \times \frac{P_{\mathrm{ress}}}{RT}, \quad (46)$$

where D_{H} is the molecular diffusivity to heat ($D_{\mathrm{H}} = 21.5 \times 10^{-6}\,\mathrm{m^2\,s^{-1}}$), P_{ress} the atmospheric pressure (in Pa), R the universal gas constant ($R = 8.314\,\mathrm{J\,mol^{-1}\,K^{-1}}$), and T the temperature of surrounding air in Kelvin. Leaf width w_{l} (m) is estimated as the square root of leaf area ($w_{\mathrm{l}} = \sqrt{\mathrm{LA}}$). g_{bHu}, the boundary layer for forced convection (in $\mathrm{mol\,m^{-2}\,s^{-1}}$), is given by

$$g_{\mathrm{bHu}} = 0.003 \times \sqrt{\frac{u}{w_{\mathrm{l}}}} \times \frac{P_{\mathrm{ress}}}{RT}, \quad (47)$$

where u is the wind speed in $\mathrm{m\,s^{-1}}$ (see Eq. 9). g_{r}, the radiation conductance in $\mathrm{mol\,m^{-2}\,s^{-1}}$, varies with T_{a} as follows (Jones, 2013, p. 101 therein).

$$g_{\mathrm{r}} = \frac{4 \times \varepsilon_{\mathrm{l}} \sigma T^3}{C_p M_{\mathrm{a}}} \quad (48)$$

g_{w}, the total conductance to water vapour, has two components that represent hydraulic resistances in series: the stomatal conductance (g_{sw}, in $\mathrm{mol\,H_2O\,m^{-2}\,s^{-1}}$, Eq. 35) and the boundary layer conductance (g_{bw} in $\mathrm{mol\,H_2O\,m^{-2}\,s^{-1}}$) to water vapour:

$$g_{\mathrm{w}} = \frac{g_{\mathrm{bw}} \times g_{\mathrm{sw}}}{g_{\mathrm{bw}} + g_{\mathrm{sw}}}, \quad (49)$$

$$\text{with } g_{\mathrm{bw}} = 1.075 \times (g_{\mathrm{bHf}} + g_{\mathrm{bHu}}), \quad (50)$$

where 1.075 accounts for the relative diffusivities of heat and water vapour in air. Equations (9) and (50) assume that all leaves are hypostomatous (stomates on the ground-facing side of the leaves only), a reasonable assumption in tropical forests (Drake et al., 2019; Muir, 2015).

2.6 Carbon allocation

2.6.1 Net carbon uptake: whole-tree integration and respiration

At each daily time step, the individual tree net primary productivity of carbon, $\mathrm{NPP_{ind}}$ (gC), is obtained by the following balance equation (Fig. 3).

$$\mathrm{NPP_{ind}} = \mathrm{GPP_{ind}} - R_{\mathrm{maintenance}} - R_{\mathrm{growth}} \quad (51)$$

$\mathrm{GPP_{ind}}$ (gC) is computed each half-hour as the carbon assimilation rate A_{n} (Eq. 19), multiplied by the leaf area in each tree crown layer (LA_l, in $\mathrm{m^2}$), then summed over tree crown layers and cumulated across the day.

Young leaves and old leaves have been reported to have lower photosynthetic capacities and activities than mature leaves (Doughty and Goulden, 2008; Kitajima et al., 2002, 1997b; Wu et al., 2016; Albert et al., 2018; Menezes et al., 2021). For each tree, total leaf area ($\mathrm{LA_t}$) is partitioned into three leaf age pools: young, mature, and old leaves so that $\mathrm{LA_t} = \mathrm{LA_{young}} + \mathrm{LA_{mature}} + \mathrm{LA_{old}}$ (all in $\mathrm{m^2}$). These three leaf age pools are assumed to be uniformly distributed within the tree crown. In young and old leaves, the net assimilation rate is a fraction $\varrho < 1$ of that of mature leaves so that

$$\mathrm{GPP_{ind}} = C_{\mathrm{GPP}} \times \frac{(\varrho \times \mathrm{LA_{young}} + \mathrm{LA_{mature}} + \varrho \times \mathrm{LA_{old}})}{\mathrm{LA}_t} \times \sum_l \sum_t A_{\mathrm{n}}(t,l) \times \mathrm{LA}_l, \quad (52)$$

where the factor C_{GPP} is a conversion factor, and t depicts the daytime half-hours and l the tree crown layers. Here we assume that the carbon uptake efficiency ϱ relative to mature leaves is the same in young and old leaves and $\varrho = 0.5$, a value consistent with observations.

TROLL 4.0 partitions autotrophic respiration into maintenance respiration and growth respiration, even if both come from the same biochemical pathways (Amthor, 1984; Thornley and Cannell, 2000). Maintenance respiration ($R_{\mathrm{maintenance}}$) has seldom been documented for stem and

roots and is inferred empirically (Cavaleri et al., 2008; Meir et al., 2001; Slot et al., 2013; Weerasinghe et al., 2014). Nighttime leaf maintenance respiration is computed using Eqs. (32) and (33), using the mean nighttime temperature. As stomatal conductance and dark respiration vary less with leaf age than carbon assimilation rate (Albert et al., 2018; Kitajima et al., 2002; Villar et al., 1995), we assumed that young and old leaves have respiration and transpiration rates equal to $\varrho' = 0.75$ that of mature leaves, leading to lower water use efficiency than mature leaves. Tree-level nighttime leaf respiration and daytime transpiration are computed as follows at each time step:

$$X_{\text{ind}} = C_X \times \frac{\left(\varrho' \times \text{LA}_{\text{young}} + \text{LA}_{\text{mature}} + \varrho' \times \text{LA}_{\text{old}}\right)}{\text{LA}_{\text{t}}} \times \sum_{l} \left(\sum_{i} X\,(i,\, l) \right) \times \text{LA}_l, \tag{53}$$

where X_{ind} is either the carbon respired by leaves during the night or the total water transpired by the tree (gC or m^3, respectively), X is the leaf dark respiration (Eqs. 32 and 33) or the leaf-level transpiration rate (Eq. 41), respectively, and C_X is a factor to convert leaf-level rates in $\mu\text{mol C m}^{-2}\,\text{s}^{-1}$ or in $\text{mol H}_2\text{O m}^{-2}\,\text{s}^{-1}$ to total fluxes per individual per day (gC or m^3, respectively).

Stem maintenance respiration (R_{stem}, in $\mu\text{mol C s}^{-1}$) was modelled assuming a constant respiration rate per volume of sapwood ($39.6\,\mu\text{mol m}^{-3}\,\text{s}^{-1}$, Ryan et al., 1994) so that

$$R_{\text{stem}} = C_{\text{sresp}} \times 39.6 \times \text{SA} \times (h - \text{cd}) \tag{54}$$

where SA is the tree sapwood area (in m^2) and C_{sresp} is a conversion factor. Stem respiration response to temperature was modelled using a Q_{10} value of 2.0 (Meir and Grace, 2002; Ryan et al., 1994) and using mean daytime and nighttime temperatures. Stahl et al. (2011) reported that R_{stem} varies among individual trees, even when controlling for sapwood volume. However, in the absence of a clear understanding of the drivers, Eq. (4) is a parsimonious choice. In TROLL 4.0, sapwood area is computed dynamically. We used an inversion of the pipe model to derive sapwood area from the tree's leaf area (LA_{t}, in m^2), height (h, m), and wood density following Fyllas et al. (2014; Eqs. 7 and 8 therein):

$$\text{SA} = C_{\text{SA}}\,\frac{2 \times \text{LA}_t}{\lambda_1 + \lambda_2 \times h + \delta_1 + \delta_2 \times \text{wsg}}, \tag{55}$$

with $\lambda_1 = 0.066\,\text{m}^2\,\text{cm}^{-2}$, $\lambda_2 = 0.017\,\text{m cm}^{-2}$, $\delta_1 = -0.018\,\text{m}^2\,\text{cm}^{-2}$, and $\delta_2 = 1.6\,\text{cm}^3\,\text{g}^{-1}$, and C_{SA} a conversion factor. In addition to Eq. (55), there are both lower and upper limits on sapwood extent. Sapwood has a minimum thickness of 0.5 cm and any newly grown wood is always considered sapwood, irrespective of leaf area. TROLL 4.0 also imposes an upper limit on sapwood growth based on stem diameter growth so that increases in living tissue cannot exceed increases in total tissue.

Other contributions of maintenance respiration were prescribed as proportions of leaf and stem maintenance respiration. Fine root maintenance respiration was assumed to be half of leaf maintenance respiration (Malhi, 2012), and coarse root and branch maintenance respirations were assumed to account for half of stem respiration (Asao et al., 2015; Cavaleri et al., 2006; Meir and Grace, 2002).

Growth respiration (R_{growth}) was assumed to account for 30 % of the carbon uptake by photosynthesis (gross primary productivity) minus the maintenance respiration (Cannell and Thornley, 2000). These assumptions are commonly made in the literature but remain a major source of uncertainty in carbon flux modelling (Atkin et al., 2014; Huntingford et al., 2013).

Contrary to the last published version of TROLL, in which the allocation of NPP_{ind} to plant organs was fully prescribed by fixed factors ($f_{\text{canopy}} = f_{\text{leaves}} + f_{\text{fruit}} + f_{\text{twigs}}$ and f_{wood}; Maréchaux and Chave, 2017), the allocation scheme implemented in TROLL 4.0 can now be additionally modulated depending on the current tree state and it includes an explicit carbon storage compartment (Sect. 2.6.2 and 2.6.3; Fig. 3).

2.6.2 Leaf production and leaf shedding

Leaf phenology is a key driver of the variation of tropical forest productivity (Manoli et al., 2018; Restrepo-Coupe et al., 2013; Wu et al., 2017). However, its underlying drivers remain poorly understood, and its representation in vegetation models remains challenging (Chen et al., 2020; Restrepo-Coupe et al., 2017). In ORCHIDEE, Chen et al. (2020, 2021) proposed a leaf phenological scheme in which the production of young leaves is partly controlled by incident shortwave radiation, while the shedding of old leaves is controlled by vapour pressure deficit. This scheme reproduces the simultaneous increase in leaf production and litterfall observed in many Amazonian rainforest sites where productivity increases during the dry season (Chave et al., 2010; Wagner et al., 2016; Yang et al., 2021), but not the observed seasonality in productivity at some sites (e.g. GUYAFLUX eddy flux site in French Guiana; Chen et al., 2020). Additionally, this scheme overlooks the contrasted leaf phenological patterns observed across canopy individuals within and across species within communities (Nicolini et al., 2012; Loubry, 1994). In ED2, Xu et al. (2016) implemented a leaf phenological scheme driven by water availability in the root zone in a seasonally dry tropical forest. Since leaf shedding is often triggered by drought-induced loss of leaf turgor in these systems (Sobrado, 1986), leaf shedding and production are assumed to depend on the difference between leaf pre-dawn water potential and leaf water potential at turgor loss point. However, such a scheme cannot simulate the simultaneous leaf production and shedding observed in moist tropical forests.

In TROLL 4.0, we propose an alternative approach. At each time step, the optimal tree total leaf area (LA_{opt}) is estimated as the leaf area beyond which producing more

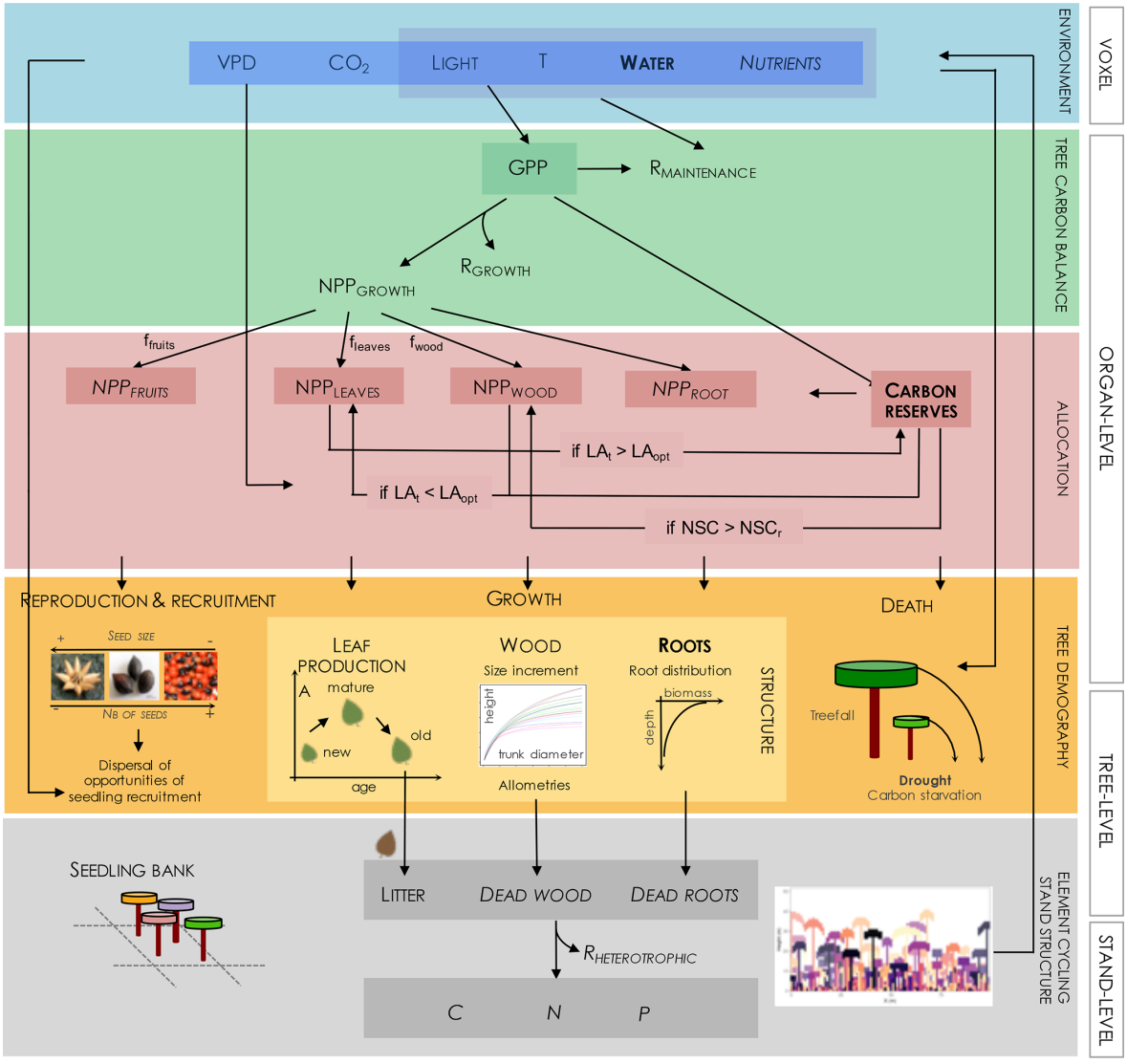

Figure 3. Diagram of structures and processes driving individual and community dynamics, as investigated under the modelling approach adopted in TROLL 4.0. Elements in bold letters refer to novel implementation in comparison to the previously published version, while italic letters refer to elements still not included in this present version. The abiotic environment is modelled at the voxel scale and drives C assimilation in the leaves (gross primary productivity, GPP) and maintenance respiration rates of the different plant organs ($R_{\mathrm{MAINTENANCE}}$). The C amount resulting from the balance between GPP and $R_{\mathrm{MAINTENANCE}}$ can be used for tissue production ($\mathrm{NPP_{FRUITS}}$, $\mathrm{NPP_{LEAVES}}$, $\mathrm{NPP_{WOOD}}$, and $\mathrm{NPP_{ROOTS}}$) or stored (CARBON RESERVES) in the different tree organs. Both allocations induce metabolic costs (R_{GROWTH} and R_{STORAGE}; but the latter is not represented nor included). CARBON RESERVES represents non-structural carbohydrates (NSC), mainly stored as sugar or starch, and its maximal storage capacity is given by $\mathrm{NSC_r}$. Allocation to these different compartments follows a hierarchical scheme initialized by default proportions (f_{fruits}, f_{leaves}, f_{wood}). If the tree leaf area ($\mathrm{LA_t}$) exceeds the optimal leaf area ($\mathrm{LA_{opt}}$, a function of both tree properties and its micro-environment), then the surplus of $\mathrm{NPP_{LEAVES}}$ is allocated to carbon reserves. If the tree leaf area is lower than optimal, then $\mathrm{NPP_{WOOD}}$ and, if further needed, carbon reserves are mobilized for leaf production. If carbon reserves surpass storage capacity ($\mathrm{NSC_r}$), then stored carbohydrates are used for woody growth. C allocated to tissue production leads to an increase in trunk diameter and height following allometric relationships and the production of new young leaves and roots. Simultaneously with tissue turnover, this leads to the update of leaf density and root biomass distribution, influencing both the abiotic environment (e.g. light diffusion and water interception) and light and element acquisition and thus carbon assimilation and metabolism. C allocated to reproduction leads to the production of seeds, which are dispersed randomly. This generates a spatially explicit seedling bank, from which winners are locally recruited depending on both light and water availability. Tree death may be triggered by environmental or mechanical constraints or carbon starvation. In a future version, litter decomposition, wood decay, and nutrient mineralization could lead to soil nutrient availability for plant uptake and take place through the action of soil microorganisms, whose activity, and hence respiration ($R_{\mathrm{HETEROTROPHIC}}$), depends particularly on temperature and soil moisture.

leaves leads to a net carbon loss due to self-shading and respiration costs. LA_{opt} depends on tree crown size and leaf area density (Sect. 2.4.2), leaf photosynthetic capacities and respiration rate (Sect. 2.5.1), and local light environment. At each time step, the amount of carbon allocated to the production of new young leaves, NPP_{leaves}, and to woody growth, NPP_{wood}, is determined by default as $NPP_{leaves} = f_{leaves} \times NPP_{ind}$, with $f_{leaves} = 0.68 \times f_{canopy}$ (Chave et al., 2008, 2010; Maréchaux and Chave, 2017) and $NPP_{wood} = 0.6 \times f_{wood} \times NPP_{ind}$, where the factor 0.6 accounts for the fact that about 40 % of woody NPP is actually used for branch fall repair (Malhi et al., 2011). When leaf area LA_t exceeds LA_{opt}, NPP_{leaves} is reduced so that $LA_t = LA_{opt}$. Second, if the carbon allocated to leaf production is not sufficient to compensate for leaf loss, then the carbon attributed by default to tree woody growth is mobilized for leaf production until leaf loss is compensated for. If not sufficient, the tree carbon storage (see Sect. 2.6.3) is then also mobilized. Hence this scheme prioritizes the maintenance of the assimilating tissues over woody growth (Schippers et al., 2015). The variation of leaf area for each leaf age pool is then computed as follows:

$$\begin{aligned}
\Delta LA_{young} &= \frac{2 \times NPP_{leaves}}{LMA} - \frac{LA_{young}}{\tau_{young}} \\
\Delta LA_{mature} &= \frac{LA_{young}}{\tau_{young}} - \frac{LA_{mature}}{\tau_{mature}} \\
\Delta LA_{old} &= \frac{LA_{mature}}{\tau_{mature}} - \frac{LA_{old}}{\tau_{old}},
\end{aligned} \tag{56}$$

where τ_{young}, τ_{mature}, and τ_{old} are the residence times in each class (in years) so that $LL = \tau_{young} + \tau_{mature} + \tau_{old}$ with LL the maximal tree leaf lifespan (in years). LL is inferred from the tree LMA using the following empirical relationships (Schmitt, 2017):

$$\begin{aligned}
LL = \frac{1}{12} \max(3, \\
12.755 \times \exp(0.007 \times LMA - 0.565 \times N))
\end{aligned} \tag{57}$$

τ_{young} was fixed to $\min(LL/3,\ 1/12)$ yr (Doughty and Goulden, 2008; Wu et al., 2016) and τ_{mature} as a third of total leaf lifespan.

The loss term LA_{old}/τ_{old} corresponds to the rate of leaf litterfall at each time step. In the previous TROLL version, litterfall resulted from the dynamics of leaf biomass with $\tau_{old} = LL - \tau_{young} - \tau_{mature}$. This leaf shedding scheme is passive and does not simulate the observed seasonality in leaf litterfall. Here we propose a new approach to simulate leaf shedding. We first observed that within species and sites, canopy trees can shed their leaves at different times, suggesting that causal environmental drivers should display fine-scale heterogeneity in space (unlike atmospheric shortwave radiation and vapour pressure deficit). In addition, old leaves display nutrient resorption before abscission (Albert et al., 2018; Kitajima et al., 1997a; Urbina et al., 2021); similarly, solute translocation from older to younger leaves can lower osmotic potential and leaf water potential at turgor loss point, thus increasing the drought tolerance of younger leaves to the detriment of older leaves (Pantin et al., 2012). We therefore used pre-dawn leaf water potential as a trigger of leaf shedding as in Xu et al. (2016), but with different thresholds for leaves of different ages, older leaves being more susceptible to a small decrease in tree water availability, while younger leaves can maintain turgor and grow at the same time. More specifically, we defined the following threshold.

$$\psi_{T,o} = \min\left(a_{T,o} \times \pi_{tlp},\ -0.01 \times h - b_{T,o}\right) \tag{58}$$

The first term in $\psi_{T,o}$ with $a_{T,o} < 1$ represents old leaves' lower ability to maintain turgor as soil dries. The second term modulates this susceptibility to drought depending on tree height (Bennett et al., 2015): it induces a susceptibility to a (small) decrease $b_{T,o} > 0$ in soil water availability for large trees, while preventing them from constantly shedding their old leaves at a fast pace (see Eq. (37) and Fig. 4). τ_{old} is then updated using a multiplying factor f_o ($0.001 \leq f_o \leq 1$). Initially, $\tau'_{old} = f_o \tau_{old}$ with $f_o = 1$, which is updated daily as follows: $f'_o = f_o - \delta_o$ when $\psi_{pd} < \psi_{T,o}$ and $f'_o = f_o + \delta_o$ when $\psi_{pd} > \psi_{T,o}$, always assuming that f_o has 0.001 as a lower bound and 1 as an upper bound.

We assumed no variation of π_{tlp} with tree height (Maréchaux et al., 2016). The threshold $\psi_{T,o}$ jointly depends on π_{tlp} and tree height h to account for drought tolerance and tree height on leaf-level water stress. Practically, the tree height above which old leaves become susceptible to a small decrease in soil water availability is $H_{T,o} = -100 \times \left(a_{T,o}\pi_{tlp} + b_{T,o}\right)$ in metres: 28 m at $\pi_{tlp} = -1.5$ MPa and 58 m at $\pi_{tlp} = -3$ MPa (when $a_{T,o} = 0.2$ and $b_{T,o} = 0.02$; see Fig. 4). While this scheme is based on process-based observations, parameters $a_{T,o}$, $b_{T,o}$, and δ_o are currently calibrated (see Schmitt et al., 2025).

2.6.3 Carbon storage

In TROLL 4.0, trees can store carbon explicitly in non-structural carbohydrates. The maximum amount of carbon a tree can store and remobilize is determined as follows:

$$NSC_r = 1000 \times 0.5 \times 0.05 \times 1.25 \times AGB, \tag{59}$$

where NSC_r stands for non-structural carbohydrates (gC), AGB is the tree aboveground biomass (in kg), and 1000×0.5 converts biomass in kilograms into C in grams (Elias and Potvin, 2003). It is assumed that NSC can account for 10 % of the tree biomass, half of which is mobilizable (Martínez-Vilalta et al., 2016), hence the factor 0.05. The other half of NSC supports critical metabolic functions or is no longer accessible. The factor 1.25 accounts for an additional 25 % biomass storage in coarse roots, so $1.25 \times AGB$ is total tree biomass (Ledo et al., 2018). AGB is computed following

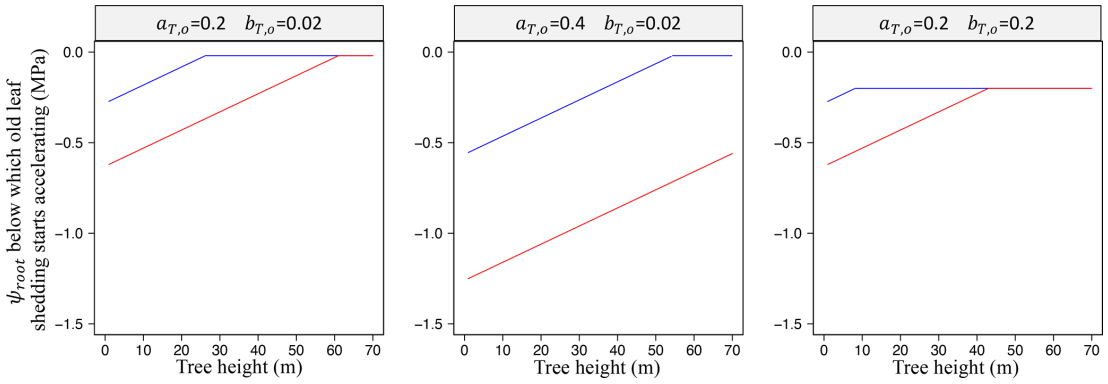

Figure 4. Effect of phenological parameters $a_{T,o}$ and $b_{T,o}$ (Eq. 58) on the height and drought tolerance dependencies of old leaf shedding. Variation of the soil water potential in the root zone (ψ_{root}; Eq. 37) below which old leaf shedding starts accelerating as a function of tree height for different values of $a_{T,o}$ and $b_{T,o}$ and two values of π_{tlp}: $\pi_{tlp} = -1.41$ MPa in blue, the least negative value reported in Maréchaux et al., 2015, and $\pi_{tlp} = -3.15$ MPa in red, the most negative value reported in Maréchaux et al. (2015), as in Fig. 2.

(Chave et al., 2014; Eq. 5 therein):

$$\mathrm{AGB} = 0.0559 \times \mathrm{wsg} \times \mathrm{dbh}^2 \times h, \tag{60}$$

where dbh is in centimetres, h in metres, and wsg in g cm^{-3}. Note that Eqs. (59) and (60), together with Eq. (61) below, induce a growth–storage trade-off mediated by wood density variation across individual and species, in agreement with observations (Signori-Müller et al., 2022). The NSC storage compartment is filled by the potential carbon surplus resulting from the allocation to leaf production, i.e. $f_{leaves} \times \mathrm{NPP_{ind}} - \mathrm{NPP_{leaves}}$, if positive. If the storage compartment has reached its maximum capacity $\mathrm{NSC_r}$, then the surplus is allocated to woody growth.

2.6.4 Growth

The net primary production allocated to woody growth, $\mathrm{NPP_{wood}}$, depends on the outcome of allocation to leaf production and carbon reserves (see Sect. 2.6.2 and 2.6.3; Fig. 3). In TROLL 4.0, hydraulic control on carbon assimilation and leaf phenology both influence carbon allocation to trunk growth (e.g. Doughty et al., 2014; Farrior et al., 2013; Friedlingstein et al., 1999), but turgor-mediated processes are not explicitly modelled (Coussement et al., 2018; Peters et al., 2023; Muller et al., 2011; Körner, 2015). $\mathrm{NPP_{wood}}$ is converted into an increment of stem volume, ΔV in m^3, as follows:

$$\Delta V = 10^{-6} \times \frac{\mathrm{NPP_{wood}}}{0.5 \times \mathrm{wsg}} \times \mathrm{Senesc}\,(\mathrm{dbh})\,, \tag{61}$$

where the factor 0.5 converts dry biomass units into carbon units (Elias and Potvin, 2003). The function Senesc (dbh) is designed so that the largest trees cannot allocate carbon as efficiently into growth, reflecting empirical evidence of a size-related relative growth decline in trees (Yoda et al., 1965; Ryan et al., 1997; Mencuccini et al., 2005; Woodruff and Meinzer, 2011; Stephenson et al., 2014). We assumed that trees cannot exceed a trunk diameter of $\mathrm{dbh_{max}} = \frac{3}{2}\mathrm{dbh_{thresh}}$, where $\mathrm{dbh_{thresh}}$ depends on species-specific information provided by the user (see Sect. 2.4.1), so that

$$\begin{aligned} &\mathrm{Senesc}\,(\mathrm{dbh}) = 1 && \text{when } \mathrm{dbh} \le \mathrm{dbh_{thresh}} \\ &\mathrm{Senesc}\,(\mathrm{dbh}) = \max\left(0;\, 3 - 2\frac{\mathrm{dbh}}{\mathrm{dbh_{thresh}}}\right) && \text{when } \mathrm{dbh} > \mathrm{dbh_{thresh}}. \end{aligned} \tag{62}$$

The trunk diameter growth increment Δdbh (m) is computed from ΔV as follows. $V = C\,\pi(\frac{\mathrm{dbh}}{2})^2 h$, where C is a form factor (Chave et al. 2014, Eq. 5 therein). The term h (m) is total tree height inferred from the dbh following Eq. (16), and this leads to an expression of V as a function of dbh only. This function can be inverted to estimate Δdbh as a function of ΔV, which is known from Eq. (61). Tree height and crown dimensions are then updated using Eqs. (16), (17), and (18).

2.7 Tree demography

2.7.1 Seed production, dispersal, and recruitment

The starting point for a tree life cycle, as represented in TROLL 4.0, is an event of seed dispersal into the seed bank. On each 1 × 1 m ground site and for each species s, a "seed" bank stores all the seeds dispersed from the mature trees as well as from an external seed rain. The seed bank is updated once a year. Here, our conceptual "seeds" represent opportunities for seedling recruitment at 1 cm dbh (henceforth denoted "reproduction opportunities") rather than as true seeds, since not all seed dispersal events are modelled explicitly, and the seed-to-seedling transition is implicit.

In TROLL 4.0 trees are assumed to become fertile above a diameter threshold $\mathrm{dbh_{mature}}$ that depends on the tree maximum size (Visser et al., 2016) as follows.

$$\mathrm{dbh_{mature}} = 0.5 \times \mathrm{dbh_{thresh}} \tag{63}$$

This relationship is drawn from direct observations of the reproductive status of tree species in the tropical forest of Barro Colorado Island, Panama, with maximal tree dbh spanning a range of 0.05 to 2 m (see Fig. S9 in Visser et al., 2016; $R^2 = 0.81$, $n = 60$ species). The number of reproduction opportunities per mature tree, n_s, is assumed to be fixed and equal for all individuals, and its value is user-defined. This assumption of a fixed reproductive opportunity per tree is predicated on the fact that there is a trade-off between seed number and seed size, itself related to seed and seedling survival. Thus, the probability of germination does not depend strongly on seed size or on the number of produced seeds and can be assumed to be a zero-sum game (Coomes and Grubb, 2003; Moles et al., 2004; Moles and Westoby, 2006). Each of the n_s events is scattered away from the tree in a random direction and at a distance randomly drawn from a Rayleigh distribution, thus allowing for potential long-dispersal events. Although seed dispersal distance is known to vary depending on dispersal syndrome and plant traits (Tamme et al., 2014; Seidler and Plotkin, 2006; Muller-Landau et al., 2008), the scale parameter σ_{disp} of the distribution is fixed here across species and individuals.

The intensity of the external seed rain is quantified by N_{tot} (number of incoming seeds per hectare) and its species composition is defined by the relative abundances of species $f_{\text{reg},s}$, both being user-defined. Hence, for each species s, $n_{\text{ext},s}$ events of dispersal due to seeds immigrating from the outside occurred, with

$$n_{\text{ext},s} = N_{\text{tot}} \times f_{\text{reg},s} \times n_{\text{ha}}, \tag{64}$$

with n_{ha} being the number of hectares of the simulated plot. These reproduction opportunities are uniformly distributed within the simulated area.

If several species are competing for recruitment in a local seed bank, one of the species is picked at random as the winner out of all the seeds present, as in a lottery model (Chesson and Warner, 1981). The recruitment event occurs only if ground-level light availability is sufficiently high. To test if this condition is met, the seedling is first attributed individual trait values depending on the species-specific averages (see Sect. 2.4.1). These trait values are then used to determine the maximum LAI (LAI_{max}) the seedling would support under average environmental conditions, with LAI_{max} defined as the threshold beyond which the seedling leaf assimilation would be less than respiration (see Sect. 2.6.2). The seedling can be recruited if the site LAI at ground level is lower than LAI_{max}.

Water availability is also key to seedling performance (Engelbrecht et al., 2006; Johnson et al., 2017; Kupers et al., 2019); hence, TROLL 4.0 now implements an additional dependence of water availability on seedling establishment (Craine et al., 2012; Paine et al., 2018). Seedling recruitment is possible only if the top-layer soil water potential is less negative than half the turgor loss point ($\pi_{\text{tlp}}/2$). Such parameterization is motivated by the fact that, at turgor loss point, the seedlings would not germinate, and a certain level of turgor is needed for germination and growth (Bradford, 1990; Daws et al., 2008; Coussement et al., 2018; Hsiao, 1973; Fatichi et al., 2016).

If both conditions on light and water availability are met, the newly recruited tree is initialized with $\text{dbh} = 0.01$ m, a total leaf area of $\text{LA}_{\text{t}} = 0.25 \times \text{LA}_{\text{opt}}$ distributed across the three leaf age pools in proportion to their relative span ($\tau_{\text{young}}/\text{LL}$, $\tau_{\text{mature}}/\text{LL}$, $\tau_{\text{old}}/\text{LL}$; see Sect. 2.6.2), and a carbon storage compartment filled at half its maximum NSC_{r} (see Sect. 2.6.3).

The assumptions here made on tree reproduction largely reflect limited knowledge of these processes, which remain major sources of uncertainty in current models (König et al., 2022; Hanbury-Brown et al., 2022; Díaz-Yáñez et al., 2024).

2.7.2 Mortality

Mortality processes also play a key role in forest structure and carbon balance (Sevanto et al., 2014; Friend et al., 2014; Johnson et al., 2016; Esquivel-Muelbert et al., 2020; McDowell et al., 2022). TROLL 4.0 explicitly represents several important mechanisms of tree mortality. At each time step, the individual tree death rate (in events per year; Sheil et al., 1995) is

$$d = d_{\text{b}} + d_{\text{starv}} + d_{\text{treefall}} + d_{\text{drought}}, \tag{65}$$

where d_{b} is a background death rate, d_{starv} represents death due to carbohydrate shortage (carbon starvation), d_{treefall} represents death due to tree fall (including trees indirectly killed by neighbouring fallen trees), and d_{drought} the drought-induced tree mortality.

Background mortality d_{b} encapsulates death events that are not attributed to any specific mechanism in the model. The mortality rate is known to vary greatly among species, and here we assume that it is negatively correlated with tree wood density, as observed pan-tropically (King et al., 2006; Kraft et al., 2010; Poorter et al., 2008; Wright et al., 2010). This dependence illustrates a trade-off between investment in construction costs and risk of mortality (Chave et al., 2009). We assumed the following relationship:

$$d_{\text{b}} = m \times \left(1 - \frac{\text{wsg}}{\text{wsg}_{\text{lim}}}\right), \tag{66}$$

where m (in events per year) is the reference background mortality rate for a species with low wood density and is user-specified. wsg_{lim} is a value large enough so that d_{b} always remains positive (here set at $1\ \text{g cm}^{-3}$).

A tree can also die because of carbohydrate shortage in the case of prolonged stress (d_{starv} in Eq. 51). In TROLL 4.0, which includes an explicit carbohydrate storage compartment, the tree dies of carbon starvation when this compartment is empty and $\text{NPP}_{\text{ind}} \leq 0$ (Eq. 51).

Tree death may be caused by tree falls (term d_{treefall} in Eq. 65). To simulate this process, we first define a stochas-

tic threshold Θ, depending on the tree maximal height and prescribed at tree birth. Then, the tree can fall with a probability equal to $1 - \frac{\Theta}{h}$ (Chave, 1999) each month. As TROLL 4.0 uses a daily time step, this probability is uniformly distributed across the days of 1 month. The parameter Θ is computed for each tree, as follows:

$$\Theta = h_{\max} \times (1 - v_{\mathrm{T}} \times |\zeta|), \tag{67}$$

where $h_{\max}$ is maximal tree height (i.e. the tree height computed using Eq. 16 at $\mathrm{dbh}_{\max}$), and v_{T} is a variance term, $|\zeta|$ is the absolute value of a random Gaussian variable with zero mean and unit standard deviation. v_{T} is modified at tree level so that high risks of tree fall ($>$ 99.5th percentile of the Gaussian variable) occur at the same height for all individuals of the same species. This implicitly introduces a growth–mortality trade-off, as more slender trees (larger ratio of height to trunk diameter) should reach this height threshold quicker. The orientation of tree falls is random. Trees on the trajectory of the falling tree can be damaged, especially if they are smaller than the fallen tree (van der Meer and Bongers, 1996). To model this effect, an individual variable *hurt* is defined. If a tree is within the trajectory of the fallen stem or of the fallen crown, its variable hurt is updated to h and $\frac{h-\mathrm{CR}}{2}$, respectively, if it was lower, where h and CR are the tree height and crown radius of the fallen tree, respectively. The probability of dying due to another tree fall is then $1-\frac{1}{2}\frac{h}{\mathrm{hurt}\times e^{\varepsilon_{h,j}}}$, where h is the height of the focal tree and $e^{\varepsilon_{h,j}}$ (see Eq. 16) accounts for the fact that slender individuals (higher tree height deviation) would be more vulnerable to tree fall. Such a tree can either fall and damage other trees itself or die standing, depending on the user choice. The hurt variable is reset to zero at each time step.

Finally, prolonged drought is also a source of mortality. Drought-induced mortality is triggered when the leaf predawn water potential ψ_{pd} is below a lethal level (ψ_{lethal}), and ψ_{lethal} is computed from the leaf water potential at turgor loss point, using the relationship provided by the global meta-analysis of Bartlett et al. (2016b; $P = 0.03$, $R^2 = 0.31$, $n = 15$ species from tropical dry and moist biomes), as follows.

$$\psi_{\mathrm{lethal}} = -0.9842 + 3.1795 \times \pi_{\mathrm{tlp}} \tag{68}$$

3 Modelling protocol

3.1 Model inputs

TROLL 4.0 requires five input files to run a simulation: (i) global parameters, (ii) species parameters, (iii) soil characteristics, and finally, meteorological drivers varying at (iv) half-hour and (v) daily steps.

The global input file contains parameters that define the simulation set-up (e.g. the number of time steps, the size of the simulated plot and of the belowground voxels) and values for biophysical parameters that remain constant throughout the simulation and are not species- or tree-specific. These include the light attenuation coefficient, allocation parameters, minimal death rate, and more (see Table A1). Parameter values can be varied across simulations to test model sensitivity, transfer across sites, or any other reason. The species input file contains mean functional traits for at least one species and with no upper bound (see Table A1). Functional trait values can be prescribed from local field measurements or retrieved from global trait databases (e.g. Kattge et al., 2020; Díaz et al., 2022).

The soil input file contains the soil variables needed for the pedotransfer functions, i.e. soil texture (proportion of silt, clay, and sand), soil organic matter content, dry bulk density, soil pH, and cation exchange capacity, for each soil layer, with the thickness of each layer. The number of soil layers is at least one and is not theoretically limited. Lacking local soil data, model users may retrieve soil parameters from online databases (e.g. Poggio et al., 2021), bearing in mind the uncertainties of such products, especially in tropical areas (Khan et al., 2024).

Meteorological drivers are provided in two files, depending on their temporal resolution in the model. Daytime temperature, vapour pressure deficit, incident irradiance, and wind speed at a reference height above the canopy are provided for every half-hour, while average nighttime temperature and cumulative rainfall are provided at a daily time step. Such data can typically be retrieved from meteorological stations embedded in eddy flux towers or from global products (Muñoz-Sabater et al., 2021), as in Schmitt et al. (2023).

3.2 Initial conditions

Two types of initial conditions are useful in most practical settings and are implemented in TROLL 4.0. First, the user can simulate forest regeneration from bare ground. In this case, forest succession is initiated by the external seed rain, the composition and intensity of which are user-defined (see above). The steady-state forest composition and structure are thus emergent properties of the community assembly mechanisms embedded in the model and the user-specified seed rain. The second option is to prescribe an initial forest state. This requires an initial forest state to be provided as an additional input file. The code is designed to adapt to the level of information provided by the inventory file, from a minimal requirement of tree dbh to the full list of individual variables for each tree. For individual variables missing in the input file, these are either computed from the model relationships or drawn at random. This second initial condition matches a real site forest state given the available data but will require careful calibration to maintain the forest state over a longer time period (e.g. Fischer et al., 2020). A more common use case is to restart new simulations from an output of a previous simulation, e.g. to perform virtual experiments controlling the initial state.

3.3 Standard outputs

TROLL 4.0 provides a range of outputs related to forest structure, forest composition and diversity, and ecosystem functioning (e.g. carbon and water fluxes; Fig. 5). It simulates forest structure and composition and provides outputs comparable to those measured in the field: tree size distribution, tree spatial distribution, biomass accumulation curve, functional trait distribution, canopy height and leaf area index maps (Maréchaux and Chave, 2017), and more generally all information that can be retrieved from a detailed field inventory or a metre-scale airborne laser scanning survey (Fischer et al., 2019). In TROLL 4.0, other outputs are also available: litterfall fluxes, carbon and water fluxes comparable to the ones provided by eddy flux towers, and soil water state (content and water potential). An evaluation of these outputs for two Amazonian forest sites is provided in a companion paper (Schmitt et al., 2025).

4 Discussion

TROLL 4.0 is part of a novel generation of forest growth models designed to bridge the gap between traditional forest growth models and process-based models informed by ecophysiology. It includes an integration of processes underlying ecosystem fluxes closer to a modern DGVM than most other forest growth simulators. It also includes representation of plant community structure and diversity at a resolution similar to that used by ecologists in the field. This enables a direct comparison with a range of field data, including forest inventories, trait distribution, fine- and large-scale remote sensing products, or eddy covariance data. Overall, these different features allow it to address a range of questions, from fundamental ones in community and theoretical ecology such as the mechanisms of species coexistence or the link between biodiversity and ecosystem functioning to more applied ones such as the design of forest management guidelines to sustain forest resilience under climate change. Here we discuss the assumptions of the water cycle newly included in the model, as well as transferability and limitations of the current model version.

4.1 Simulating water fluxes and forest responses to water availability

Previous versions of TROLL assume that water availability does not limit ecosystem fluxes and dynamics, a strong but reasonable assumption in a light-limited forest like in eastern Amazonia (Guan et al., 2015; Wagner et al., 2016; Maréchaux and Chave, 2017). However, such a simplification does not allow accounting for drought-induced interannual variability in forest dynamics (Bonal et al., 2008; Aguilos et al., 2018; Leitold et al., 2018) or transferring the model to sites where water availability is limiting. As droughts will be important drivers for tropical ecosystems in the future (Duffy et al., 2015), such a simplification does not allow projecting future states of forest under climate change.

In TROLL 4.0, we implemented a full water cycle. We introduced a belowground field with a hydraulic state coupled to the vegetation and a representation of the response of leaf gas exchanges to local atmospheric conditions and their control by the leaf boundary layer. This detailed representation is commonplace in DGVMs (Prentice et al., 2007), but to our knowledge, it is new for an individual-based spatially explicit forest dynamic simulator. This paves the way for explorations and projections of the independent effects of soil water availability and atmospheric demand on ecosystem functioning (Novick et al., 2016; Santos et al., 2018), community composition, and structure (Esquivel-Muelbert et al., 2019; Fauset et al., 2012; Slik, 2004; Feeley et al., 2011).

These developments have striven to follow the parsimonious principle: more complex representations do not systematically result in increased model reliability and robustness, especially if the additional parameters are poorly constrained (Mahnken et al., 2022; Prentice et al., 2015). The soil hydraulic state is simulated using a bucket model (Budyko, 1961; Manabe, 1969; Vargas Godoy et al., 2021). In the future, more complex representations of soil water dynamics could be implemented at finer temporal and spatial resolutions, such as the implementation of Richards' equation (Richards, 1931), and integration of lateral flows, but this would be at a serious computational cost. These could be compared with the current simpler representation to assess the relevance of increasing complexity in various contexts and soil data availability (Van Nes and Scheffer, 2005). However, two aspects were considered to be needed in the current version based on biological considerations. First, we implemented a multi-layer soil model, a more detailed representation compared with other models using a bucket model approach (e.g. Fischer et al., 2014; Laio et al., 2001). This was motivated by the need to account for contrasting rooting strategies and access to water among coexisting plants, which is an underexplored, but likely key, aspect of community dynamics in forests (Brum et al., 2019; De Deurwaerder et al., 2018; Ivanov et al., 2012). Second, we assumed that the depth of tree water uptake is controlled not only by the distribution of root biomass (as in Naudts et al., 2015; Sakschewski et al., 2021; Paschalis et al., 2024), but also by soil water state and its vertical variation (as in Williams et al., 1996; Duursma and Medlyn, 2012). These improvements are relevant to the temporal variation of water retrieval depth (Bruno et al., 2006) and the sustained dry-season productivity in rainforest ecosystems (Restrepo-Coupe et al., 2017).

The control of leaf gas exchange by water availability has been implemented by means of multiplicative soil water stress factors. Although the use of such factors has been debated (Powell et al., 2013; Joetzjer et al., 2014) and may underestimate the reduction of gas exchanges at midday under high evaporative demand, it has been preferred over a more explicit representation of the water flow through the plant

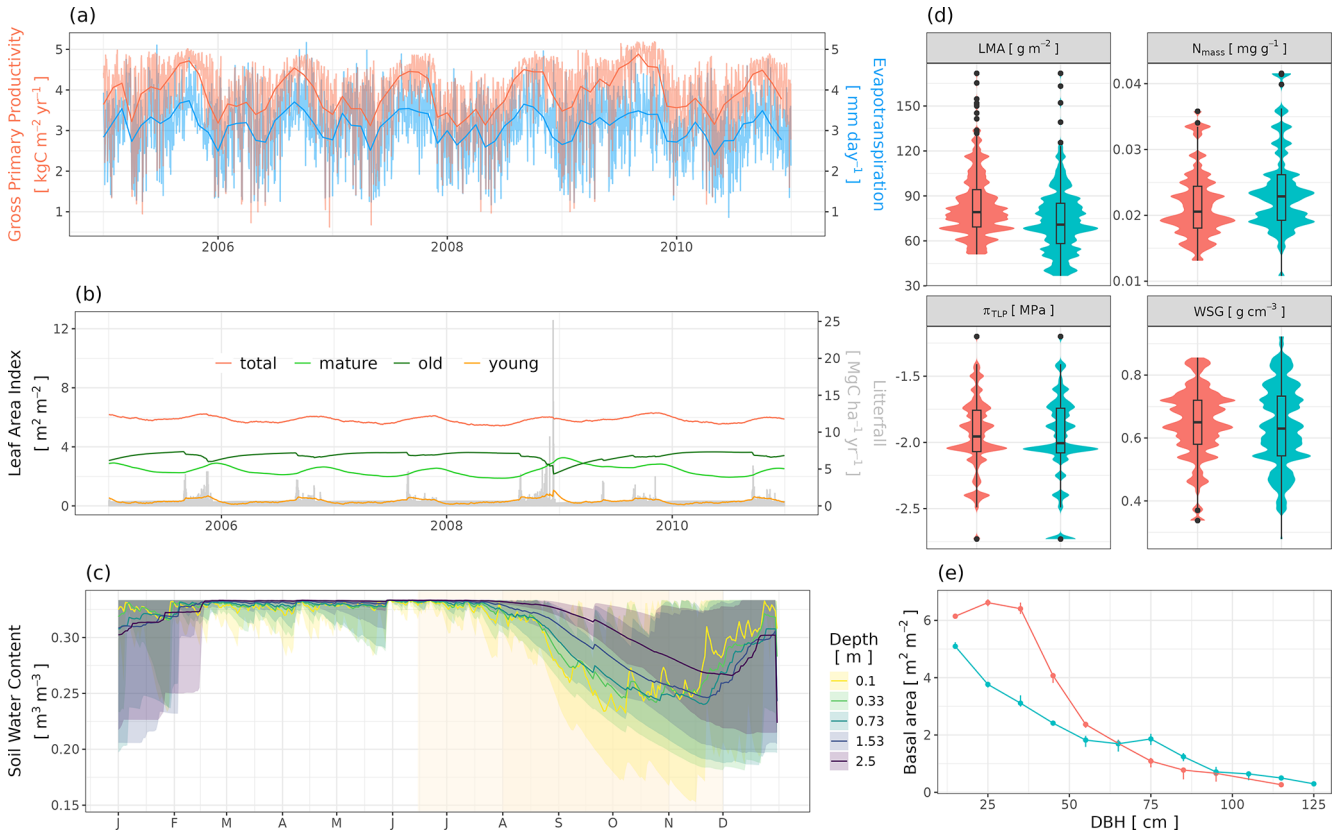

Figure 5. Examples of outputs provided by TROLL 4.0 related to ecosystem functioning, diversity, and structure. **(a)** Temporal variations of gross primary productivity (red) and evapotranspiration (blue) within and across years. **(b)** Variation in total leaf area index (red line) and leaf area index per leaf age cohort (young, mature, and old are represented by yellow, light green, and dark green lines, respectively), together with litterfall (grey bars), within and across years. **(c)** Mean seasonal variations of water content in soil layers of different depths, with the vertical yellow band in the background depicting the dry season. **(d)** Distribution of functional traits. **(e)** Distributions of basal area per diameter class. Panels **(a)**, **(b)**, and **(c)** show outputs for an Amazonian forest site (Paracou), and panels **(d)** and **(e)** show outputs for two Amazonian sites (Paracou, red; Tapajos, blue); see Schmitt et al. (2025) for details on simulation set-ups.

column (e.g. Yao et al., 2022; Christoffersen et al., 2016; Cochard et al., 2021; De Cáceres et al., 2023). Although the stem hydraulic traits that would be needed for parameterizing an explicit plant water flow module have been increasingly measured over the past decades, data availability for tropical tree species remains low in regards to the actual number of species coexisting in these communities. Alternatively, correlative relationships have been used to infer these traits from more easily measured traits (Christoffersen et al., 2016; Xu et al., 2016). However, these are context-dependent (Brodribb, 2017; Rosas et al., 2019) and have at best low statistical support in rainforest communities that are loosely constrained by water availability (Dwyer and Laughlin, 2017; Delhaye et al., 2020; Maréchaux et al., 2020). Innovative methods alleviate the difficulties of robustly measuring the vulnerability of tropical trees to embolism (Cochard et al., 2016; Sergent et al., 2020; Garcia et al., 2023), and this could provide a key motivation for a more explicit module of plant water flow in TROLL (Kennedy et al., 2019; Paschalis et al., 2024). Such developments could be necessary to correctly represent the legacy of drought in forest ecosystems (Paschalis et al., 2024; Anderegg et al., 2015). However, two important aspects were taken into account in the implementation of the multiplicative water stress factors in TROLL 4.0. These factors were parameterized based on soil water potential as an independent variable, and not soil water content, the former directly controlling water availability for plants, while the effect of soil water content is strongly mediated by soil properties (Novick et al., 2022). Also, different water stress factors were used for stomatal and non-stomatal limitations in order to capture the sequence of effects of decreasing water availability on plant function (Trueba et al., 2019; Fatichi et al., 2016; Hsiao, 1973).

The effects of water availability on plant function and tree demography were implemented through trait-based parameterization, which allows a range of responses between trees and species. This was made possible through the use of leaf water potential at turgor loss point (π_{tlp}), a leaf-level trait that

is mechanistically linked to plant responses to water availability (Bartlett et al., 2016b) and that is measurable at the community scale in diverse systems through a well-validated method (Maréchaux et al., 2016; Griffin-Nolan et al., 2019; Sun et al., 2020; Bartlett et al., 2012a). Leaf water potential at turgor loss point varies greatly across species within Amazonian forest communities (Maréchaux et al., 2015; Ziegler et al., 2019), and this diversity explains contrasting responses to water availability at the leaf and plant levels (Martin-StPaul et al., 2017; Maréchaux et al., 2018; Powell et al., 2017) and species distribution at local, regional, and global scales (Bartlett et al., 2016a; Baltzer et al., 2008; Lenz et al., 2006; Bartlett et al., 2012b). The relationships implemented here involving π_{tlp} have a mechanistic basis, as discussed above. However, the relationships controlling the effect of water availability on (1) leaf shedding, (2) seed germination and seedling recruitment, and (3) drought-induced mortality would deserve in-depth exploration. More generally, these three processes remain key aspects of community dynamics and ecosystem functioning in high need of sustained empirical investigation (Albert et al., 2019; Díaz-Yáñez et al., 2024; McDowell et al., 2022).

4.2 Model–data integration, transferability, and limitations

TROLL 4.0 simulates forest structure and diversity, while expanding the types of data with which its results can be compared (Schmitt et al., 2025). The individual-based species-specific representation of forest yields virtual forest inventories, including the location of each individual, their botanical identity, their dimensions, and virtual airborne laser scanning point clouds (Fischer et al., 2019; Schmitt et al., 2023). TROLL 4.0 additionally provides water, carbon, and litter flux dynamics that are directly comparable to eddy flux tower data and litter trap monitoring at fine temporal resolutions, and this specificity has numerous advantages.

The knowledge derived from field data can be directly assimilated into TROLL 4.0. As opposed to most DGVMs whose representation of vegetation does not allow this type of assimilation, this offers new perspectives for inference or calibration (Dietze et al., 2013; Fer et al., 2018; Hartig et al., 2012; LeBauer et al., 2013), which could help inform the development of DGVMs. For example, TROLL 4.0 may act as an integrator of data of different types, such as field inventories and remote sensing, to constrain allometries that would be biased or poorly grounded if relying on a unique data source (Fischer et al., 2019). Also, as many uncertainties in current DGVMs have been related to their aggregated representation of vegetation structure and biodiversity, TROLL 4.0 can be used to directly test the sensitivity of a range of processes shared with DGVMs to such representation, for example by performing simulations with different numbers and identities of species or spatial resolutions, to then inform DGVMs on the corresponding needed developments. TROLL 4.0 is also easy to use and test by field ecologists as it simulates trees, not cohorts, PFTs, or gap patches: it can reproduce classical experiments in community or ecosystem ecology (e.g. Crawford et al., 2021; Schmitt et al., 2020) while overcoming known empirical challenges such as low repeatability (Schnitzer and Carson, 2016) or limited spatial footprint (Estes et al., 2018). TROLL 4.0 can be compared with data under the control of different biophysical processes supporting a more robust evaluation and limiting equifinality issues (Franks et al., 1997; Medlyn et al., 2005). Finally, the model is parameterized based on traits directly measured in the field, improving model transferability (Rau et al., 2022a).

The individual-scale and spatially explicit representation of TROLL 4.0 comes with a computational burden. For a reference 4 ha area starting from bare ground and 600 years of simulation on a single CPU, the computational cost of TROLL 4.0 is about 1820 min compared with TROLL 2.3 (Maréchaux and Chave, 2017) of about 12 min. While the shift from a monthly to a daily time step explains the multiplication by a factor of 30 between the two versions, the addition of a belowground field and an iterative scheme to simulate leaf gas exchanges explains to a great extent the remaining factor of 5. Several developments should reduce this computational cost: tree demographic processes do not need to be simulated at the daily time step and could be represented at a monthly resolution; vegetation models already implement such nested timescales (Moorcroft, 2006). We are also confident that further computer time reduction will be brought about by code optimization. Finally, several strategies can be implemented to up-scale the outputs of individual-based models at reduced computational costs, especially by leveraging large-scale remote sensing products (Rödig et al., 2017; Sato et al., 2007; Shugart et al., 2015).

4.3 Current and future developments

TROLL 4.0 aims to reflect the state of the art in plant physiology and ecology and, as a result, reflects the corresponding knowledge gaps, which can lead to an unbalanced representation across processes. TROLL is being continuously developed, as knowledge and data availability progress, specific questions to address with the model emerge, or important limitations are identified. In a companion paper (Schmitt et al., companion paper), we use data from forest inventories, litter traps, eddy flux towers, and remote sensing products to evaluate and discuss the performance and limitations of TROLL 4.0 at two forest sites. We mention several ongoing or future developments here.

Empirical findings suggest that the contribution of undisturbed tropical forests to the global carbon sink is declining (Hubau et al., 2020; Qie et al., 2017), pointing to the need for integrated modelling to understand and predict such trends (Yao et al., 2023, 2024; Koch et al., 2021). Among the possible steps forward with TROLL 4.0 are an improved representation of stomatal conductance and its coupling with pho-

tosynthesis (Lamour et al., 2022; Dewar et al., 2018), as well as respiration response and acclimation to climatic drivers (Smith and Dukes, 2013; Collalti et al., 2020; Slot et al., 2013; Rowland et al., 2015). This notably includes the integration of light-driven plasticity in leaf traits, which has been recently highlighted as an important model development to robustly up-scale leaf-level gas exchange into ecosystem-level water and carbon balance (Fisher and Koven, 2020; Lamour et al., 2023b; Xu et al., 2021; Xu and Trugman, 2021). Improvements on the carbon budget would also be important, with more explicit carbon allocation to respiration, reproductive organs, and belowground structures, under the control of environmental drivers (Fig. 3). However, such developments would rely on limited empirical or experimental knowledge belowground (Cusack et al., 2024) and scarce information on tree reproductive strategies (Igarashi et al., 2024; Vacchiano et al., 2018; Norden et al., 2007). An improved representation and evaluation of drought-induced tree mortality would be another important step forward as it might play a key role in the observed changing dynamics and functional and floristic turnover (Esquivel-Muelbert et al., 2019; Feeley et al., 2011; Hubau et al., 2020; Qie et al., 2017). Information provided by long-term throughfall exclusion experiments would offer interesting opportunities for model development and evaluation (Powell et al., 2013; Yao et al., 2022).

Tropical forest disturbance by land use change, fire regimes, and other degradations is an important source of carbon emissions (Lapola et al., 2023) and must be represented in models. For instance, it is important to understand how edge effects affect the forest micro-climate and consequently forest dynamics, functioning, and composition (Camargo and Kapos, 1995; Nunes et al., 2022). To this end, micro-climate models could be coupled to or embedded within TROLL (Gril et al., 2023a; Maclean and Klinges, 2021). Fragmentation also impacts seed dispersal and thus seed rain and seed bank intensity and composition (Warneke et al., 2022; Cubiña and Aide, 2001). Improving TROLL's representation of seed dispersal ability and germination as a function of plant trait and dispersal mode is key to capturing the effect of forest loss and fragmentation on forest functioning and biodiversity (Seidler and Plotkin, 2006; Muller-Landau et al., 2008; Tamme et al., 2014; Chase et al., 2020; Riva and Fahrig, 2023). More generally, one overarching objective is to improve the model's representation of processes involved in forest regeneration to simulate secondary forest dynamics and resilience to disturbances (Hanbury-Brown et al., 2022; Díaz-Yáñez et al., 2024; Poorter et al., 2023; Albrich et al., 2020).

Finally, TROLL 4.0 includes major developments that should facilitate its transferability across sites. The explicit integration of the ecosystem water balance and vegetation responses to soil water availability now allows it to consider spatio-temporal extrapolation along water stress gradients. The integration of soil topography and heterogeneity would also be an important advance for improved generality. As nutrient availability is being altered by human activities (Peñuelas et al., 2013), the explicit integration of a nutrient cycle with nitrogen and phosphorous co-limitation will be a useful advance in the future (Fernández-Martínez et al., 2014; Turner et al., 2018). Similarly, the extension of tree functioning responses to a broader range of temperatures should support the transferability of TROLL to temperate and boreal forests.

5 Conclusions

TROLL 4.0 represents an advance over previous versions as it bridges forest model types, while maintaining a representation consistent with field ecology and ecosystem science. TROLL 4.0 simulates the responses of tropical forests to water availability through the explicit representation of water dynamics belowground and its coupling with leaf-level gas exchanges and demographic processes. This comes at a computational cost, and a future task is to conduct code optimization and parallelization, as well as up-scaling in combination with remote sensing products. The representation of processes in TROLL 4.0 mirrors an unbalanced state of the art, but its ability to dialogue with a range of data of various nature makes it a valuable tool to take up the fundamental and applied research challenges on tropical forests. TROLL 4.0 has benefited from observations and field experiments that feed the development of models (Medlyn et al., 2015; Paschalis et al., 2020), while modelling exercises inform and guide empirical approaches (Medlyn et al., 2016; Norby et al., 2016; Pacala and Rees, 1998). This is possible because of the fine-scale representation of forest structure and diversity and the trait-based parameterization of processes in the model.

Appendix A

Table A1. List of symbols and variables.

Symbols	Definition	Units	Nature	Equations
Physical constants				
M_w	Molar mass of water vapour	$kg\,mol^{-1}$	Constant	(12)
R	Ideal gas constant	$J\,mol^{-1}\,K^{-1}$	Constant	(12)–(13), (28)–(31), (46)–(47)
V_w	Partial molal volume of water	$m^3\,mol^{-1}$	Constant	(13)
κ	von Kármán constant	unitless	Constant	(8), (15)
g	Gravity constant	$m\,s^{-2}$	Constant	(37)
ρ	Density of water	$kg\,m^{-3}$	Constant	(37)
M_a	Molecular mass of air	$kg\,mol^{-1}$	Constant	(41), (48)
C_p	Heat capacity of air	$J\,kg^{-1}\,K^{-1}$	Constant	(41), (48)
γ	Psychrometric constant	$Pa\,K^{-1}$	Constant	(41)
D_H	Molecular diffusivity to heat	$m^2\,s^{-1}$	Constant	(46)
σ	Stefan–Boltzmann constant	$W\,m^{-2}\,K^{-4}$	Constant	(44), (48)
Aboveground environment				
$PPFD_{top}$	Photosynthetic photon flux density at canopy top	$\mu mol\ photons\ m^{-2}\,s^{-1}$	Updated at half-hourly step, given as input	(1)
T_{top}	Temperature at canopy top	°C	Updated at half-hourly step, given as input	(4), (6), (44)
VPD_{top}	Vapour pressure deficit at canopy top	kPa	Updated at half-hourly step, given as input	(5), (7)
u_{top}	Wind speed at a reference height above the canopy	$m\,s^{-1}$	Updated at half-hourly step, given as input	Sect. 2.1 and 2.2
T_{night}	Nighttime temperature	°C	Updated daily, given as input	Sect. 2.2
PPFD	Incident photosynthetic photon flux density	$\mu mol\ photons\ m^{-2}\,s^{-1}$	Computed every half-hour	(1), (25)
T	Temperature	°C	Computed every half-hour	(4), (42), (46)–(48)
VPD	Vapour pressure deficit	kPa	Computed every half-hour	(5)
u	Wind speed	$m\,s^{-1}$	Computed every half-hour	(8), (9), (15), (47)
c_a	CO_2 concentration	$\mu mol\,mol^{-1}$ (ppm)	Constant	Sect. 2.5
P_{ress}	Atmospheric pressure	Pa	Constant	(46)–(47)
$PPFD_{abs}$	Absorbed photosynthetic photon flux density	$\mu mol\ photons\ m^{-2}\,s^{-1}$	Computed every half-hour	(2)
T_{mean}	Temperature, averaged per crown layer	°C	Computed every half-hour	(6)
VPD_{mean}	Vapour pressure deficit, averaged per crown layer	kPa	Computed every half-hour	(7)
LAI	Cumulated leaf area per ground area	$m^2\,m^{-2}$	Computed daily for each voxel	(1)–(3), (11), (43)
dens	Averaged leaf area density per unit ground area	$m^2\,m^{-2}$	Computed daily, averaged per layer	(3), (6)–(7)
k	Effective light extinction coefficient	unitless	Fixed, computed from k_{geom} and $absorptance_{leaves}$	(1)
k_{geom}	Light extinction coefficient reflecting the geometric arrangement of leaves	unitless	Constant, given as input	(1)

Table A1. Continued.

Symbols	Definition	Units	Nature	Equations
Physical constants				
$\text{absorptance}_{\text{leaves}}$	Fraction of absorbed light within a single leaf	unitless	Constant, given as input	(1)
LAI_{sat}	LAI threshold for computing micro-environmental variation within the canopy	$\text{m}^2\ \text{m}^{-2}$	Constant	(4)–(7)
ΔT	Parameter of the within-canopy variation in temperature	°C	Constant	(4), (6)
C_{VPD0}	Parameter of the within-canopy variation in vapour pressure deficit	unitless	Constant	(5), (7)
u^*	Friction velocity	m s^{-1}	Constant	
d	Zero-plane displacement height	m	Computed from the locally averaged canopy height (H)	(8)
z_0	Aerodynamic roughness	m	Computed from the locally averaged canopy height (H)	(8)
H	Top canopy height	m	Computed daily	(8)–(9)
α	Parameter of wind speed decrease within the canopy	unitless	Constant	(9)
Water balance				
P	Precipitation	mm	Updated daily, given as input	(10)
I	Interception	mm	Computed daily	(10), (11)
Q	Run-off	m^3	Computed daily	(10)
E	Evaporation from the soil	$\text{kg m}^{-2}\ \text{s}^{-1}$	Computed daily	(10), (12)
T	Tree transpiration	m^3	Computed daily	(10)
L	Leakage	m^3	Computed daily	(10)
K	Parameter for rainfall interception	mm	Constant	(11)
T_{s}	Temperature at soil surface	K	Computed daily	(12), (13)
e_{s}	Vapour pressure of the soil surface	Pa	Computed daily	(12)
e_{a}	Vapour pressure of air above the soil surface	Pa	Computed daily	(12)
e_{sat}	Saturated vapour pressure	Pa	Computed daily	(13)
r_{soil}	Soil surface resistance	s m^{-1}	Computed daily	(12), (14)
r_{aero}	Aerodynamic resistance to heat transfer	s m^{-1}	Computed daily	(12), (15)
Z	Reference height for r_{aero} computation	m	Constant	(15)
Z_{m}	Momentum soil roughness	m	Constant	(15)
ψ_l	Soil water potential of layer l	MPa	Computed daily	(21)
K_l	Soil hydraulic conductivity of layer l	$\text{kg m}^{-2}\ \text{s}^{-1}$	Computed daily	(22)
$\psi_{\text{soil, top}}$	Water potential of the topsoil belowground voxel	MPa	Computed daily	(13)
θ_{top}	Water content of the topsoil belowground voxel	m^3	Computed daily	(14)
$\theta_{\text{fc, top}}$	water content at field capacity of the topsoil belowground voxel	m^3	Computed daily	(14)

Table A1. Continued.

Symbols	Definition	Units	Nature	Equations
Species and tree characteristics				
LMA	Leaf mass per area	$g\,m^{-2}$	Species-specific means: constant, provided as input; tree-specific values: randomly attributed at tree birth	(26), (27), (32), (56)
LA	Leaf area	cm^2	Species-specific means: constant, provided as input; tree-specific values: randomly attributed at tree birth	(46)–(47)
N	Leaf nitrogen content per dry mass	$mg\,g^{-1}$	Species-specific means: constant, provided as input; tree-specific values: randomly attributed at tree birth	(26), (27), (32)
P	Leaf phosphorous content per dry mass	$mg\,g^{-1}$	Species-specific means: constant, provided as input; tree-specific values: randomly attributed at tree birth	(26), (27), (32)
wsg	Wood specific gravity	$g\,cm^{-3}$	Species-specific means: constant, provided as input; tree-specific values: randomly attributed at tree birth	(36), (55), (60)–(61), (66)
π_{tlp}	Leaf water potential at turgor loss point	MPa	Species-specific means: constant, provided as input; tree-specific values: randomly attributed at tree birth	(39)–(40), (58), (68), Sect. 2.7.1
dbh_{thres}	Threshold diameter at breast height, beyond which growth senescence starts	m	Species-specific means: constant, provided as input; tree-specific values: randomly attributed at tree birth	(62), (63)
dbh_{max}	Maximal tree diameter at breast height	m	Computed once per tree	Sect. 2.6.4
h_{lim}	Asymptotic height (parameter of the Michaelis–Menten function)	m	Species-specific means: constant, provided as input	(16)
h_{max}	Maximal tree height	m	Species-specific means: constant, provided as input	(67)
a_h	Parameter of the Michaelis–Menten function	m	Species-specific means: constant, provided as input	(16)
$f_{reg,s}$	Relative abundance of species s in the external seed rain	unitless	Species-specific, provide as input	(64)
w_l	Leaf width	m	Computed for each tree	(46)–(47)
LL	Leaf lifespan	year	Computed for each tree	(57)
$\varepsilon_{i,j}$	Individual effects for trait or variable i and tree j	See traits	Randomly attributed at tree birth	Sect. 2.4.1 and 2.4.2
σ_i	Standard deviation for intraspecific variability in trait or variable i	See traits	Constant, provided as input	Sect. 2.4.1 and 2.4.2
dbh	Tree diameter at breast height	m	Tree variable, updated at each time step	(16), (17), (19), (60)–(62)
h	Tree height	m	Tree variable, updated at each time step	(16), (37), (54)–(55), (58), (60)
cr	Tree crown radius	m	Tree variable, updated at each time step	(17)
cd	Tree crown depth	m	Tree variable, updated at each time step	(18), (54)
a_{cr}	Coefficients of crown radius allometry	unitless	Species-independent constant, provided as input	(17)
b_{cr}	Coefficients of crown radius allometry	unitless	Species-independent constant, provided as input	(17)
a_{cd}	Coefficients of crown depth allometry	m	Species-independent constant, provided as input	(18)
b_{cd}	Coefficients of crown depth allometry	unitless	Species-independent constant, provided as input	(18)

Table A1. Continued.

Symbols	Definition	Units	Nature	Equations
shape_crown	Ratio between the radius of the crown at the top of the tree to the radius at the bottom of the crown being a global parameter	unitless	Global parameter, provided as input	Sect. 2.4.2
f_{gap}	Fraction of gaps (openings) in tree crowns	unitless	Constant, provided as input	Sect. 2.4.2
RD	Tree root depth	m	Tree variable, updated at each time step	(19)
RB_t	Total tree fine root biomass	g	Tree variable, updated at each time step	(20)
RB_l	Tree fine root biomass in layer l	g	Tree variable, updated at each time step	(20)
ψ_{root}	Soil water potential in the tree root zone	MPa	Tree variable, updated at each time step	(21), (37)
$\psi_{R,min}$	Root water potential below which there is no soil water uptake	MPa	Constant	(21)
G_l	Soil-to-root water conductance in layer l	$mmol\,H_2O\,m^{-2}\,s^{-1}\,MPa^{-1}$	Variable, computed for each tree and layer at each time step	(21), (22)
$L_{a,l}$	Tree total root length per unit area in layer l	$m\,m^{-2}$	Variable, computed for each tree and layer at each time step	(22)
$L_{v,l}$	Tree total root length per unit soil volume in layer l	$m\,m^{-3}$	Variable, computed for each tree and layer at each time step	(23)
SRL	Specific root length	$m\,g^{-1}$	Constant	(22)
r_s	Mean fine root radius	m	Constant	(22)
r_s	Half of the mean distance between roots	m	Variable, computed for each tree and layer at each time step	(22), (23)
Leaf physiology				
T_l	Leaf temperature	°C	Computed half-hourly for each crown layer	(24), (25), (28)–(31), (33), (46)
VPD_s	Vapour pressure deficit at the leaf surface	kPa	Computed half-hourly for each crown layer	(35)
c_s	CO_2 concentration at the leaf surface	$\mu mol\,mol^{-1}$ (ppm or µbar)	Computed half-hourly for each crown layer	(34)
c_i	CO_2 concentration at carboxylation sites	$\mu mol\,mol^{-1}$ (ppm or µbar)	Computed half-hourly for each crown layer	(24), (34)
A_n	Leaf-level net carbon assimilation rate	$\mu mol\,CO_2\,m^{-2}\,s^{-1}$	Computed half-hourly for each crown layer	(24), (52)
A_v	Leaf-level net carbon assimilation rate limited by Rubisco activity	$\mu mol\,CO_2\,m^{-2}\,s^{-1}$	Computed half-hourly for each crown layer	(24)
A_j	Leaf-level net carbon assimilation rate limited by RuBP regeneration	$\mu mol\,CO_2\,m^{-2}\,s^{-1}$	Computed half-hourly for each crown layer	(24)
R_p	Photorespiration rate	$\mu mol\,C\,m^{-2}\,s^{-1}$	Computed half-hourly for each crown layer	(24)
R_d	Leaf dark respiration rate	$\mu mol\,C\,m^{-2}\,s^{-1}$	Computed half-hourly for each crown layer	(33)
R_{d-M}	Leaf dark respiration rate on a leaf dry mass basis	$nmol\,CO_2\,g^{-1}\,s^{-1}$	Computed half-hourly for each crown layer	(32)

Table A1. Continued.

Symbols	Definition	Units	Nature	Equations
V_{cmax}	Maximum rate of carboxylation	µmol CO_2 m^{-2} s^{-1}	Computed half-hourly for each crown layer	(24), (26), (28)
$V_{cmax\text{-}M}$	Maximum rate of carboxylation on a leaf dry mass basis	µmol CO_2 g^{-1} s^{-1}	Computed half-hourly for each crown layer	(26)
J	Electron transport rate	µmol e^- m^{-2} s^{-1}	Computed half-hourly for each crown layer	(24), (25)
J_{max}	Maximal electron transport capacity	µmol e^- m^{-2} s^{-1}	Computed half-hourly for each crown layer	(25), (29)
J_{max-M}	Maximal electron transport capacity on a leaf dry mass basis	µmol e^- g^{-1} s^{-1}	Computed half-hourly for each crown layer	(27)
Γ^*	CO_2 compensation point in the absence of dark respiration	µbar	Computed half-hourly for each crown layer	(24), (30)
K_m	Apparent kinetic constant of the Rubisco	µbar	Computed half-hourly for each crown layer	(24), (31)
θ	Curvature factor	unitless	Constant	(25)
α	Apparent quantum yield to electron transport	mol e^- mol photons^{-1}	Constant	(25)
LSQ	Effective spectral quality of light	unitless	Constant	(25)
g_s	Stomatal conductance to CO_2	mol CO_2 m^{-2} s^{-1}	Computed half-hourly for each crown layer	(34)
g_{sw}	Stomatal conductance to water vapour	mol H_2O m^{-2} s^{-1}	Computed half-hourly for each crown layer	(35)
g_0	Minimum leaf conductance for water vapour	mol H_2O m^{-2} s^{-1}	Constant, provided by the user	(35)
g_1	Parameter of the stomatal conductance model	$kPa^{0.5}$	Computed daily for each tree	(35), (36)
ψ_{pd}	Leaf pre-dawn water potential	MPa	Tree variable, computed daily	(24), (25), (28), (29), (36)–(40)
WSF_{ns}	Water stress factor for non-stomatal limitation	unitless	Tree variable, computed daily	(28), (29), (40)
WSF_s	Water stress factor for stomatal limitation	unitless	Tree variable, computed daily	(36), (38)–(39)
a	Parameter of WSF_{ns}	unitless	Constant	(40)
b	Parameter of WSF_s	unitless	Computed from tree-specific ψ_{tlp}	(38), (39)
E_l	Leaf-level transpiration rate	mol H_2O m^{-2} s^{-1}	Computed half-hourly for each crown layer	(41)
λ	Latent heat of water vapour	J mol^{-1}	Computed half-hourly for each crown layer	(41), (42)
s	Slope of the (locally linearized) relationship between saturated vapour pressure and temperature	Pa K^{-1}	Computed half-hourly for each crown layer	(41)
R_{ni}	Isothermal net radiation	J m^{-2} s^{-1}	Computed half-hourly for each crown layer	(41), (43)
g_H	Total leaf conductance to heat	mol m^{-2} s^{-1}	Computed half-hourly for each crown layer	(41), (45)
g_{bHf}	Boundary layer conductance for free convection	mol m^{-2} s^{-1}	Computed half-hourly for each crown layer	(45), (46), (50)
g_{bHu}	Boundary layer for forced convection	mol m^{-2} s^{-1}	Computed half-hourly for each crown layer	(45), (47), (50)

Table A1. Continued.

Symbols	Definition	Units	Nature	Equations
g_r	Radiation conductance	$mol\,m^{-2}\,s^{-1}$	Computed half-hourly for each crown layer	(45), (48)
g_w	Total leaf conductance to water vapour	$mol\,H_2O\,m^{-2}\,s^{-1}$	Computed half-hourly for each crown layer	(41), (49)
g_{bw}	Boundary layer conductance to water vapour	$mol\,H_2O\,m^{-2}\,s^{-1}$	Computed half-hourly for each crown layer	(49), (50)
S_{abs}	Absorbed solar radiation (PAR and NIR)	$J\,m^{-2}\,s^{-1}$	Computed half-hourly for each crown layer	(43)
$B_{n,0}$	Net longwave radiation at the top of the canopy	$J\,m^{-2}\,s^{-1}$	Computed every half-hour	(43), (44)
k_d	Coefficient of extinction of longwave radiation	Unitless	Constant	(43)
ε_l	Emissivity of the canopy leaves	Unitless	Constant	(44), (48)
ε_a	Emissivity of the atmosphere	Unitless	Computed every half-hour	(44)
Tree carbon allocation and demography				
GPP_{ind}	Tree-level gross primary productivity	gC	Computed daily	(51)
NPP_{ind}	Tree-level net primary productivity	gC	Computed daily	(51)
NPP_{leaves}	Tree-level net primary productivity allocated to leaf production	gC	Computed daily	(56)
NPP_{wood}	Tree-level net primary productivity allocated to woody growth	gC	Computed daily	(61)
AGB	Tree aboveground biomass	kg	Computed daily	(59)–(60)
$R_{maintenance}$	Tree-level maintenance respiration	gC	Computed daily	(51)
R_{stem}	Stem maintenance respiration	$\mu mol\,C\,s^{-1}$	Computed daily	(54)
R_{growth}	Tree-level growth respiration	gC	Computed daily	(51)
LA_t	Tree-level total leaf area	m^2	Updated daily	(55)
LA_{opt}	Optimal tree leaf area	m^2	Updated daily	Sect. 2.6.2
LA_l	Leaf area in tree crown layer l	m^2	Updated daily	(51), (52)–(53)
LA_{young}	Tree-level young leaf area	m^2	Updated daily	(52)–(53), (56)
LA_{mature}	Tree-level mature leaf area	m^2	Updated daily	(52)–(53), (56)
LA_{old}	Tree-level old leaf area	m^2	Updated daily	(52)–(53), (56)
ϱ	Ratio of young or old leaf assimilation rate over mature leaf assimilation rate	unitless	Constant	(52)
ϱ'	Ratio of young or old leaf respiration rate over mature leaf respiration rate	unitless	Constant	(53)
τ_{young}	Leaf residence time in the young age pool	year	Computed for each tree	(56)
τ_{mature}	Leaf residence time in the young age pool	year	Computed for each tree	(56)
τ_{old}	Leaf residence time in the young age pool	year	Computed for each tree	(56)
SA	Tree sapwood area	m^2	Updated daily	(54), (55)

Table A1. Continued.

Symbols	Definition	Units	Nature	Equations
λ_1	Parameter for sapwood area computation	$m^2\,cm^{-2}$	Constant	(55)
λ_2	Parameter for sapwood area computation	$m\,cm^{-2}$	Constant	(55)
δ_1	Parameter for sapwood area computation	$m^2\,cm^{-2}$	Constant	(55)
δ_2	Parameter for sapwood area computation	$cm^3\,g^{-1}$	Constant	(55)
f_{canopy}	Fraction of NPP_{ind} allocated to tree canopy (including leaves, fruits and twigs)	unitless	Constant, given as input	Sect. 2.6.1 and 2.6.2
f_{leaves}	Fraction of NPP_{ind} allocated to leaves	unitless	Constant	Sect. 2.6.2, (56)
f_{fruit}	Fraction of NPP_{ind} allocated to fruits	unitless	Constant	Sect. 2.6.1
f_{twigs}	Fraction of NPP_{ind} allocated to twigs	unitless	Constant	Sect. 2.6.1
f_{wood}	Fraction of NPP_{ind} allocated to wood	unitless	Constant, given as input	Sect. 2.6.2
$\psi_{T,o}$	Water potential threshold for accelerating old leaf shedding	MPa	Computed daily for each tree	(58)
$a_{T,o}$	Parameter to compute $\psi_{T,o}$ (modulates old leaf drought tolerance)	unitless	Constant, given as input	(58)
$b_{T,o}$	Parameter to compute $\psi_{T,o}$ (modulates the height dependence of leaf susceptibility to drought)	MPa	Constant, given as input	(58)
f_o	Factor of the acceleration of old leaf shedding	unitless	Updated daily for each tree	Sect. 2.6.2
δ_o	Parameter controlling the pace of old leaf shedding acceleration (Δf_0)	unitless	Constant, given as input	
NSC_r	Maximal amount of stored non-structural carbohydrates	gC	Updated daily for each tree	(59)
ΔV	Increment of stem volume	m^3	Computed daily for each tree	(61)
Senesc	Growth senescence factor	unitless	Computed daily for each tree	(61)–(62)
Δdbh	Trunk diameter growth	m	Computed daily for each tree	Sect. 2.6.4
dbh_{mature}	Diameter threshold beyond which the tree is fertile	m	Computed once for each tree	(63)
σ_{disp}	Scale parameter of the Rayleigh distribution for seed dispersal	m	Constant	Sect. 2.7.1
n_s	Number of reproduction opportunities per mature tree	number of seeds	Constant	Sect. 2.7.1
N_{tot}	Intensity of the external seed rain	number of seeds per hectare	Constant, given as input	(64)
$n_{ext,s}$	Species-specific number of dispersal events due to the external seed rain	number of seeds	Computed once for each species	(64)
n_{ha}	Area of the simulated plot	ha	Constant, computed from dimensions given as input	(64)
LAI_{max}	LAI threshold beyond which the seedling leaf carbon balance is negative	$m^2\,m^{-2}$	Computed once for each tree	Sect. 2.7.1

Table A1. Continued.

Symbols	Definition	Units	Nature	Equations
d	Tree death rate	events per year	Updated daily at tree level	(65)–(66)
d_{b}	Background death rate	events per year	Computed once per tree	(65)
m	Reference background mortality rate	events per year	Constant, provided as input	(66)
$\mathrm{wsg}_{\mathrm{lim}}$	Parameter of d_{b}	$\mathrm{g\,cm^{-3}}$	Constant	(66)
d_{starv}	Death rate due to carbon starvation	events per year	Updated daily at tree level	(65)
d_{treefall}	Death rate due to tree fall	events per year	Updated daily at tree level	(65)
Θ	Parameter of tree fall probability	m	Computed once per tree	(67)
d_{drought}	Death rate due to drought	events per year	Updated daily at tree level	(65)
v_{T}	Variance for tree fall probability	unitless	Computed once per tree	(67)
hurt	Parameter of secondary tree fall probability	m	Updated daily for each tree	Sect. 2.7.2
ψ_{lethal}	Water potential threshold for drought-induced mortality	MPa	Computed once per tree	(68)

Appendix B

Table B1. Representation of stomatal conductance, water stress effect on leaf gas exchange, and tree transpiration in several vegetation models. g_0: cuticular or minimal stomatal conductance; i.e. g_s when $A \to 0$. A: CO_2 assimilation rate. c_s: CO_2 concentration at the leaf surface. D_s: vapour pressure deficit at the leaf surface. h_s: fractional relative humidity at the leaf surface. Γ: CO_2 compensation point. V_{cmax} and J_{max} are the maximum carboxylation rate and electron transport rate. All 0 subscripts denote the values without water stress (except for g_0 by convention). Note that stomatal conductance to H_2O is 1.6 times higher than stomatal conductance to CO_2, and here we only represent stomatal conductance to H_2O.

Vegetation model			Stomatal conductance		Water stress effect on leaf gas exchange		Tree transpiration	Comments
Name	Reference	Type	Model	Reference/type	Stomatal limitations	Non-stomatal limitations		
ED2	Longo et al. (2018), Medvigy et al. (2009)	Cohort-based vegetation model	$g_s = g_0 + \frac{a_1 \times A}{(c_s - \Gamma)(1 + \frac{D_s}{D_0})}$	Leuning (1995)/ empirical model	The plant net CO_2 assimilation and evapotranspiration rates (x_{net}) are computed as a linear combination of their rates under open (x_o) and closed (x_c) stomata: $x_{net} = f x_o + (1 - f) x_c$ with $f = \frac{1}{1 + \frac{\text{Demand}}{\text{Supply}}} = \frac{1}{1 + \frac{E_0 \times \text{LA}}{K \times W_{\text{avail, tot}} \times B_{\text{root}}}}$ where E_0 is the evapotranspiration rate under conditions of open stomata times and LA the total plant leaf surface area, and $W_{\text{avail, tot}}$ is the amount of water accessible by the vegetation layer, B_{root} the plant root biomass, and K an optimized constant	Computed with $E_0 = \varphi_0 \times \text{SLA} \times B_{\text{leaf}}$ with B_{leaf} the tree leaf biomass and φ_0 its evapotranspiration rate, obtained by solving a set of 6 equations of 6 unknowns (after determining the leaf temperature using a surface energy balance submodel), among which $\varphi_0 = g_{bw} \times (e_s - e_a)$ $\varphi_0 = g_s \times (e_l - e_s)$		
ED2-hydro	Powell et al. (2018), Xu et al. (2016)	ED2 with a new module of plant hydraulics	Solution of $\frac{\partial}{\partial g_w}(A_{net} - \lambda g_w D_a) = 0$ with $g_w = \frac{g_s g_b}{g_s + g_b}$ and λ is the Lagrangian multiplier of the optimization problem, representing the marginal water use efficiency (marginal increase in A_{net} per unit change of water loss)	Vico et al. (2013)/optimization model, under CO_2 (Rubisco) and light (RuBP regeneration/electron transport) co-limitations	$\lambda = \lambda_0 \times \exp(\beta \times \psi_{pd})$ with λ_0 the value of λ when there is no water stress and β an empirical factor taken from Manzoni et al. (2011)	$V_{cmax} = V_{cmax,0} \times \left[1 + \left(\frac{\psi_{leaf}}{\pi_{tlp}}\right)^a\right]^{-1}$ $J_{max} = J_{max,0} \times \left[1 + \left(\frac{\psi_{leaf}}{\pi_{tlp}}\right)^a\right]^{-1}$ where $V_{cmax,0}$ and $J_{max,0}$ denote the photosynthetic capacities without water stress, and a is a shape factor estimated from Brodribb et al. (2003)	Similarly to Medvigy et al. (2009), $E_0 = \frac{g_s g_b}{g_s + g_b} \times D_a \times \text{LA}$ well as ψ_{stem} based on soil–root, root–leaf, and leaf–atmosphere conductances and water fluxes from the previous step	ψ_{leaf} is updated at each time step (10 min) as

Table B1. Continued.

Vegetation model			Stomatal conductance		Water stress effect on leaf gas exchange		Tree transpiration	Comments
Name	Reference	Type	Model	Reference/type	Stomatal limitations	Non-stomatal limitations		
TFS	Fyllas et al. (2014)		$g_s = g_0 + 1.6 \times (1 + \frac{g_1}{\sqrt{D_s}}) \times \frac{A}{c_s}$ g_1 is an empirical coefficient*, associated with the water use efficiency (the Lagrangian)	Medlyn et al. (2011)/ optimization, for electron-transport-limited photosynthesis (light limitation)	$g_s = g_{s,0} \times \frac{\theta_i - \theta_{wp}}{\theta_{fc} - \theta_{wp}}$ where θ_{wp}, θ_{fc}, and θ_{wp} are the actual soil water available for tree i, and the soil water content at field capacity and wilting point, respectively	–	Following MAESTRA (Medlyn et al., 2007), an iterative procedure is used to solve the energy balance of the canopy of each tree, under which the Penman–Monteith equation is used to estimate canopy transpiration	Soil water content variation is computed using a single-layer bucket model and a root depth proportional to root biomass
TFS-Hydro	Christoffersen et al. (2016)	TFS with a new module of plant hydraulics	"	"	$g_s = g_{s,0} \times \left[1 + \left(\frac{\psi_{leaf}}{\psi_{gs,50}}\right)^{a_{gs}}\right]^{-1}$ where $\psi_{gs,50}$ is the leaf water potential at 50 % stomatal closure (assumed a 1 : 1 relationship between $\psi_{gs,50}$ and the water potential at 20 % loss of xylem hydraulic conductivity ($P_{20,x}$), following results from Brodribb et al., 2003), and a_{gs} is the slope of the curve at $\psi_{leaf} = \psi_{gs,50}$, computed from $\psi_{gs,50}$ using the same relationship that relates a_x and $P_{50,x}$	–	"	ψ_{leaf} is updated at each time step (hourly) by the hydraulic module, based on a continuous porous media approach $P_{20,x}$ is itself derived from xylem vulnerability function with $P_{50,x}$ (derived from an inferred relationship with wood density, $R^2 = 0.34$, based on a meta-analysis) and slope a_x (derived from an inferred relationship with $P_{50,x}$, based on a meta-analysis, $R^2 = 0.38$); did not consider vertical distribution of soil water and roots

Table B1. Continued.

Vegetation model			Stomatal conductance		Water stress effect on leaf gas exchange			Tree transpiration	Comments
Name	Reference	Type	Model	Reference/type	Stomatal limitations	Non-stomatal limitations	limita-		
Multi-layer CLM4.5	Bonan et al. (2014)	DGVM	$g_s = g_0 + g_1 \times A \times \frac{h_s}{c_s}$	Ball et al. (1987), Collatz et al. (1991)/empirical	$g_0 = g_{0,0} \times \sum_j r_j \frac{\psi_j - \psi_c}{\psi_o - \psi_c}$ where ψ_j is the soil water potential of soil layer j, ψ_o and ψ_c are the soil water potential at which the stomata are fully open and fully closed, respectively, and r_j is the relative root fraction of soil layer j	$V_{c,max} = V_{c,max,0} \times \sum_j r_j \frac{\psi_j - \psi_c}{\psi_o - \psi_c}$		Iterative procedure	Without soil moisture stress, the performance of the SPA stomatal model was comparable to or slightly better than the CLM Ball–Berry model in flux tower simulations but was significantly better than the CLM Ball–Berry model when there was soil moisture stress
			g_s is iteratively computed such that (1) further opening does not yield a sufficient carbon gain per unit water loss (defined by a stomatal efficiency parameter) or (2) further opening causes leaf water potential to decrease below the minimum sustainable leaf water potential that prevents xylem cavitation	Inspired from the SPA model (Williams et al., 1996)/optimization within limitations imposed by water use efficiency, plant water storage, and soil-to-leaf water transport	The optimization includes a dependence on ψ_{leaf}, where ψ_{leaf} is computed at each time step (30–60 min) with Darcy's law (soil-to-leaf pathway, including capacitance)		–		

Table B1. Continued.

Vegetation model			Stomatal conductance		Water stress effect on leaf gas exchange		Tree transpiration	Comments
Name	Reference	Type	Model	Reference/type	Stomatal limitations	Non-stomatal limitations		
CLM5	Kennedy et al. (2019	Stand-based physiological model	$g_s = g_0 + 1.6 \times (1 + \frac{g_1}{\sqrt{D_s}}) \times \frac{A}{c_s}$ g_1, is an empirical coefficient*, associated with the water use efficiency (the Lagrangian)	Medlyn et al. (2011/optimization, under light limitation (RuBP regeneration)	–	CML4.5 default: $V_{c,max} = V_{c,max,0} \times \sum_j r_j \frac{\psi_j - \psi_c}{\psi_o - \psi_c}$	An iterative procedure is used to solve the energy balance (determine the leaf temperature and internal CO_2 concentration), under which transpiration is computed as $E_0 = \frac{g_s g_b}{g_s + g_b} \times D_a \times LA$	The new version results in reductions in transpiration and soil moisture biases relative to a control model under both ambient and exclusion conditions (Caixuana Throughfall Exclusion Experiment), correcting excessive dry season soil moisture stress in the control model
					–	$V_{c,max} = V_{c,max,0} \times 2^{-\left(\frac{\psi_{leaf}}{\psi_{gs,50}}\right)^{a_{gs}}}$ where $\psi_{g_s,50}$ is the leaf water potential at 50 % loss of stomatal conductance and a_{g_s} is a shape-fitting parameter; the solution for vegetation water potential is the set of values that matches supply with demand, maintaining water balance across each of the vegetation water potential nodes (ψ_{root}, ψ_{stem}, $\psi_{sunlit\text{-}leaf}$, $\psi_{shade\text{-}leaf}$) based on Darcy's law (without capacitance)		
MAESPA	Duursma et al. (2012)	Individual- and stand-based model	$g_s = g_0 + 1.6 \times \frac{A}{c_s} \times \frac{1 + e^{s_f \psi_f}}{1 + e^{s_f (\psi_f - \psi_{leaf})}}$ where ψ_{leaf} is computed at each time step using Darcy's law ($E_L = k_L \times (\psi_{soil} - \psi_{leaf})$)	Tuzet et al. (2003)/empirical	Already implemented in g_s computation	–	Following MAESTRA (Medlyn et al., 2007), an iterative procedure is used to solve the energy balance of the canopy of each tree, under which the Penman–Monteith equation is used to estimate canopy transpiration	Transpiration is used to yield ψ_{leaf}, which is the solution to the Tuzet model of stomatal conductance

Table B1. Continued.

Vegetation model			Stomatal conductance		Water stress effect on leaf gas exchange		Tree transpiration	Comments
Name	Reference	Type	Model	Reference/type	Stomatal limitations	Non-stomatal limitations		
CABLE	De Kauwe et al. (2015a, b)	DGVM (vegetation is represented using a single-layer, two-leaf canopy model separated into sunlit and shaded leaves)	$g_s = g_0 + 1.6 \times (1 + \frac{g_1}{\sqrt{D_s}}) \times \frac{A}{c_s}$	Medlyn et al. (2011)/optimization, under light limitation (RuBP regeneration) (was the model of Leuning (1995) in previous versions of CABLE (Wang et al., 2011))	Standard version of CABLE (De Kauwe et al., 2015b)	–	Transpiration from the vegetation to the atmosphere is controlled by several resistances operating in series, both above (aerodynamic) and within the canopy (stomatal and leaf boundary layer), and a longwave radiative balance through radiative conductance on net available energy; these resistances in serial result in a relatively weak coupling between the canopy surface and the atmosphere	The new expression of drought sensitivity of gas exchange with variable parameter values across species improves the model predictions across a latitudinal gradient in Europe in the 2003 heatwave
					$g_1 = g_{1,0} \times \sum_j r_j \frac{\theta_j - \theta_{wp}}{\theta_{fc} - \theta_{wp}}$ with θ_l the volumetric soil water content, r_i the fraction of root mass in soil layer j, and θ_{wp} the soil wilting point and θ_{fc} its field capacity			
					New expression for drought sensitivity of gas exchange			
					$g_1 = g_{1,0} \times \exp(b \times \psi_{pd})$, where b is a fitted (species-specific) parameter representing the sensitivity of g_1 to leaf pre-dawn water potential ψ_{pd} and taken from Zhou et al. (2013, 2014), while $g_{1,0}$ values are drawn from (Lin et al., 2015)	$V_{c,max} = V_{c,max,0} \times \frac{1+e^{sf\psi_f}}{1+e^{sf(\psi_f - \psi_{pd})}}$ where sf and ψ_f are fitted (species-specific) parameters drawn from Zhou et al. (2013, 2014)		

Table B1. Continued.

Vegetation model			Stomatal conductance		Water stress effect on leaf gas exchange		Tree transpiration	Comments
Name	Reference	Type	Model	Reference/type	Stomatal limitations	Non-stomatal limitations		
ORCHIDEE	Krinner et al. (2005), Naudts et al. (2015)	DGVM	$g_s = mA\frac{h_r}{c_a} + b$ with m and b derived from laboratory measurements	Ball et al. (1987)	In the version of (Krinner et al., 2005)			In the hydraulic scheme implemented in the CAN version, the leaf water potential is a PFT-specific minimal leaf water potential and is thus fixed, assuming that plants maximize water uptake by lowering their leaf water potential to the minimum. The loss of sapwood conductance as a result of cavitation is implemented using a s-shaped vulnerability curve using the soil water potential in the rooting zone (computed as the sum of soil water potential in each soil layer weighted by the relative share of roots in that layer, added to a modulator (empirical tuned parameter).
					–	The photosynthetic capacities, V_{cmax} and J_{max}, are multiplied by a water stress factor, which is $1 \; if \; f_w > f_o$ $1 - \frac{f_w - f_c}{f_o - f_c}$ if $f_c < f_w < f_o$ 0 if $f_w < f_c$ with f_w the water fraction available for the plant in the root zone, and f_c and f_o the soil water fractions inducing, respectively, closure and maximum opening of stomata		
					In the CAN version of Naudts et al. (2015)			
					The model calculates plant water supply according to the implementation of hydraulic architecture by Hickler et al. (2006), i.e. using Darcy's law and accounting for the hydraulic resistances of fine roots, sapwood, and leaves; if the transpiration calculated by the energy budget exceeds the amount of water a plant can transport from the soil to its stomata, transpiration is limited to the plant water supply, and stomatal conductance is then recalculated such that the transpiration equals the amount of water a plant can transport – the energy budget and photosynthesis are then recalculated, and this may require up to 10 iterations to converge	–		

https://doi.org/10.5194/gmd-18-5143-2025

Table B1. Continued.

Vegetation model			Stomatal conductance		Water stress effect on leaf gas exchange		Tree transpiration	Comments
Name	Reference	Type	Model	Reference/type	Stomatal limitations	Non-stomatal limitations		
LPJ	Sitch et al. (2003)	DGVM	The model uses the Farquhar model of photosynthesis as generalized for global modelling purposes by Collatz et al. (1991); in the absence of water stress, canopy conductance is derived from the daytime carbon assimilation rate: $g_c = g_{min} + \frac{1.6A}{c_a(1-\lambda)}$	Collatz et al. (1991)	Under water stress, i.e. when $\min[1; \frac{E_{supply}}{E_{dema,d}}] < 1$, the equations of evapotranspiration rate, assimilation rate, and the one related to assimilation rate and canopy conductance are solved simultaneously to yield values of canopy conductance consistent with the transpiration rate		Daily evapotranspiration is calculated for each PFT as the minimum of a plant- and soil-limited supply function (E_{supply}) and the atmospheric demand (E_{demand}); E_{supply} is the product of a plant-root-weighted soil moisture availability and a maximum transpiration rate; E_{demand} is calculated following Monteith's empirical relation between evaporation efficiency and surface conductance that uses g_{pot}, the non-water-stressed potential canopy conductance calculated by the photosynthesis routine	Scheme used in Sakschewski et al. (2015, 2016) that combined LPJmL (LPJ with a "managed land" module; Bondeau et al., 2007) with a gap model approach (following LPJ-GUESS,; Smith et al., 2001) in which individual trees with a unique trait combination are modelled, but not species

* Although fitted empirically to leaf exchange experimental data (Lin et al., 2015), attempts have been made to relate g_1 to functional traits and/or climatological variables (wood density, Lin et al., 2015; leaf $\delta^{13}C$, Franks et al., 2018) based on the premise that water use efficiency should be associated with functional strategies. See also values reported in Domingues et al. (2014).

Table B2. Examples of observational or experimental studies that explored the relative roles of stomatal and non-stomatal limitations of photosynthesis under drought conditions.

Key message for vegetation models	Reference	Studied system	Main results
Stomatal limitation only	Santos et al. (2018)	57 canopy and understorey trees within a central Amazonian forest	Photosynthesis decreased during the extreme dry season, and this was only related to stomatal closure (decline in stomatal conductance) and not to leaf biochemical changes (sustained chlorophyll concentration and fluorescence, as well as nutrient concentration)
	Rowland et al. (2015)	Trees in the throughfall exclusion and control plots in Caixuana, Amazonia	No differences in V_{cmax} and J_{max} between the throughfall exclusion plot and the control plot
	Trueba et al. (2019)	Mature individuals of 10 angiosperms species located on the campus of UCLA and a park in LA	The stomatal and leaf hydraulic systems (50 % lost of g_s, K_{leaf}) show early functional declines before cell integrity is lost; substantial damage to the photochemical apparatus (maximum quantum yield of the photosystem) occurs at extreme dehydration, after turgor loss and complete stomatal closure, and seems to be irreversible
Both stomatal and non-stomatal limitations	Zhou et al. (2013)	Meta-analysis of 22 experimental datasets where photosynthesis, stomatal conductance, and pre-dawn leaf water potential were measured at increasing water stress, spanning a range of plant functional types	Photosynthesis was found almost universally to decrease more than could be explained by the reduction in g_1 (parameter of the Medlyn model), implying a decline in apparent carboxylation capacity (V_{cmax})
	Zhou et al. (2014)	Two experiments, one in Australia on eucalyptus and one in Spain on Quercus, on plants grown in glasshouses under control conditions; the non-stomatal response was partitioned into effects on mesophyll conductance (g_m), the maximum Rubisco activity (V_{cmax}), and the maximum electron transport rate (J_{max})	They consistency found among the drought responses of g_1, g_m, V_{cmax}, and J_{max} suggests that drought imposes limitations on Rubisco activity and RuBP regeneration capacity concurrently with declines in stomatal and mesophyll conductance; within each experiment, the more xeric species showed relatively high g_1 under moist conditions, low drought sensitivity of g_1, g_m, V_{cmax}, and J_{max}, and more negative values of the critical pre-dawn water potential at which V_{cmax} declines most steeply, compared with the more mesic species Results showed that the decline in V_{cmax} is not explained just by the decline in g_m, but by the decline in both g_m and V_{cmax}
	Egea et al. (2011)	Outputs from a coupled A–g_s model that uses a soil-water-content-dependent water stress factor were compared to leaf-level values obtained from the literature	The sensitivity analyses emphasized the necessity to combine both stomatal and non-stomatal limitations of A in coupled A–g_s models to accurately capture the observed functional relationships A vs. g_s and A/g_s vs. g_s in response to drought; accounting for water stress in coupled A–g_s models by imposing either stomatal or biochemical limitations of A, as commonly practised in most ecosystem models, failed to reproduce the observed functional relationship between key leaf gas exchange attributes
	Drake et al. (2017)	Plants in pots of four tree species originating from contrasting hydrological environments, placed in the field under rainout shelters; comparison with coupled stomatal conductance–photosynthesis model	As soil water content (θ) was reduced under increasing drought, all species responded by reducing g_s, resulting in reduced C_i and A_{sat}; however, A_{sat} was reduced to a larger degree than would be predicted only by stomatal reduction of C_i, indicating a coincident reduction in photosynthetic capacity with declining θ – the best model includes both stomatal and non-stomatal limitations

Code and data availability. The code of TROLL 4.0 is publicly available as a C++ standalone at https://github.com/TROLL-code/TROLL (last access: 11 July 2025) (https://doi.org/10.5281/zenodo.14013147, Maréchaux et al., 2024). Additionally, TROLL 4.0 can be set up and run and its outputs can be analysed with an updated version of the R package rcontroll: https://github.com/sylvainschmitt/rcontroll/tree/TROLLV4 (last access: 11 July 2025, https://doi.org/10.5281/zenodo.14012116, Schmitt et al., 2024). It is also available in R through the following command: `devtools::install_github("sylvainschmitt/rcontroll", ref = "TROLLV4")`

Author contributions. IM led TROLL 4.0 and designed the implementation of the water cycle and its coupling to vegetation. FJF coled TROLL 4.0 and designed the new implementation of intraspecific variability and crown shapes. SyS and JC contributed ideas and discussions. IM wrote the paper with contributions from all authors.

Competing interests. The contact author has declared that none of the authors has any competing interests.

Disclaimer. Publisher's note: Copernicus Publications remains neutral with regard to jurisdictional claims made in the text, published maps, institutional affiliations, or any other geographical representation in this paper. While Copernicus Publications makes every effort to include appropriate place names, the final responsibility lies with the authors.

Acknowledgements. We acknowledge Nicolas Martin-StPaul and Rémi Vezy for useful discussions on the representation of gas exchanges and water fluxes in models; Nicolas Barbier, Gregoire Vincent, and James Ball for sharing data and useful discussions on leaf phenology; Philippe Verley and Thomas Arsouze for IT support; and Marie Boscher for help in designing Fig. 1. This work was carried out with the support of the MESO@LR Platform at the University of Montpellier.

Financial support. This research has been supported by funding from the ANR (the French National Research Agency) under the "Investissements d'avenir" programme with the references ANR-16-IDEX-0006, ANR-10-LABX-25-01, and ANR-10-LABX-0041; the Amazonian Landscapes in Transition ANR project (ALT); the CNES Biomass-Valo project; and ESA CCI-BIOMASS.

Review statement. This paper was edited by Dalei Hao and reviewed by Xiangtao Xu and two anonymous referees.

References

Aguilos, M., Hérault, B., Burban, B., Wagner, F., and Bonal, D.: What drives long-term variations in carbon flux and balance in a tropical rainforest in French Guiana?, Agr. Forest Meteorol., 253–254, 114–123, https://doi.org/10.1016/j.agrformet.2018.02.009, 2018.

Albert, L. P., Restrepo-Coupe, N., Smith, M. N., Wu, J., Chavana-Bryant, C., Prohaska, N., Taylor, T. C., Martins, G. A., Ciais, P., Mao, J., Arain, M. A., Li, W., Shi, X., Ricciuto, D. M., Huxman, T. E., McMahon, S. M., and Saleska, S. R.: Cryptic phenology in plants: Case studies, implications, and recommendations, Glob. Change Biol., 25, 3591–3608, https://doi.org/10.1111/gcb.14759, 2019.

Albert, L. P., Wu, J., Prohaska, N., de Camargo, P. B., Huxman, T. E., Tribuzy, E. S., Ivanov, V. Y., Oliveira, R. S., Garcia, S., Smith, M. N., Oliveira Junior, R. C., Restrepo-Coupe, N., da Silva, R., Stark, S. C., Martins, G. A., Penha, D. V., and Saleska, S. R.: Age-dependent leaf physiology and consequences for crown-scale carbon uptake during the dry season in an Amazon evergreen forest, New Phytol., 219, 870–884, https://doi.org/10.1111/nph.15056, 2018.

Albrich, K., Rammer, W., Turner, M. G., Ratajczak, Z., Braziunas, K. H., Hansen, W. D., and Seidl, R.: Simulating forest resilience: A review, Global Ecol. Biogeogr., 29, 2082–2096, https://doi.org/10.1111/geb.13197, 2020.

Amthor, J. S.: The role of maintenance respiration in plant growth, Plant Cell Environ., 7, 561–569, https://doi.org/10.1111/1365-3040.ep11591833, 1984.

Anderegg, W. R. L., Schwalm, C., Biondi, F., Camarero, J. J., Koch, G., Litvak, M., Ogle, K., Shaw, J. D., Shevliakova, E., Williams, A. P., Wolf, A., Ziaco, E., and Pacala, S.: Pervasive drought legacies in forest ecosystems and their implications for carbon cycle models, Science, 349, 528–532, https://doi.org/10.1126/science.aab1833, 2015.

Anderegg, W. R. L., Wolf, A., Arango-Velez, A., Choat, B., Chmura, D. J., Jansen, S., Kolb, T., Li, S., Meinzer, F., Pita, P., Dios, V. R. de, Sperry, J. S., Wolfe, B. T., and Pacala, S.: Plant water potential improves prediction of empirical stomatal models, PLOS ONE, 12, e0185481, https://doi.org/10.1371/journal.pone.0185481, 2017.

Anderegg, W. R. L., Wolf, A., Arango-Velez, A., Choat, B., Chmura, D. J., Jansen, S., Kolb, T., Li, S., Meinzer, F. C., Pita, P., Dios, V. R. de, Sperry, J. S., Wolfe, B. T., and Pacala, S.: Woody plants optimise stomatal behaviour relative to hydraulic risk, Ecol. Lett., 21, 968–977, https://doi.org/10.1111/ele.12962, 2018.

Arora, V. K. and Boer, G. J.: A Representation of Variable Root Distribution in Dynamic Vegetation Models, Earth Interact., 7, 1–19, https://doi.org/10.1175/1087-3562(2003)007<0001:AROVRD>2.0.CO;2, 2003.

Asao, S., Bedoya-Arrieta, R., and Ryan, M. G.: Variation in foliar respiration and wood CO_2 efflux rates among species and canopy layers in a wet tropical forest, Tree Physiol., 35, 148–159, https://doi.org/10.1093/treephys/tpu107, 2015.

Atkin, O. K., Evans, J. R., Ball, M. C., Lambers, H., and Pons, T. L.: Leaf respiration of snow gum in the light and dark. Interactions between temperature and irradiance, Plant Physiol., 122, 915–924, https://doi.org/10.1104/pp.122.3.915, 2000.

Atkin, O. K., Meir, P., and Turnbull, M. H.: Improving representation of leaf respiration in large-scale predictive climate–vegetation models, New Phytol., 202, 743–748, https://doi.org/10.1111/nph.12686, 2014.

Atkin, O. K., Bloomfield, K. J., Reich, P. B., Tjoelker, M. G., Asner, G. P., Bonal, D., Bönisch, G., Bradford, M. G., Cernusak, L. A., Cosio, E. G., Creek, D., Crous, K. Y., Domingues, T. F., Dukes, J. S., Egerton, J. J. G., Evans, J. R., Farquhar, G. D., Fyllas, N. M., Gauthier, P. P. G., Gloor, E., Gimeno, T. E., Griffin, K. L., Guerrieri, R., Heskel, M. A., Huntingford, C., Ishida, F. Y., Kattge, J., Lambers, H., Liddell, M. J., Lloyd, J., Lusk, C. H., Martin, R. E., Maksimov, A. P., Maximov, T. C., Malhi, Y., Medlyn, B. E., Meir, P., Mercado, L. M., Mirotchnick, N., Ng, D., Niinemets, Ü., O'Sullivan, O. S., Phillips, O. L., Poorter, L., Poot, P., Prentice, I. C., Salinas, N., Rowland, L. M., Ryan, M. G., Sitch, S., Slot, M., Smith, N. G., Turnbull, M. H., VanderWel, M. C., Valladares, F., Veneklaas, E. J., Weerasinghe, L. K., Wirth, C., Wright, I. J., Wythers, K. R., Xiang, J., Xiang, S., and Zaragoza-Castells, J.: Global variability in leaf respiration in relation to climate, plant functional types and leaf traits, New Phytol., 206, 614–636, https://doi.org/10.1111/nph.13253, 2015.

Ball, J. T., Woodrow, I. E., and Berry, J. A.: A model predicting stomatal conductance and its contribution to the control of photosynthesis under different environmental conditions, in: Progress in photosynthesis research, edited by: Biggins, J., Springer Netherlands, 221–224, https://doi.org/10.1007/978-94-017-0519-6_48, 1987.

Baltzer, J. L., Davies, S. J., Bunyavejchewin, S., and Noor, N. S. M.: The role of desiccation tolerance in determining tree species distributions along the Malay–Thai Peninsula, Funct. Ecol., 22, 221–231, https://doi.org/10.1111/j.1365-2435.2007.01374.x, 2008.

Baraloto, C., Paine, C. E. T., Patiño, S., Bonal, D., Hérault, B., and Chave, J.: Functional trait variation and sampling strategies in species-rich plant communities, Funct. Ecol., 24, 208–216, https://doi.org/10.1111/j.1365-2435.2009.01600.x, 2010a.

Baraloto, C., Timothy Paine, C. E., Poorter, L., Beauchene, J., Bonal, D., Domenach, A.-M., Hérault, B., Patiño, S., Roggy, J.-C., and Chave, J.: Decoupled leaf and stem economics in rain forest trees, Ecol. Lett., 13, 1338–1347, https://doi.org/10.1111/j.1461-0248.2010.01517.x, 2010b.

Bartlett, M. K., Scoffoni, C., Ardy, R., Zhang, Y., Sun, S., Cao, K., and Sack, L.: Rapid determination of comparative drought tolerance traits: using an osmometer to predict turgor loss point, Methods Ecol. Evol., 3, 880–888, https://doi.org/10.1111/j.2041-210X.2012.00230.x, 2012a.

Bartlett, M. K., Scoffoni, C., and Sack, L.: The determinants of leaf turgor loss point and prediction of drought tolerance of species and biomes: a global meta-analysis, Ecol. Lett., 15, 393–405, https://doi.org/10.1111/j.1461-0248.2012.01751.x, 2012b.

Bartlett, M. K., Zhang, Y., Yang, J., Kreidler, N., Sun, S.-W., Lin, L., Hu, Y.-H., Cao, K.-F., and Sack, L.: Drought tolerance as a driver of tropical forest assembly: resolving spatial signatures for multiple processes, Ecology, 97, 503–514, https://doi.org/10.1890/15-0468.1, 2016a.

Bartlett, M. K., Klein, T., Jansen, S., Choat, B., and Sack, L.: The correlations and sequence of plant stomatal, hydraulic, and wilting responses to drought, P. Natl. Acad. Sci. USA, 113, 13098–13103, https://doi.org/10.1073/pnas.1604088113, 2016b.

Beer, C., Reichstein, M., Tomelleri, E., Ciais, P., Jung, M., Carvalhais, N., Rödenbeck, C., Arain, M. A., Baldocchi, D., Bonan, G. B., Bondeau, A., Cescatti, A., Lasslop, G., Lindroth, A., Lomas, M., Luyssaert, S., Margolis, H., Oleson, K. W., Roupsard, O., Veenendaal, E., Viovy, N., Williams, C., Woodward, F. I., and Papale, D.: Terrestrial gross carbon dioxide uptake: global distribution and covariation with climate, Science, 329, 834–838, https://doi.org/10.1126/science.1184984, 2010.

Bennett, A. C., McDowell, N. G., Allen, C. D., and Anderson-Teixeira, K. J.: Larger trees suffer most during drought in forests worldwide, Nat. Plants, 1, 15139, https://doi.org/10.1038/nplants.2015.139, 2015.

Bernacchi, C. J., Pimentel, C., and Long, S. P.: In vivo temperature response functions of parameters required to model RuBP-limited photosynthesis, Plant Cell Environ., 26, 1419–1430, https://doi.org/10.1046/j.0016-8025.2003.01050.x, 2003.

Berzaghi, F., Wright, I. J., Kramer, K., Oddou-Muratorio, S., Bohn, F. J., Reyer, C. P. O., Sabaté, S., Sanders, T. G. M., and Hartig, F.: Towards a New Generation of Trait-Flexible Vegetation Models, Trends Ecol. Evol., 35, 191–205, https://doi.org/10.1016/j.tree.2019.11.006, 2020.

Blanchard, G., Barbier, N., Vieilledent, G., Ibanez, T., Hequet, V., McCoy, S., and Birnbaum, P.: UAV-Lidar reveals that canopy structure mediates the influence of edge effects on forest diversity, function and microclimate, J. Ecol., 111, 1411–1427, https://doi.org/10.1111/1365-2745.14105, 2023.

Bohlman, S. and O'Brien, S.: Allometry, adult stature and regeneration requirement of 65 tree species on Barro Colorado Island, Panama, J. Trop. Ecol., 22, 123–136, https://doi.org/10.1017/S0266467405003019, 2006.

Bonal, D., Bosc, A., Ponton, S., Goret, J.-Y., Burban, B., Gross, P., Bonnefond, J.-M., Elbers, J., Longdoz, B., Epron, D., Guehl, J.-M., and Granier, A.: Impact of severe dry season on net ecosystem exchange in the Neotropical rainforest of French Guiana, Glob. Change Biol., 14, 1917–1933, https://doi.org/10.1111/j.1365-2486.2008.01610.x, 2008.

Bonan, G. B.: Forests and Climate Change: Forcings, Feedbacks, and the Climate Benefits of Forests, Science, 320, 1444–1449, https://doi.org/10.1126/science.1155121, 2008.

Bonan, G. B., Williams, M., Fisher, R. A., and Oleson, K. W.: Modeling stomatal conductance in the earth system: linking leaf water-use efficiency and water transport along the soil–plant–atmosphere continuum, Geosci. Model Dev., 7, 2193–2222, https://doi.org/10.5194/gmd-7-2193-2014, 2014.

Bondeau, A., Smith, P. C., Zaehle, S., Schaphoff, S., Lucht, W., Cramer, W., Gerten, D., Lotze-Campen, H., Müller, C., Reichstein, M., and Smith, B.: Modelling the role of agriculture for the 20th century global terrestrial carbon balance, Glob. Change Biol., 13, 679–706, https://doi.org/10.1111/j.1365-2486.2006.01305.x, 2007.

Botkin, D. B., Janak, J. F., and Wallis, J. R.: Some Ecological Consequences of a Computer Model of Forest Growth, J. Ecol., 60, 849–872, https://doi.org/10.2307/2258570, 1972.

Bradford, K. J.: A Water Relations Analysis of Seed Germination Rates, Plant Physiol., 94, 840–849, https://doi.org/10.1104/pp.94.2.840, 1990.

Braghiere, R. K., Quaife, T., Black, E., He, L., and Chen, J. M.: Underestimation of Global Photosynthesis in Earth System Models Due to Representation of Vegeta-

tion Structure, Global Biogeochem. Cy., 33, 1358–1369, https://doi.org/10.1029/2018GB006135, 2019.

Braghiere, R. K., Wang, Y., Doughty, R., Sousa, D., Magney, T., Widlowski, J.-L., Longo, M., Bloom, A. A., Worden, J., Gentine, P., and Frankenberg, C.: Accounting for canopy structure improves hyperspectral radiative transfer and sun-induced chlorophyll fluorescence representations in a new generation Earth System model, Remote Sens. Environ., 261, 112497, https://doi.org/10.1016/j.rse.2021.112497, 2021.

Brodribb, T. J.: Progressing from "functional" to mechanistic traits, New Phytol., 215, 9–11, https://doi.org/10.1111/nph.14620, 2017.

Brodribb, T. J., Holbrook, N. M., and Gutiérrez, M. V.: Hydraulic and photosynthetic co-ordination in seasonally dry tropical forest trees, Plant Cell Environ., 25, 1435–1444, https://doi.org/10.1046/j.1365-3040.2002.00919.x, 2002.

Brodribb, T. J., Holbrook, N. M., Edwards, E. J., and Gutiérrez, M. V.: Relations between stomatal closure, leaf turgor and xylem vulnerability in eight tropical dry forest trees, Plant Cell Environ., 26, 443–450, https://doi.org/10.1046/j.1365-3040.2003.00975.x, 2003.

Brooks, R. H. and Corey, A. T.: Hydraulic properties of porous media. Hydrology Paper No. 3, Civil Engineering Department, Colorado State University, Fort Collins, 1964.

Brum, M., Vadeboncoeur, M. A., Ivanov, V., Asbjornsen, H., Saleska, S., Alves, L. F., Penha, D., Dias, J. D., Aragão, L. E. O. C., Barros, F., Bittencourt, P., Pereira, L., and Oliveira, R. S.: Hydrological niche segregation defines forest structure and drought tolerance strategies in a seasonal Amazon forest, J. Ecol., 107, 318–333, https://doi.org/10.1111/1365-2745.13022, 2019.

Bruno, R. D., da Rocha, H. R., de Freitas, H. C., Goulden, M. L., and Miller, S. D.: Soil moisture dynamics in an eastern Amazonian tropical forest, Hydrol. Process., 20, 2477–2489, https://doi.org/10.1002/hyp.6211, 2006.

Bucci, S., Scholz, F. G., Goldstein, G., Meinzer, F. C., Hinojosa, J. A., Hoffman, W. A., and Franco, A. C.: Processes preventing nocturnal equilibration between leaf and soil water potential in tropical savanna woody species, Tree Physiol., 24, 1119–1127, 2004.

Buchmann, N., Guehl, J.-M., Barigah, T. S., and Ehleringer, J. R.: Interseasonal comparison of CO_2 concentrations, isotopic composition, and carbon dynamics in an Amazonian rainforest (French Guiana), Oecologia, 110, 120–131, https://doi.org/10.1007/s004420050140, 1997.

Budyko, M. I.: The Heat Balance of the Earth's Surface, Soviet Geography, 2, 3–13, https://doi.org/10.1080/00385417.1961.10770761, 1961.

Bugmann, H.: A review of forest gap models, Climatic Change, 51, 259–305, https://doi.org/10.1023/A:1012525626267, 2001.

Burgess, S. S. O., Adams, M. A., Turner, N. C., and Ong, C. K.: The redistribution of soil water by tree root systems, Oecologia, 115, 306–311, https://doi.org/10.1007/s004420050521, 1998.

Camargo, J. L. C. and Kapos, V.: Complex edge effects on soil moisture and microclimate in central Amazonian forest, J. Trop. Ecol., 11, 205–221, 1995.

Canadell, J., Jackson, R. B., Ehleringer, J. R., Mooney, H. A., Sala, O. E., and Schulze, E. D.: Maximum rooting depth of vegetation types at the global scale, Oecologia, 108, 583–595, https://doi.org/10.1007/BF00329030, 1996.

Cannell, M. G. R. and Thornley, J. H. M.: Modelling the components of plant respiration: some guiding principles, Ann. Bot., 85, 45–54, https://doi.org/10.1006/anbo.1999.0996, 2000.

Cavaleri, M. A., Oberbauer, S. F., and Ryan, M. G.: Wood CO_2 efflux in a primary tropical rain forest, Glob. Change Biol., 12, 2442–2458, https://doi.org/10.1111/j.1365-2486.2006.01269.x, 2006.

Cavaleri, M. A., Oberbauer, S. F., and Ryan, M. G.: Foliar and ecosystem respiration in an old-growth tropical rain forest, Plant Cell Environ., 31, 473–483, https://doi.org/10.1111/j.1365-3040.2008.01775.x, 2008.

Charney, J. G.: Dynamics of deserts and drought in the Sahel, Q. J. Roy. Meteor. Soc., 101, 193–202, https://doi.org/10.1002/qj.49710142802, 1975.

Chase, J. M., Blowes, S. A., Knight, T. M., Gerstner, K., and May, F.: Ecosystem decay exacerbates biodiversity loss with habitat loss, Nature, 584, 238–243, https://doi.org/10.1038/s41586-020-2531-2, 2020.

Chave: Study of structural, successional and spatial patterns in tropical rain forests using TROLL, a spatially explicit forest model, Ecol. Model., 124, 233–254, https://doi.org/10.1016/S0304-3800(99)00171-4, 1999.

Chave, J., Olivier, J., Bongers, F., Châtelet, P., Forget, P.-M., van der Meer, P., Norden, N., Riéra, B., and Charles-Dominique, P.: Above-ground biomass and productivity in a rain forest of eastern South America, J. Trop. Ecol., 24, 355–366, https://doi.org/10.1017/S0266467408005075, 2008.

Chave, J., Coomes, D., Jansen, S., Lewis, S. L., Swenson, N. G., and Zanne, A. E.: Towards a worldwide wood economics spectrum, Ecol. Lett., 12, 351–366, https://doi.org/10.1111/j.1461-0248.2009.01285.x, 2009.

Chave, J., Navarrete, D., Almeida, S., Álvarez, E., Aragão, L. E. O. C., Bonal, D., Châtelet, P., Silva-Espejo, J. E., Goret, J.-Y., von Hildebrand, P., Jiménez, E., Patiño, S., Peñuela, M. C., Phillips, O. L., Stevenson, P., and Malhi, Y.: Regional and seasonal patterns of litterfall in tropical South America, Biogeosciences, 7, 43–55, https://doi.org/10.5194/bg-7-43-2010, 2010.

Chave, J., Réjou-Méchain, M., Búrquez, A., Chidumayo, E., Colgan, M. S., Delitti, W. B. C., Duque, A., Eid, T., Fearnside, P. M., Goodman, R. C., Henry, M., Martínez-Yrízar, A., Mugasha, W. A., Muller-Landau, H. C., Mencuccini, M., Nelson, B. W., Ngomanda, A., Nogueira, E. M., Ortiz-Malavassi, E., Pélissier, R., Ploton, P., Ryan, C. M., Saldarriaga, J. G., and Vieilledent, G.: Improved allometric models to estimate the aboveground biomass of tropical trees, Glob. Change Biol., 20, 3177–3190, https://doi.org/10.1111/gcb.12629, 2014.

Chen, X., Maignan, F., Viovy, N., Bastos, A., Goll, D., Wu, J., Liu, L., Yue, C., Peng, S., Yuan, W., da Conceição, A. C., O'Sullivan, M., and Ciais, P.: Novel Representation of Leaf Phenology Improves Simulation of Amazonian Evergreen Forest Photosynthesis in a Land Surface Model, J. Adv. Model. Earth Sy., 12, e2018MS001565, https://doi.org/10.1029/2018MS001565, 2020.

Chen, X., Ciais, P., Maignan, F., Zhang, Y., Bastos, A., Liu, L., Bacour, C., Fan, L., Gentine, P., Goll, D., Green, J., Kim, H., Li, L., Liu, Y., Peng, S., Tang, H., Viovy, N., Wigneron, J.-P., Wu, J., Yuan, W., and Zhang, H.: Vapor Pressure Deficit and Sunlight Explain Seasonality of Leaf Phenology and Photosynthesis Across Amazonian

Evergreen Broadleaved Forest, Global Biogeochem. Cy., 35, e2020GB006893, https://doi.org/10.1029/2020GB006893, 2021.

Chen, Y., Ryder, J., Bastrikov, V., McGrath, M. J., Naudts, K., Otto, J., Ottlé, C., Peylin, P., Polcher, J., Valade, A., Black, A., Elbers, J. A., Moors, E., Foken, T., van Gorsel, E., Haverd, V., Heinesch, B., Tiedemann, F., Knohl, A., Launiainen, S., Loustau, D., Ogée, J., Vessala, T., and Luyssaert, S.: Evaluating the performance of land surface model ORCHIDEE-CAN v1.0 on water and energy flux estimation with a single- and multi-layer energy budget scheme, Geosci. Model Dev., 9, 2951–2972, https://doi.org/10.5194/gmd-9-2951-2016, 2016.

Chesson, P. L. and Warner, R. R.: Environmental variability promotes coexistence in lottery competitive systems, Am. Natural., 117, 923–943, 1981.

Christoffersen, B. O., Gloor, M., Fauset, S., Fyllas, N. M., Galbraith, D. R., Baker, T. R., Kruijt, B., Rowland, L., Fisher, R. A., Binks, O. J., Sevanto, S., Xu, C., Jansen, S., Choat, B., Mencuccini, M., McDowell, N. G., and Meir, P.: Linking hydraulic traits to tropical forest function in a size-structured and trait-driven model (TFS v.1-Hydro), Geosci. Model Dev., 9, 4227–4255, https://doi.org/10.5194/gmd-9-4227-2016, 2016.

Chuine, I. and Beaubien, E. G.: Phenology is a major determinant of tree species range, Ecol. Lett., 4, 500–510, https://doi.org/10.1046/j.1461-0248.2001.00261.x, 2001.

Clark, D. B., Mercado, L. M., Sitch, S., Jones, C. D., Gedney, N., Best, M. J., Pryor, M., Rooney, G. G., Essery, R. L. H., Blyth, E., Boucher, O., Harding, R. J., Huntingford, C., and Cox, P. M.: The Joint UK Land Environment Simulator (JULES), model description – Part 2: Carbon fluxes and vegetation dynamics, Geosci. Model Dev., 4, 701–722, https://doi.org/10.5194/gmd-4-701-2011, 2011.

Cochard, H.: A new mechanism for tree mortality due to drought and heatwaves, Peer Community Journal, 1, e36, https://doi.org/10.24072/pcjournal.45, 2021.

Cochard, H., Torres-Ruiz, J. M., and Delzon, S.: Let plant hydraulics catch the wave, J. Plant Hydraul., 3, e002–e002, https://doi.org/10.20870/jph.2016.e002, 2016.

Cochard, H., Pimont, F., Ruffault, J., and Martin-StPaul, N.: SurEau: a mechanistic model of plant water relations under extreme drought, Ann. Forest Sci., 78, 55, https://doi.org/10.1007/s13595-021-01067-y, 2021.

Collalti, A., Tjoelker, M. G., Hoch, G., Mäkelä, A., Guidolotti, G., Heskel, M., Petit, G., Ryan, M. G., Battipaglia, G., Matteucci, G., and Prentice, I. C.: Plant respiration: Controlled by photosynthesis or biomass?, Glob. Change Biol., 26, 1739–1753, https://doi.org/10.1111/gcb.14857, 2020.

Collatz, G. J., Ball, J. T., Grivet, C., and Berry, J. A.: Physiological and environmental regulation of stomatal conductance, photosynthesis and transpiration: a model that includes a laminar boundary layer, Agr. Forest Meteorol., 54, 107–136, https://doi.org/10.1016/0168-1923(91)90002-8, 1991.

Coomes, D. A. and Grubb, P. J.: Colonization, tolerance, competition and seed-size variation within functional groups, Trend. Ecol. Evol., 18, 283–291, https://doi.org/10.1016/S0169-5347(03)00072-7, 2003.

Cosby, B. J., Hornberger, G. M., Clapp, R. B., and Ginn, T. R.: A Statistical Exploration of the Relationships of Soil Moisture Characteristics to the Physical Properties of Soils, Water Resour. Res., 20, 682–690, https://doi.org/10.1029/WR020i006p00682, 1984.

Costa, F. R. C., Schietti, J., Stark, S. C., and Smith, M. N.: The other side of tropical forest drought: do shallow water table regions of Amazonia act as large-scale hydrological refugia from drought?, New Phytol., 237, 714–733, https://doi.org/10.1111/nph.17914, 2023.

Coussement, J. R., De Swaef, T., Lootens, P., Roldán-Ruiz, I., and Steppe, K.: Introducing turgor-driven growth dynamics into functional–structural plant models, Ann. Bot., 121, 849–861, https://doi.org/10.1093/aob/mcx144, 2018.

Cox, P. M., Betts, R. A., Jones, C. D., Spall, S. A., and Totterdell, I. J.: Acceleration of global warming due to carbon-cycle feedbacks in a coupled climate model, Nature, 408, 184–187, https://doi.org/10.1038/35041539, 2000.

Craine, J. M., Engelbrecht, B. M. J., Lusk, C. H., McDowell, N. G., and Poorter, H.: Resource limitation, tolerance, and the future of ecological plant classification, Front. Plant Sci., 3, https://doi.org/10.3389/fpls.2012.00246, 2012.

Crawford, M. S., Barry, K. E., Clark, A. T., Farrior, C. E., Hines, J., Ladouceur, E., Lichstein, J. W., Maréchaux, I., May, F., Mori, A. S., Reineking, B., Turnbull, L. A., Wirth, C., and Rüger, N.: The function-dominance correlation drives the direction and strength of biodiversity–ecosystem functioning relationships, Ecol. Lett., 24, 1762–1775, https://doi.org/10.1111/ele.13776, 2021.

Cubiña, A. and Aide, T. M.: The Effect of Distance from Forest Edge on Seed Rain and Soil Seed Bank in a Tropical Pasture, Biotropica, 33, 260–267, https://doi.org/10.1646/0006-3606(2001)033[0260:TEODFF]2.0.CO;2, 2001.

Cusack, D. F., Christoffersen, B., Smith-Martin, C. M., Andersen, K. M., Cordeiro, A. L., Fleischer, K., Wright, S. J., Guerrero-Ramírez, N. R., Lugli, L. F., McCulloch, L. A., Sanchez-Julia, M., Batterman, S. A., Dallstream, C., Fortunel, C., Toro, L., Fuchslueger, L., Wong, M. Y., Yaffar, D., Fisher, J. B., Arnaud, M., Dietterich, L. H., Addo-Danso, S. D., Valverde-Barrantes, O. J., Weemstra, M., Ng, J. C., and Norby, R. J.: Toward a coordinated understanding of hydro-biogeochemical root functions in tropical forests for application in vegetation models, New Phytol., 242, 351–371, https://doi.org/10.1111/nph.19561, 2024.

Damour, G., Simonneau, T., Cochard, H., and Urban, L.: An overview of models of stomatal conductance at the leaf level, Plant Cell Environ., 33, 1419–1438, https://doi.org/10.1111/j.1365-3040.2010.02181.x, 2010.

Daws, M. I., Crabtree, L. M., Dalling, J. W., Mullins, C. E., and Burslem, D. F. R. P.: Germination Responses to Water Potential in Neotropical Pioneers Suggest Large-seeded Species Take More Risks, Ann. Bot., 102, 945–951, https://doi.org/10.1093/aob/mcn186, 2008.

Dawson, T. E.: Hydraulic lift and water use by plants: implications for water balance, performance and plant-plant interactions, Oecologia, 95, 565–574, https://doi.org/10.1007/BF00317442, 1993.

De Cáceres, M., Molowny-Horas, R., Cabon, A., Martínez-Vilalta, J., Mencuccini, M., García-Valdés, R., Nadal-Sala, D., Sabaté, S., Martin-StPaul, N., Morin, X., D'Adamo, F., Batllori, E., and Améztegui, A.: MEDFATE 2.9.3: a trait-enabled model to simulate Mediterranean forest function and dynamics at regional scales, Geosci. Model Dev., 16, 3165–3201, https://doi.org/10.5194/gmd-16-3165-2023, 2023.

De Deurwaerder, H., Hervé-Fernández, P., Stahl, C., Burban, B., Petronelli, P., Hoffman, B., Bonal, D., Boeckx, P., and Verbeeck, H.: Liana and tree below-ground water competition – evidence for water resource partitioning during the dry season, Tree Physiol., 38, 1071–1083, https://doi.org/10.1093/treephys/tpy002, 2018.

De Frenne, P., Zellweger, F., Rodríguez-Sánchez, F., Scheffers, B. R., Hylander, K., Luoto, M., Vellend, M., Verheyen, K., and Lenoir, J.: Global buffering of temperatures under forest canopies, Nat. Ecol. Evol., 3, 744–749, https://doi.org/10.1038/s41559-019-0842-1, 2019.

De Frenne, P., Lenoir, J., Luoto, M., Scheffers, B. R., Zellweger, F., Aalto, J., Ashcroft, M. B., Christiansen, D. M., Decocq, G., De Pauw, K., Govaert, S., Greiser, C., Gril, E., Hampe, A., Jucker, T., Klinges, D. H., Koelemeijer, I. A., Lembrechts, J. J., Marrec, R., Meeussen, C., Ogée, J., Tyystjärvi, V., Vangansbeke, P., and Hylander, K.: Forest microclimates and climate change: Importance, drivers and future research agenda, Glob. Change Biol., 27, 2279–2297, https://doi.org/10.1111/gcb.15569, 2021.

De Kauwe, M. G., Zhou, S.-X., Medlyn, B. E., Pitman, A. J., Wang, Y.-P., Duursma, R. A., and Prentice, I. C.: Do land surface models need to include differential plant species responses to drought? Examining model predictions across a mesic-xeric gradient in Europe, Biogeosciences, 12, 7503–7518, https://doi.org/10.5194/bg-12-7503-2015, 2015a.

De Kauwe, M. G., Kala, J., Lin, Y.-S., Pitman, A. J., Medlyn, B. E., Duursma, R. A., Abramowitz, G., Wang, Y.-P., and Miralles, D. G.: A test of an optimal stomatal conductance scheme within the CABLE land surface model, Geosci. Model Dev., 8, 431–452, https://doi.org/10.5194/gmd-8-431-2015, 2015b.

De Kauwe, M. G., Medlyn, B. E., Knauer, J., and Williams, C. A.: Ideas and perspectives: how coupled is the vegetation to the boundary layer?, Biogeosciences, 14, 4435–4453, https://doi.org/10.5194/bg-14-4435-2017, 2017.

Delhaye, G., Bauman, D., Séleck, M., Ilunga wa Ilunga, E., Mahy, G., and Meerts, P.: Interspecific trait integration increases with environmental harshness: A case study along a metal toxicity gradient, Funct. Ecol., 34, 1428–1437, https://doi.org/10.1111/1365-2435.13570, 2020.

Dewar, R., Mauranen, A., Mäkelä, A., Hölttä, T., Medlyn, B., and Vesala, T.: New insights into the covariation of stomatal, mesophyll and hydraulic conductances from optimization models incorporating nonstomatal limitations to photosynthesis, New Phytol., 217, 571–585, https://doi.org/10.1111/nph.14848, 2018.

Díaz, S., Kattge, J., Cornelissen, J. H. C., Wright, I. J., Lavorel, S., Dray, S., Reu, B., Kleyer, M., Wirth, C., Colin Prentice, I., Garnier, E., Bönisch, G., Westoby, M., Poorter, H., Reich, P. B., Moles, A. T., Dickie, J., Gillison, A. N., Zanne, A. E., Chave, J., Joseph Wright, S., Sheremet'ev, S. N., Jactel, H., Baraloto, C., Cerabolini, B., Pierce, S., Shipley, B., Kirkup, D., Casanoves, F., Joswig, J. S., Günther, A., Falczuk, V., Rüger, N., Mahecha, M. D., and Gorné, L. D.: The global spectrum of plant form and function, Nature, 529, 167–171, https://doi.org/10.1038/nature16489, 2016.

Díaz, S., Kattge, J., Cornelissen, J. H. C., Wright, I. J., Lavorel, S., Dray, S., Reu, B., Kleyer, M., Wirth, C., Prentice, I. C., Garnier, E., Bönisch, G., Westoby, M., Poorter, H., Reich, P. B., Moles, A. T., Dickie, J., Zanne, A. E., Chave, J., Wright, S. J., Sheremetiev, S. N., Jactel, H., Baraloto, C., Cerabolini, B. E. L., Pierce, S., Shipley, B., Casanoves, F., Joswig, J. S., Günther, A., Falczuk, V., Rüger, N., Mahecha, M. D., Gorné, L. D., Amiaud, B., Atkin, O. K., Bahn, M., Baldocchi, D., Beckmann, M., Blonder, B., Bond, W., Bond-Lamberty, B., Brown, K., Burrascano, S., Byun, C., Campetella, G., Cavender-Bares, J., Chapin, F. S., Choat, B., Coomes, D. A., Cornwell, W. K., Craine, J., Craven, D., Dainese, M., de Araujo, A. C., de Vries, F. T., Domingues, T. F., Enquist, B. J., Fagúndez, J., Fang, J., Fernández-Méndez, F., Fernandez-Piedade, M. T., Ford, H., Forey, E., Freschet, G. T., Gachet, S., Gallagher, R., Green, W., Guerin, G. R., Gutiérrez, A. G., Harrison, S. P., Hattingh, W. N., He, T., Hickler, T., Higgins, S. I., Higuchi, P., Ilic, J., Jackson, R. B., Jalili, A., Jansen, S., Koike, F., König, C., Kraft, N., Kramer, K., Kreft, H., Kühn, I., Kurokawa, H., Lamb, E. G., Laughlin, D. C., Leishman, M., Lewis, S., Louault, F., Malhado, A. C. M., Manning, P., Meir, P., Mencuccini, M., Messier, J., Miller, R., Minden, V., Molofsky, J., Montgomery, R., Montserrat-Martí, G., Moretti, M., Müller, S., Niinemets, Ü., Ogaya, R., Öllerer, K., Onipchenko, V., Onoda, Y., Ozinga, W. A., Pausas, J. G., Peco, B., Penuelas, P., Pillar, V. D., Pladevall, C., Römermann, C., Sack, L., Salinas, N., Sandel, B., Sardans, J., Schamp, B., Scherer-Lorenzen, M., Schulze, E.-D., Schweingruber, F., Shiodera, S., Sosinski, Ê., Soudzilovskaia, N., Spasojevic, M. J., Swaine, E., Swenson, N., Tautenhahn, S., Thompson, K., Totte, A., Urrutia-Jalabert, R., Valladares, F., van Bodegom, P., Vasseur, F., Verheyen, K., Vile, D., Violle, C., von Holle, B., Weigelt, P., Weiher, E., Wiemann, M. C., Williams, M., Wright, J., and Zotz, G.: The global spectrum of plant form and function: enhanced species-level trait dataset, Sci. Data, 9, 755, https://doi.org/10.1038/s41597-022-01774-9, 2022.

Díaz-Yáñez, O., Käber, Y., Anders, T., Bohn, F., Braziunas, K. H., Brůna, J., Fischer, R., Fischer, S. M., Hetzer, J., Hickler, T., Hochauer, C., Lexer, M. J., Lischke, H., Mairota, P., Merganič, J., Merganičová, K., Mette, T., Mina, M., Morin, X., Nieberg, M., Rammer, W., Reyer, C. P. O., Scheiter, S., Scherrer, D., and Bugmann, H.: Tree regeneration in models of forest dynamics: A key priority for further research, Ecosphere, 15, e4807, https://doi.org/10.1002/ecs2.4807, 2024.

Dietze, M. C., Lebauer, D. S., and Kooper, R.: On improving the communication between models and data, Plant Cell Environ., 36, 1575–1585, https://doi.org/10.1111/pce.12043, 2013.

Dilley, A. C. and O'Brien, D. M.: Estimating downward clear sky long-wave irradiance at the surface from screen temperature and precipitable water, Q. J. Roy. Meteor. Soc., 124, 1391–1401, https://doi.org/10.1002/qj.49712454903, 1998.

Domingues, T. F., Meir, P., Feldpausch, T. R., Saiz, G., Veenendaal, E. M., Schrodt, F., Bird, M., Djagbletey, G., Hien, F., Compaore, H., Diallo, A., Grace, J., and Lloyd, J.: Co-limitation of photosynthetic capacity by nitrogen and phosphorus in West Africa woodlands, Plant Cell Environ., 33, 959–980, https://doi.org/10.1111/j.1365-3040.2010.02119.x, 2010.

Domingues, T. F., Martinelli, L. A., and Ehleringer, J. R.: Seasonal patterns of leaf-level photosynthetic gas exchange in an eastern Amazonian rain forest, Plant Ecol. Divers., 7, 189–203, https://doi.org/10.1080/17550874.2012.748849, 2014.

Donovan, L. A., Richards, J. H., and Linton, M. J.: Magnitude and mechanisms of disequilibrium between predawn plant and soil water potentials, Ecology, 84, 463–470, https://doi.org/10.1890/0012-9658(2003)084[0463:MAMODB]2.0.CO;2, 2003.

d'Orgeval, T., Polcher, J., and de Rosnay, P.: Sensitivity of the West African hydrological cycle in ORCHIDEE to infiltration processes, Hydrol. Earth Syst. Sci., 12, 1387–1401, https://doi.org/10.5194/hess-12-1387-2008, 2008.

Dormann, C. F., Schymanski, S. J., Cabral, J., Chuine, I., Graham, C., Hartig, F., Kearney, M., Morin, X., Römermann, C., Schröder, B., and Singer, A.: Correlation and process in species distribution models: bridging a dichotomy, J. Biogeogr., 39, 2119–2131, https://doi.org/10.1111/j.1365-2699.2011.02659.x, 2012.

Doughty, C. E. and Goulden, M. L.: Seasonal patterns of tropical forest leaf area index and CO_2 exchange, J. Geophys. Res., 113, G00B06, https://doi.org/10.1029/2007JG000590, 2008.

Doughty, C. E., Malhi, Y., Araujo-Murakami, A., Metcalfe, D. B., Silva-Espejo, J. E., Arroyo, L., Heredia, J. P., Pardo-Toledo, E., Mendizabal, L. M., Rojas-Landivar, V. D., Vega-Martinez, M., Flores-Valencia, M., Sibler-Rivero, R., Moreno-Vare, L., Viscarra, L. J., Chuviru-Castro, T., Osinaga-Becerra, M., and Ledezma, R.: Allocation trade-offs dominate the response of tropical forest growth to seasonal and interannual drought, Ecology, 95, 2192–2201, https://doi.org/10.1890/13-1507.1, 2014.

Doughty, C. E., Gaillard, C., Burns, P., Keany, J. M., Abraham, A. J., Malhi, Y., Aguirre-Gutierrez, J., Koch, G., Jantz, P., Shenkin, A., and Tang, H.: Tropical forests are mainly unstratified especially in Amazonia and regions with lower fertility or higher temperatures, Environ. Res. Ecol., 2, 035002, https://doi.org/10.1088/2752-664X/ace723, 2023.

Drake, J. E., Power, S. A., Duursma, R. A., Medlyn, B. E., Aspinwall, M. J., Choat, B., Creek, D., Eamus, D., Maier, C., Pfautsch, S., Smith, R. A., Tjoelker, M. G., and Tissue, D. T.: Stomatal and non-stomatal limitations of photosynthesis for four tree species under drought: A comparison of model formulations, Agr. Forest Meteorol., 247, 454–466, https://doi.org/10.1016/j.agrformet.2017.08.026, 2017.

Drake, P. L., Boer, H. J. de, Schymanski, S. J., and Veneklaas, E. J.: Two sides to every leaf: water and CO_2 transport in hypostomatous and amphistomatous leaves, New Phytol., 222, 1179–1187, https://doi.org/10.1111/nph.15652, 2019.

Duffy, P. B., Brando, P., Asner, G. P., and Field, C. B.: Projections of future meteorological drought and wet periods in the Amazon, P. Natl. Acad. Sci. USA, 112, 13172–13177, https://doi.org/10.1073/pnas.1421010112, 2015.

Dunne, T. and Black, R. D.: An Experimental Investigation of Runoff Production in Permeable Soils, Water Resour. Res., 6, 478–490, https://doi.org/10.1029/WR006i002p00478, 1970.

Duursma, R. A.: Plantecophys – An R Package for Analysing and Modelling Leaf Gas Exchange Data, PLOS ONE, 10, e0143346, https://doi.org/10.1371/journal.pone.0143346, 2015.

Duursma, R. A. and Medlyn, B. E.: MAESPA: a model to study interactions between water limitation, environmental drivers and vegetation function at tree and stand levels, with an example application to $[CO_2]$ × drought interactions, Geosci. Model Dev., 5, 919–940, https://doi.org/10.5194/gmd-5-919-2012, 2012.

Duursma, R. A., Blackman, C. J., Lopéz, R., Martin-StPaul, N. K., Cochard, H., and Medlyn, B. E.: On the minimum leaf conductance: its role in models of plant water use, and ecological and environmental controls, New Phytol., 221, 693–705, https://doi.org/10.1111/nph.15395, 2019.

Dwyer, J. M. and Laughlin, D. C.: Constraints on trait combinations explain climatic drivers of biodiversity: the importance of trait covariance in community assembly, Ecol. Lett., 20, 872–882, https://doi.org/10.1111/ele.12781, 2017.

Egea, G., Verhoef, A., and Vidale, P. L.: Towards an improved and more flexible representation of water stress in coupled photosynthesis–stomatal conductance models, Agr. Forest Meteorol., 151, 1370–1384, https://doi.org/10.1016/j.agrformet.2011.05.019, 2011.

Elias, M. and Potvin, C.: Assessing inter- and intra-specific variation in trunk carbon concentration for 32 neotropical tree species, Can. J. For. Res., 33, 1039–1045, https://doi.org/10.1139/x03-018, 2003.

Elith, J. and Leathwick, J. R.: Species Distribution Models: Ecological Explanation and Prediction Across Space and Time, Annu. Rev. Ecol. Evol. S., 40, 677–697, https://doi.org/10.1146/annurev.ecolsys.110308.120159, 2009.

Engelbrecht, B. M. J., Dalling, J. W., Pearson, T. R. H., Wolf, R. L., Galvez, D. A., Koehler, T., Tyree, M. T., and Kursar, T. A.: Short dry spells in the wet season increase mortality of tropical pioneer seedlings, Oecologia, 148, 258–269, https://doi.org/10.1007/s00442-006-0368-5, 2006.

Esquivel-Muelbert, A., Baker, T. R., Dexter, K. G., Lewis, S. L., Brienen, R. J. W., Feldpausch, T. R., Lloyd, J., Monteagudo-Mendoza, A., Arroyo, L., Álvarez-Dávila, E., Higuchi, N., Marimon, B. S., Marimon-Junior, B. H., Silveira, M., Vilanova, E., Gloor, E., Malhi, Y., Chave, J., Barlow, J., Bonal, D., Cardozo, N. D., Erwin, T., Fauset, S., Hérault, B., Laurance, S., Poorter, L., Qie, L., Stahl, C., Sullivan, M. J. P., Steege, H. ter, Vos, V. A., Zuidema, P. A., Almeida, E., de Oliveira, E. A., Andrade, A., Vieira, S. A., Aragão, L., Araujo-Murakami, A., Arets, E., C, G. A. A., Baraloto, C., Camargo, P. B., Barroso, J. G., Bongers, F., Boot, R., Camargo, J. L., Castro, W., Moscoso, V. C., Comiskey, J., Valverde, F. C., da Costa, A. C. L., Pasquel, J. del A., Fiore, A. D., Duque, L. F., Elias, F., Engel, J., Llampazo, G. F., Galbraith, D., Fernández, R. H., Coronado, E. H., Hubau, W., Jimenez-Rojas, E., Lima, A. J. N., Umetsu, R. K., Laurance, W., Lopez-Gonzalez, G., Lovejoy, T., Cruz, O. A. M., Morandi, P. S., Neill, D., Vargas, P. N., Camacho, N. C. P., Gutierrez, A. P., Pardo, G., Peacock, J., Peña-Claros, M., Peñuela-Mora, M. C., Petronelli, P., Pickavance, G. C., Pitman, N., Prieto, A., Quesada, C., Ramírez-Angulo, H., Réjou-Méchain, M., Correa, Z. R., Roopsind, A., Rudas, A., Salomão, R., Silva, N., Espejo, J. S., Singh, J., Stropp, J., Terborgh, J., Thomas, R., Toledo, M., Torres-Lezama, A., Gamarra, L. V., van de Meer, P. J., van der Heijden, G., van der Hout, P., Vasquez Martinez, R., Vela, C., Célia, I., Vieira, G., and Phillips, O. L.: Compositional response of Amazon forests to climate change, Glob. Change Biol., 25, 39–56, https://doi.org/10.1111/gcb.14413, 2019.

Esquivel-Muelbert, A., Phillips, O. L., Brienen, R. J. W., Fauset, S., Sullivan, M. J. P., Baker, T. R., Chao, K.-J., Feldpausch, T. R., Gloor, E., Higuchi, N., Houwing-Duistermaat, J., Lloyd, J., Liu, H., Malhi, Y., Marimon, B., Marimon Junior, B. H., Monteagudo-Mendoza, A., Poorter, L., Silveira, M., Torre, E. V., Dávila, E. A., del Aguila Pasquel, J., Almeida, E., Loayza, P. A., Andrade, A., Aragão, L. E. O. C., Araujo-Murakami, A., Arets, E., Arroyo, L., Aymard C. G. A., Baisie, M., Baraloto, C., Camargo, P. B., Barroso, J., Blanc, L., Bonal, D., Bongers, F., Boot, R., Brown, F., Burban, B., Camargo, J. L., Castro, W., Moscoso, V. C., Chave, J., Comiskey, J., Valverde, F. C., da Costa, A. L., Cardozo, N. D., Di Fiore, A., Dourdain, A., Erwin, T., Llam-

pazo, G. F., Vieira, I. C. G., Herrera, R., Honorio Coronado, E., Huamantupa-Chuquimaco, I., Jimenez-Rojas, E., Killeen, T., Laurance, S., Laurance, W., Levesley, A., Lewis, S. L., Ladvocat, K. L. L. M., Lopez-Gonzalez, G., Lovejoy, T., Meir, P., Mendoza, C., Morandi, P., Neill, D., Nogueira Lima, A. J., Vargas, P. N., de Oliveira, E. A., Camacho, N. P., Pardo, G., Peacock, J., Peña-Claros, M., Peñuela-Mora, M. C., Pickavance, G., Pipoly, J., Pitman, N., Prieto, A., Pugh, T. A. M., Quesada, C., Ramirez-Angulo, H., de Almeida Reis, S. M., Rejou-Machain, M., Correa, Z. R., Bayona, L. R., Rudas, A., Salomão, R., Serrano, J., Espejo, J. S., Silva, N., Singh, J., Stahl, C., Stropp, J., Swamy, V., Talbot, J., ter Steege, H., Terborgh, J., Thomas, R., Toledo, M., Torres-Lezama, A., Valenzuela Gamarra, L., van der Heijden, G., van der Meer, P., van der Hout, P., Vasquez Martinez, R., Aparecida Vieira, S., Villalobos Cayo, J., Vos, V., Zagt, R., Zuidema, P., and Galbraith, D.: Tree mode of death and mortality risk factors across Amazon forests, Nat. Commun., 11, 5515, https://doi.org/10.1038/s41467-020-18996-3, 2020.

Estes, L., Elsen, P. R., Treuer, T., Ahmed, L., Caylor, K., Chang, J., Choi, J. J., and Ellis, E. C.: The spatial and temporal domains of modern ecology, Nat. Ecol. Evol., 2, 819–826, https://doi.org/10.1038/s41559-018-0524-4, 2018.

Evans, M. R.: Modelling ecological systems in a changing world, Phil. Trans. R. Soc. B, 367, 181–190, https://doi.org/10.1098/rstb.2011.0172, 2012.

Farrior, C. E., Dybzinski, R., Levin, S. A., and Pacala, S. W.: Competition for Water and Light in Closed-Canopy Forests: A Tractable Model of Carbon Allocation with Implications for Carbon Sinks, Am. Nat., 181, 314–330, https://doi.org/10.1086/669153, 2013.

Farquhar, G. D., Caemmerer, S. von, and Berry, J. A.: A biochemical model of photosynthetic CO_2 assimilation in leaves of C3 species, Planta, 149, 78–90, 1980.

Farrell, C., Szota, C., and Arndt, S. K.: Does the turgor loss point characterize drought response in dryland plants?, Plant Cell Environ., 40, 1500–1511, https://doi.org/10.1111/pce.12948, 2017.

Fatichi, S., Pappas, C., and Ivanov, V. Y.: Modeling plant–water interactions: an ecohydrological overview from the cell to the global scale, WIREs Water, 3, 327–368, https://doi.org/10.1002/wat2.1125, 2016.

Fauset, S., Baker, T. R., Lewis, S. L., Feldpausch, T. R., Affum-Baffoe, K., Foli, E. G., Hamer, K. C., and Swaine, M. D.: Drought-induced shifts in the floristic and functional composition of tropical forests in Ghana, Ecol. Lett., 15, 1120–1129, https://doi.org/10.1111/j.1461-0248.2012.01834.x, 2012.

Feeley, K. J., Davies, S. J., Perez, R., Hubbell, S. P., and Foster, R. B.: Directional changes in the species composition of a tropical forest, Ecology, 92, 871–882, 2011.

Fer, I., Kelly, R., Moorcroft, P. R., Richardson, A. D., Cowdery, E. M., and Dietze, M. C.: Linking big models to big data: efficient ecosystem model calibration through Bayesian model emulation, Biogeosciences, 15, 5801–5830, https://doi.org/10.5194/bg-15-5801-2018, 2018.

Fernández-Martínez, M., Vicca, S., Janssens, I. A., Sardans, J., Luyssaert, S., Campioli, M., Chapin Iii, F. S., Ciais, P., Malhi, Y., Obersteiner, M., Papale, D., Piao, S. L., Reichstein, M., Rodà, F., and Peñuelas, J.: Nutrient availability as the key regulator of global forest carbon balance, Nat.Clim. Change, 4, 471–476, https://doi.org/10.1038/nclimate2177, 2014.

Ferrier, S. and Guisan, A.: Spatial modelling of biodiversity at the community level, J. Appl. Ecol., 43, 393–404, https://doi.org/10.1111/j.1365-2664.2006.01149.x, 2006.

Fichtner, A., Härdtle, W., Bruelheide, H., Kunz, M., Li, Y., and Oheimb, G.: Neighbourhood interactions drive overyielding in mixed-species tree communities, Nat. Commun., 9, 1144, https://doi.org/10.1038/s41467-018-03529-w, 2018.

Fischer, F. J.: Inferring the structure and dynamics of tropical rain forests with individual-based forest growth models, Doctoral Dissertation, Université Paul Sabatier-Toulouse III, 2019.

Fischer, F. J., Maréchaux, I., and Chave, J.: Improving plant allometry by fusing forest models and remote sensing, New Phytol., 223, 1159–1165, https://doi.org/10.1111/nph.15810, 2019.

Fischer, F. J., Labrière, N., Vincent, G., Hérault, B., Alonso, A., Memiaghe, H., Bissiengou, P., Kenfack, D., Saatchi, S., and Chave, J.: A simulation method to infer tree allometry and forest structure from airborne laser scanning and forest inventories, Remote Sens. Environ., 251, 112056, https://doi.org/10.1016/j.rse.2020.112056, 2020.

Fischer, R., Armstrong, A., Shugart, H. H., and Huth, A.: Simulating the impacts of reduced rainfall on carbon stocks and net ecosystem exchange in a tropical forest, Environ. Model. Softw., 52, 200–206, https://doi.org/10.1016/j.envsoft.2013.10.026, 2014.

Fisher, J. B., Huntzinger, D. N., Schwalm, C. R., and Sitch, S.: Modeling the Terrestrial Biosphere, Annu. Rev. Environ. Resour., 39, 91–123, https://doi.org/10.1146/annurev-environ-012913-093456, 2014.

Fisher, R. A., Williams, M., Do Vale, R. L., Da Costa, A. L., and Meir, P.: Evidence from Amazonian forests is consistent with isohydric control of leaf water potential, Plant Cell Environ., 29, 151–165, https://doi.org/10.1111/j.1365-3040.2005.01407.x, 2006.

Fisher, R. A., Williams, M., Da Costa, A. L., Malhi, Y., Da Costa, R. F., Almeida, S., and Meir, P.: The response of an Eastern Amazonian rain forest to drought stress: results and modelling analyses from a throughfall exclusion experiment, Glob. Change Biol., 13, 2361–2378, https://doi.org/10.1111/j.1365-2486.2007.01417.x, 2007.

Fisher, R. A., Muszala, S., Verteinstein, M., Lawrence, P., Xu, C., McDowell, N. G., Knox, R. G., Koven, C., Holm, J., Rogers, B. M., Spessa, A., Lawrence, D., and Bonan, G.: Taking off the training wheels: the properties of a dynamic vegetation model without climate envelopes, CLM4.5(ED), Geosci. Model Dev., 8, 3593–3619, https://doi.org/10.5194/gmd-8-3593-2015, 2015.

Fisher, R. A., Koven, C. D., Anderegg, W. R. L., Christoffersen, B. O., Dietze, M. C., Farrior, C. E., Holm, J. A., Hurtt, G. C., Knox, R. G., Lawrence, P. J., Lichstein, J. W., Longo, M., Matheny, A. M., Medvigy, D., Muller-Landau, H. C., Powell, T. L., Serbin, S. P., Sato, H., Shuman, J. K., Smith, B., Trugman, A. T., Viskari, T., Verbeeck, H., Weng, E., Xu, C., Xu, X., Zhang, T., and Moorcroft, P. R.: Vegetation demographics in Earth System Models: A review of progress and priorities, Glob. Change Biol., 24, 35–54, https://doi.org/10.1111/gcb.13910, 2018.

Fisher, R. A. and Koven, C. D.: Perspectives on the Future of Land Surface Models and the Challenges of Representing Complex Terrestrial Systems, J. Adv. Model. Earth Sy., 12, e2018MS001453, https://doi.org/10.1029/2018MS001453, 2020.

Flexas, J., Bota, J., Loreto, F., Cornic, G., and Sharkey, T. D.: Diffusive and Metabolic Limitations to Photosynthesis under Drought and Salinity in C3 Plants, Plant Biol., 6, 269–279, https://doi.org/10.1055/s-2004-820867, 2004.

Flexas, J., Galmes, J., Ribas-Carbo, M., and Medrano, H.: The Effects of Water Stress on Plant Respiration, in: Plant Respiration, Springer, Dordrecht, 85–94, https://doi.org/10.1007/1-4020-3589-6_6, 2005.

Flexas, J., Bota, J., Galmés, J., Medrano, H., and Ribas-Carbó, M.: Keeping a positive carbon balance under adverse conditions: responses of photosynthesis and respiration to water stress, Physiol. Plant., 127, 343–352, https://doi.org/10.1111/j.1399-3054.2006.00621.x, 2006.

Flexas, J., Barbour, M. M., Brendel, O., Cabrera, H. M., Carriquí, M., Díaz-Espejo, A., Douthe, C., Dreyer, E., Ferrio, J. P., Gago, J., Gallé, A., Galmés, J., Kodama, N., Medrano, H., Niinemets, Ü., Peguero-Pina, J. J., Pou, A., Ribas-Carbó, M., Tomás, M., Tosens, T., and Warren, C. R.: Mesophyll diffusion conductance to CO_2: An unappreciated central player in photosynthesis, Plant Science, 193–194, 70–84, https://doi.org/10.1016/j.plantsci.2012.05.009, 2012.

Franks, P. J., Bonan, G. B., Berry, J. A., Lombardozzi, D. L., Holbrook, N. M., Herold, N., and Oleson, K. W.: Comparing optimal and empirical stomatal conductance models for application in Earth system models, Glob. Change Biol., 24, 5708–5723, https://doi.org/10.1111/gcb.14445, 2018.

Franks, S. W., Beven, K. J., Quinn, P. F., and Wright, I. R.: On the sensitivity of soil-vegetation-atmosphere transfer (SVAT) schemes: equifinality and the problem of robust calibration, Agr. Forest Meteorol., 86, 63–75, https://doi.org/10.1016/S0168-1923(96)02421-5, 1997.

Friedlingstein, P., Joel, G., Field, C. B., and Fung, I. Y.: Toward an allocation scheme for global terrestrial carbon models, Glob. Change Biol., 5, 755–770,https://doi.org/10.1046/j.1365-2486.1999.00269.x, 1999.

Friend, A. D., Lucht, W., Rademacher, T. T., Keribin, R., Betts, R., Cadule, P., Ciais, P., Clark, D. B., Dankers, R., Falloon, P. D., Ito, A., Kahana, R., Kleidon, A., Lomas, M. R., Nishina, K., Ostberg, S., Pavlick, R., Peylin, P., Schaphoff, S., Vuichard, N., Warszawski, L., Wiltshire, A., and Woodward, F. I.: Carbon residence time dominates uncertainty in terrestrial vegetation responses to future climate and atmospheric CO_2, P. Natl. Acad. Sci. USA, 111, 3280–3285, https://doi.org/10.1073/pnas.1222477110, 2014.

Fyllas, N. M., Gloor, E., Mercado, L. M., Sitch, S., Quesada, C. A., Domingues, T. F., Galbraith, D. R., Torre-Lezama, A., Vilanova, E., Ramírez-Angulo, H., Higuchi, N., Neill, D. A., Silveira, M., Ferreira, L., Aymard C., G. A., Malhi, Y., Phillips, O. L., and Lloyd, J.: Analysing Amazonian forest productivity using a new individual and trait-based model (TFS v.1), Geosci. Model Dev., 7, 1251–1269, https://doi.org/10.5194/gmd-7-1251-2014, 2014.

Garcia, M. N., Domingues, T. F., Oliveira, R. S., and Costa, F. R. C.: The biogeography of embolism resistance across resource gradients in the Amazon, Global Ecol. Biogeogr., 32, 2199–2211, https://doi.org/10.1111/geb.13765, 2023.

Gardner, W. R.: Relation of Root Distribution to Water Uptake and Availability, Agron. J., 56, 41–45, https://doi.org/10.2134/agronj1964.00021962005600010013x, 1964.

Gash, J. H. C.: An analytical model of rainfall interception by forests, Q. J. Roy. Meteor. Soc., 105, 43–55, https://doi.org/10.1002/qj.49710544304, 1979.

Gash, J. H. C., Lloyd, C. R., and Lachaud, G.: Estimating sparse forest rainfall interception with an analytical model, J. Hydrol., 170, 79–86, https://doi.org/10.1016/0022-1694(95)02697-N, 1995.

Girard-Tercieux, C., Maréchaux, I., Clark, A. T., Clark, J. S., Courbaud, B., Fortunel, C., Guillemot, J., Künstler, G., le Maire, G., Pélissier, R., Rüger, N., and Vieilledent, G.: Rethinking the nature of intraspecific variability and its consequences on species coexistence, Ecol. Evol., 13, e9860, https://doi.org/10.1002/ece3.9860, 2023.

Girard-Tercieux, C., Vieilledent, G., Clark, A., Clark, J. S., Courbaud, B., Fortunel, C., Kunstler, G., Pélissier, R., Rüger, N., and Maréchaux, I.: Beyond variance: simple random distributions are not a good proxy for intraspecific variability in systems with environmental structure, Peer Community Journal, 4, e28, https://doi.org/10.24072/pcjournal.360, 2024.

Gourlet-Fleury, S., Blanc, L., Picard, N., Sist, P., Dick, J., Nasi, R., Swaine, M. D., and Forni, E.: Grouping species for predicting mixed tropical forest dynamics: looking for a strategy, Ann. Forest Sci., 62, 12, https://doi.org/10.1051/forest:2005084, 2005.

Griffin-Nolan, R. J., Ocheltree, T. W., Mueller, K. E., Blumenthal, D. M., Kray, J. A., and Knapp, A. K.: Extending the osmometer method for assessing drought tolerance in herbaceous species, Oecologia, 189, 353–363, https://doi.org/10.1007/s00442-019-04336-w, 2019.

Gril, E., Spicher, F., Greiser, C., Ashcroft, M. B., Pincebourde, S., Durrieu, S., Nicolas, M., Richard, B., Decocq, G., Marrec, R., and Lenoir, J.: Slope and equilibrium: A parsimonious and flexible approach to model microclimate, Methods Ecol. Evol., 14, 885–897, https://doi.org/10.1111/2041-210X.14048, 2023a.

Gril, E., Laslier, M., Gallet-Moron, E., Durrieu, S., Spicher, F., Le Roux, V., Brasseur, B., Haesen, S., Van Meerbeek, K., Decocq, G., Marrec, R., and Lenoir, J.: Using airborne LiDAR to map forest microclimate temperature buffering or amplification, Remote Sens. Environ., 298, 113820, https://doi.org/10.1016/j.rse.2023.113820, 2023b.

Grisebach, A.: Die Vegetation der Erde nach ihrer klimatischen Anordnung: Ein Abriss der vergleichenden Geographie der Pflanzen. Bd. I und II, Verlag von Wilhelm Engelmann, Leipzig, http://archive.org/details/dievegetationde01grisgoog (last access: 24 July 2025), 1872.

Gu, L., Shugart, H. H., Fuentes, J. D., Black, T. A., and Shewchuk, S. R.: Micrometeorology, biophysical exchanges and NEE decomposition in a two-story boreal forest – development and test of an integrated model, Agr. Forest Meteorol., 94, 123–148, https://doi.org/10.1016/S0168-1923(99)00006-4, 1999.

Guan, K., Pan, M., Li, H., Wolf, A., Wu, J., Medvigy, D., Caylor, K. K., Sheffield, J., Wood, E. F., Malhi, Y., Liang, M., Kimball, J. S., Saleska, S. R., Berry, J., Joiner, J., and Lyapustin, A. I.: Photosynthetic seasonality of global tropical forests constrained by hydroclimate, Nat. Geosci., 8, 284–289, https://doi.org/10.1038/ngeo2382, 2015.

Guerrero-Ramírez, N. R., Mommer, L., Freschet, G. T., Iversen, C. M., McCormack, M. L., Kattge, J., Poorter, H., van der Plas, F., Bergmann, J., Kuyper, T. W., York, L. M., Bruelheide, H., Laughlin, D. C., Meier, I. C., Roumet, C., Semchenko, M., Sweeney, C. J., van Ruijven, J., Valverde-Barrantes, O. J., Aubin, I., Catford,

J. A., Manning, P., Martin, A., Milla, R., Minden, V., Pausas, J. G., Smith, S. W., Soudzilovskaia, N. A., Ammer, C., Butterfield, B., Craine, J., Cornelissen, J. H. C., de Vries, F. T., Isaac, M. E., Kramer, K., König, C., Lamb, E. G., Onipchenko, V. G., Peñuelas, J., Reich, P. B., Rillig, M. C., Sack, L., Shipley, B., Tedersoo, L., Valladares, F., van Bodegom, P., Weigelt, P., Wright, J. P., and Weigelt, A.: Global root traits (GRooT) database, Global Ecol. Biogeogr., 30, 25–37, https://doi.org/10.1111/geb.13179, 2021.

Guillemot, J., Kunz, M., Schnabel, F., Fichtner, A., Madsen, C. P., Gebauer, T., Härdtle, W., von Oheimb, G., and Potvin, C.: Neighbourhood-mediated shifts in tree biomass allocation drive overyielding in tropical species mixtures, New Phytol., 228, 1256–1268, https://doi.org/10.1111/nph.16722, 2020.

Guimberteau, M., Ducharne, A., Ciais, P., Boisier, J. P., Peng, S., De Weirdt, M., and Verbeeck, H.: Testing conceptual and physically based soil hydrology schemes against observations for the Amazon Basin, Geosci. Model Dev., 7, 1115–1136, https://doi.org/10.5194/gmd-7-1115-2014, 2014.

Guisan, A. and Thuiller, W.: Predicting species distribution: offering more than simple habitat models, Ecol. Lett., 8, 993–1009, https://doi.org/10.1111/j.1461-0248.2005.00792.x, 2005.

Guisan, A., Thuiller, W., and Zimmermann, N. E.: Habitat Suitability and Distribution Models: with Applications in R, Cambridge University Press, 513 pp., https://doi.org/10.1017/9781139028271, 2017.

Gutiérrez, A. G., Armesto, J. J., Díaz, M. F., and Huth, A.: Increased Drought Impacts on Temperate Rainforests from Southern South America: Results of a Process-Based, Dynamic Forest Model, PLOS ONE, 9, e103226, https://doi.org/10.1371/journal.pone.0103226, 2014.

Haesen, S., Lenoir, J., Gril, E., De Frenne, P., Lembrechts, J. J., Kopecký, M., Macek, M., Man, M., Wild, J., and Van Meerbeek, K.: Microclimate reveals the true thermal niche of forest plant species, Ecol. Lett., 26, 2043–2055, https://doi.org/10.1111/ele.14312, 2023.

Hanbury-Brown, A. R., Ward, R. E., and Kueppers, L. M.: Forest regeneration within Earth system models: current process representations and ways forward, New Phytol., 235, 20–40, https://doi.org/10.1111/nph.18131, 2022.

Harper, A., Baker, I. T., Denning, A. S., Randall, D. A., Dazlich, D., and Branson, M.: Impact of evapotranspiration on dry season climate in the Amazon forest, J. Climate, 27, 574–591, https://doi.org/10.1175/JCLI-D-13-00074.1, 2013.

Hartig, F., Dyke, J., Hickler, T., Higgins, S. I., O'Hara, R. B., Scheiter, S., and Huth, A.: Connecting dynamic vegetation models to data – an inverse perspective, J. Biogeogr., 39, 2240–2252, https://doi.org/10.1111/j.1365-2699.2012.02745.x, 2012.

Hasselquist, N. J., Allen, M. F., and Santiago, L. S.: Water relations of evergreen and drought-deciduous trees along a seasonally dry tropical forest chronosequence, Oecologia, 164, 881–890, https://doi.org/10.1007/s00442-010-1725-y, 2010.

Hengl, T., Jesus, J. M. de, Heuvelink, G. B. M., Gonzalez, M. R., Kilibarda, M., Blagotić, A., Shangguan, W., Wright, M. N., Geng, X., Bauer-Marschallinger, B., Guevara, M. A., Vargas, R., MacMillan, R. A., Batjes, N. H., Leenaars, J. G. B., Ribeiro, E., Wheeler, I., Mantel, S., and Kempen, B.: SoilGrids250m: Global gridded soil information based on machine learning, PLOS ONE, 12, e0169748, https://doi.org/10.1371/journal.pone.0169748, 2017.

Héroult, A., Lin, Y.-S., Bourne, A., Medlyn, B. E., and Ellsworth, D. S.: Optimal stomatal conductance in relation to photosynthesis in climatically contrasting Eucalyptus species under drought, Plant Cell Environ., 36, 262–274, https://doi.org/10.1111/j.1365-3040.2012.02570.x, 2013.

Heskel, M. A., O'Sullivan, O. S., Reich, P. B., Tjoelker, M. G., Weerasinghe, L. K., Penillard, A., Egerton, J. J. G., Creek, D., Bloomfield, K. J., Xiang, J., Sinca, F., Stangl, Z. R., la Torre, A. M., Griffin, K. L., Huntingford, C., Hurry, V., Meir, P., Turnbull, M. H., and Atkin, O. K.: Convergence in the temperature response of leaf respiration across biomes and plant functional types, P. Natl. Acad. Sci. USA, 113, 3832–3837, https://doi.org/10.1073/pnas.1520282113, 2016.

Hickler, T., Prentice, I. C., Smith, B., Sykes, M. T., and Zaehle, S.: Implementing plant hydraulic architecture within the LPJ Dynamic Global Vegetation Model, Global Ecol. Biogeogr., 15, 567–577, https://doi.org/10.1111/j.1466-8238.2006.00254.x, 2006.

Hodnett, M. G. and Tomasella, J.: Marked differences between van Genuchten soil water-retention parameters for temperate and tropical soils: a new water-retention pedo-transfer functions developed for tropical soils, Geoderma, 108, 155–180, https://doi.org/10.1016/S0016-7061(02)00105-2, 2002.

Horton, R. E.: The role of infiltration in the hydrologic cycle, Eos, T. Am. Geophys. Un., 14, 446–460, https://doi.org/10.1029/TR014i001p00446, 1933.

Hsiao, T. C.: Plant Responses to Water Stress, Annu. Rev. Plant Physiol., 24, 519–570, https://doi.org/10.1146/annurev.pp.24.060173.002511, 1973.

Huaraca Huasco, W., Riutta, T., Girardin, C. A. J., Hancco Pacha, F., Puma Vilca, B. L., Moore, S., Rifai, S. W., del Aguila-Pasquel, J., Araujo Murakami, A., Freitag, R., Morel, A. C., Demissie, S., Doughty, C. E., Oliveras, I., Galiano Cabrera, D. F., Durand Baca, L., Farfán Amézquita, F., Silva Espejo, J. E., da Costa, A. C. L., Oblitas Mendoza, E., Quesada, C. A., Evouna Ondo, F., Edzang Ndong, J., Jeffery, K. J., Mihindou, V., White, L. J. T., N'ssi Bengone, N., Ibrahim, F., Addo-Danso, S. D., Duah-Gyamfi, A., Djaney Djagbletey, G., Owusu-Afriyie, K., Amissah, L., Mbou, A. T., Marthews, T. R., Metcalfe, D. B., Aragão, L. E. O., Marimon-Junior, B. H., Marimon, B. S., Majalap, N., Adu-Bredu, S., Abernethy, K. A., Silman, M., Ewers, R. M., Meir, P., and Malhi, Y.: Fine root dynamics across pantropical rainforest ecosystems, Glob. Change Biol., 27, 3657–3680, https://doi.org/10.1111/gcb.15677, 2021.

Hubau, W., Lewis, S. L., Phillips, O. L., Affum-Baffoe, K., Beeckman, H., Cuní-Sanchez, A., Daniels, A. K., Ewango, C. E. N., Fauset, S., Mukinzi, J. M., Sheil, D., Sonké, B., Sullivan, M. J. P., Sunderland, T. C. H., Taedoumg, H., Thomas, S. C., White, L. J. T., Abernethy, K. A., Adu-Bredu, S., Amani, C. A., Baker, T. R., Banin, L. F., Baya, F., Begne, S. K., Bennett, A. C., Benedet, F., Bitariho, R., Bocko, Y. E., Boeckx, P., Boundja, P., Brienen, R. J. W., Brncic, T., Chezeaux, E., Chuyong, G. B., Clark, C. J., Collins, M., Comiskey, J. A., Coomes, D. A., Dargie, G. C., de Haulleville, T., Kamdem, M. N. D., Doucet, J.-L., Esquivel-Muelbert, A., Feldpausch, T. R., Fofanah, A., Foli, E. G., Gilpin, M., Gloor, E., Gonmadje, C., Gourlet-Fleury, S., Hall, J. S., Hamilton, A. C., Harris, D. J., Hart, T. B., Hockemba, M. B. N., Hladik, A., Ifo, S. A., Jeffery, K. J., Jucker, T., Yakusu, E. K., Kearsley, E., Kenfack, D., Koch, A., Leal, M. E., Levesley,

A., Lindsell, J. A., Lisingo, J., Lopez-Gonzalez, G., Lovett, J. C., Makana, J.-R., Malhi, Y., Marshall, A. R., Martin, J., Martin, E. H., Mbayu, F. M., Medjibe, V. P., Mihindou, V., Mitchard, E. T. A., Moore, S., Munishi, P. K. T., Bengone, N. N., Ojo, L., Ondo, F. E., Peh, K. S.-H., Pickavance, G. C., Poulsen, A. D., Poulsen, J. R., Qie, L., Reitsma, J., Rovero, F., Swaine, M. D., Talbot, J., Taplin, J., Taylor, D. M., Thomas, D. W., Toirambe, B., Mukendi, J. T., Tuagben, D., Umunay, P. M., van der Heijden, G. M. F., Verbeeck, H., Vleminckx, J., Willcock, S., Wöll, H., Woods, J. T., and Zemagho, L.: Asynchronous carbon sink saturation in African and Amazonian tropical forests, Nature, 579, 80–87, https://doi.org/10.1038/s41586-020-2035-0, 2020.

Humbel, F.-X.: Caractérisation, par des mesures physiques, hydriques et d'enracinement, de sols de Guyane francaise à dynamique de l'eau superficielle, Sciences du sol, 2, 83–94, 1978.

Huntingford, C., Zelazowski, P., Galbraith, D., Mercado, L. M., Sitch, S., Fisher, R., Lomas, M., Walker, A. P., Jones, C. D., Booth, B. B. B., Malhi, Y., Hemming, D., Kay, G., Good, P., Lewis, S. L., Phillips, O. L., Atkin, O. K., Lloyd, J., Gloor, E., Zaragoza-Castells, J., Meir, P., Betts, R., Harris, P. P., Nobre, C., Marengo, J., and Cox, P. M.: Simulated resilience of tropical rainforests to CO_2-induced climate change, Nat. Geosci., 6, 268–273, https://doi.org/10.1038/ngeo1741, 2013.

Hutchinson, G. E.: Concluding remarks, Cold Spring Harbor Symposia on Quantitative Biology, 22, 415–427, 1957.

Igarashi, S., Yoshida, S., Kenzo, T., Sakai, S., Nagamasu, H., Hyodo, F., Tayasu, I., Mohamad, M., and Ichie, T.: No evidence of carbon storage usage for seed production in 18 dipterocarp masting species in a tropical rain forest, Oecologia, 204, 717–726, https://doi.org/10.1007/s00442-024-05527-w, 2024.

Iida, Y., Poorter, L., Sterck, F. J., Kassim, A. R., Kubo, T., Potts, M. D., and Kohyama, T. S.: Wood density explains architectural differentiation across 145 co-occurring tropical tree species, Funct. Ecol., 26, 274–282, https://doi.org/10.1111/j.1365-2435.2011.01921.x, 2012.

Ivanov, V. Y., Hutyra, L. R., Wofsy, S. C., Munger, J. W., Saleska, S. R., Oliveira, R. C. de, and Camargo, P. B. de: Root niche separation can explain avoidance of seasonal drought stress and vulnerability of overstory trees to extended drought in a mature Amazonian forest, Water Resour. Res., 48, W12507, https://doi.org/10.1029/2012WR011972, 2012.

Jackson, R. B., Canadell, J., Ehleringer, J. R., Mooney, H. A., Sala, O. E., and Schulze, E. D.: A global analysis of root distributions for terrestrial biomes, Oecologia, 108, 389–411, https://doi.org/10.1007/BF00333714, 1996.

Jackson, R. B., Moore, L. A., Hoffmann, W. A., Pockman, W. T., and Linder, C. R.: Ecosystem rooting depth determined with caves and DNA, P. Natl. Acad. Sci. USA, 96, 11387–11392, https://doi.org/10.1073/pnas.96.20.11387, 1999.

Jarvis, P. G. and McNaughton, K. G.: Stomatal Control of Transpiration: Scaling Up from Leaf to Region, Adv. Ecol. Res., 15, 1–49, https://doi.org/10.1016/S0065-2504(08)60119-1, 1986.

Joetzjer, E., Delire, C., Douville, H., Ciais, P., Decharme, B., Fisher, R., Christoffersen, B., Calvet, J. C., da Costa, A. C. L., Ferreira, L. V., and Meir, P.: Predicting the response of the Amazon rainforest to persistent drought conditions under current and future climates: a major challenge for global land surface models, Geosci. Model Dev., 7, 2933–2950, https://doi.org/10.5194/gmd-7-2933-2014, 2014.

Joetzjer, E., Maignan, F., Chave, J., Goll, D., Poulter, B., Barichivich, J., Maréchaux, I., Luyssaert, S., Guimberteau, M., Naudts, K., Bonal, D., and Ciais, P.: Effect of tree demography and flexible root water uptake for modeling the carbon and water cycles of Amazonia, Ecol. Modell., 469, 109969, https://doi.org/10.1016/j.ecolmodel.2022.109969, 2022.

Johnson, D. J., Condit, R., Hubbell, S. P., and Comita, L. S.: Abiotic niche partitioning and negative density dependence drive tree seedling survival in a tropical forest, Proc. R. Soc. B, 284, 20172210, https://doi.org/10.1098/rspb.2017.2210, 2017.

Johnson, M. O., Galbraith, D., Gloor, M., De Deurwaerder, H., Guimberteau, M., Rammig, A., Thonicke, K., Verbeeck, H., von Randow, C., Monteagudo, A., Phillips, O. L., Brienen, R. J. W., Feldpausch, T. R., Lopez Gonzalez, G., Fauset, S., Quesada, C. A., Christoffersen, B., Ciais, P., Sampaio, G., Kruijt, B., Meir, P., Moorcroft, P., Zhang, K., Alvarez-Davila, E., Alves de Oliveira, A., Amaral, I., Andrade, A., Aragao, L. E. O. C., Araujo-Murakami, A., Arets, E. J. M. M., Arroyo, L., Aymard, G. A., Baraloto, C., Barroso, J., Bonal, D., Boot, R., Camargo, J., Chave, J., Cogollo, A., Cornejo Valverde, F., Lola da Costa, A. C., Di Fiore, A., Ferreira, L., Higuchi, N., Honorio, E. N., Killeen, T. J., Laurance, S. G., Laurance, W. F., Licona, J., Lovejoy, T., Malhi, Y., Marimon, B., Marimon, B. H., Matos, D. C. L., Mendoza, C., Neill, D. A., Pardo, G., Peña-Claros, M., Pitman, N. C. A., Poorter, L., Prieto, A., Ramirez-Angulo, H., Roopsind, A., Rudas, A., Salomao, R. P., Silveira, M., Stropp, J., ter Steege, H., Terborgh, J., Thomas, R., Toledo, M., Torres-Lezama, A., van der Heijden, G. M. F., Vasquez, R., Guimarães Vieira, I. C., Vilanova, E., Vos, V. A., and Baker, T. R.: Variation in stem mortality rates determines patterns of above-ground biomass in Amazonian forests: implications for dynamic global vegetation models, Glob. Change Biol., 22, 3996–4013, https://doi.org/10.1111/gcb.13315, 2016.

Jones, H. G.: Plants and Microclimate: A Quantitative Approach to Environmental Plant Physiology, 3rd Edn., Cambridge University Press, Cambridge, https://doi.org/10.1017/CBO9780511845727, 2013.

Jourdan, M., Kunstler, G., and Morin, X.: How neighbourhood interactions control the temporal stability and resilience to drought of trees in mountain forests, J. Ecol., 108, 666–677, https://doi.org/10.1111/1365-2745.13294, 2020.

Journé, V., Barnagaud, J.-Y., Bernard, C., Crochet, P.-A., and Morin, X.: Correlative climatic niche models predict real and virtual species distributions equally well, Ecology, 101, e02912, https://doi.org/10.1002/ecy.2912, 2020.

Jucker, T., Hardwick, S. R., Both, S., Elias, D. M. O., Ewers, R. M., Milodowski, D. T., Swinfield, T., and Coomes, D. A.: Canopy structure and topography jointly constrain the microclimate of human-modified tropical landscapes, Glob. Change Biol., 24, 5243–5258, https://doi.org/10.1111/gcb.14415, 2018.

Kattge, J. and Knorr, W.: Temperature acclimation in a biochemical model of photosynthesis: a reanalysis of data from 36 species, Plant Cell Environ., 30, 1176–1190, https://doi.org/10.1111/j.1365-3040.2007.01690.x, 2007.

Kattge, J., Díaz, S., Lavorel, S., Prentice, I. C., Leadley, P., Bönisch, G., Garnier, E., Westoby, M., Reich, P. B., Wright, I. J., Cornelissen, J. H. C., Violle, C., Harrison, S. P., Van Bodegom, P. M., Reichstein, M., Enquist, B. J., Soudzilovskaia, N. A., Ackerly, D. D., Anand, M., Atkin, O., Bahn, M., Baker, T. R., Bal-

docchi, D., Bekker, R., Blanco, C. C., Blonder, B., Bond, W. J., Bradstock, R., Bunker, D. E., Casanoves, F., Cavender-bares, J., Chambers, J. Q., Chapin III, F. S., Chave, J., Coomes, D., Cornwell, W. K., Craine, J. M., Dobrin, B. H., Duarte, L., Durka, W., Elser, J., Esser, G., Estiarte, M., Fagan, W. F., Fang, J., Fernández-méndez, F., Fidelis, A., Finegan, B., Flores, O., Ford, H., Frank, D., Freschet, G. T., Fyllas, N. M., Gallagher, R. V., Green, W. A., Gutierrez, A. G., Hickler, T., Higgins, S. I., Hodgson, J. G., Jalili, A., Jansen, S., Joly, C. A., Kerkhoff, A. J., Kirkup, D., Kitajima, K., Kleyer, M., Klotz, S., Knops, J. M. H., Kramer, K., Kühn, I., Kurokawa, H., Laughlin, D., Lee, T. D., Leishman, M., Lens, F., Lenz, T., Lewis, S. L., Lloyd, J., Llusià, J., Louault, F., Ma, S., Mahecha, M. D., Manning, P., Massad, T., Medlyn, B. E., Messier, J., Moles, A. T., Müller, S. C., Nadrowski, K., Naeem, S., Niinemets, Ü., Nöllert, S., Nüske, A., Ogaya, R., Oleksyn, J., Onipchenko, V. G., Onoda, Y., Ordoñez, J., Overbeck, G., Ozinga, W. A., Patiño, S., Paula, S., Pausas, J.G., Peñuelas, J., Phillips, O. L., Pillar, V., Poorter, H., Poorter, L., Poschlod, P., Prinzing, A., Proulx, R., Rammig, A., Reinsch, S., Reu, B., Sack, L., Salgado-Negret, B., Sardans, J., Shiodera, S., Shipley, B., Siefert, A., Sosinski, E., Soussana, J.-F., Swaine, E., Swenson, N., Thompson, K., Thornton, P., Waldram, M., Weiher, E., White, M., White, S., Wright, S. J., Yguel, B., Zaehle, S., Zanne, A. E., and Wirth, C.: TRY – a global database of plant traits, Glob. Change Biol., 17, 2905–2935, https://doi.org/10.1111/j.1365-2486.2011.02451.x, 2011.

Kattge, J., Bönisch, G., Díaz, S., Lavorel, S., Prentice, I. C., Leadley, P., Tautenhahn, S., Werner, G. D. A., Aakala, T., Abedi, M., Acosta, A. T. R., Adamidis, G. C., Adamson, K., Aiba, M., Albert, C. H., Alcántara, J. M., C, C. A., Aleixo, I., Ali, H., Amiaud, B., Ammer, C., Amoroso, M. M., Anand, M., Anderson, C., Anten, N., Antos, J., Apgaua, D. M. G., Ashman, T.-L., Asmara, D. H., Asner, G. P., Aspinwall, M., Atkin, O., Aubin, I., Baastrup-Spohr, L., Bahalkeh, K., Bahn, M., Baker, T., Baker, W. J., Bakker, J. P., Baldocchi, D., Baltzer, J., Banerjee, A., Baranger, A., Barlow, J., Barneche, D. R., Baruch, Z., Bastianelli, D., Battles, J., Bauerle, W., Bauters, M., Bazzato, E., Beckmann, M., Beeckman, H., Beierkuhnlein, C., Bekker, R., Belfry, G., Belluau, M., Beloiu, M., Benavides, R., Benomar, L., Berdugo-Lattke, M. L., Berenguer, E., Bergamin, R., Bergmann, J., Carlucci, M. B., Berner, L., Bernhardt-Römermann, M., Bigler, C., Bjorkman, A. D., Blackman, C., Blanco, C., Blonder, B., Blumenthal, D., Bocanegra-González, K. T., Boeckx, P., Bohlman, S., Böhning-Gaese, K., Boisvert-Marsh, L., Bond, W., Bond-Lamberty, B., Boom, A., Boonman, C. C. F., Bordin, K., Boughton, E. H., Boukili, V., Bowman, D. M. J. S., Bravo, S., Brendel, M. R., Broadley, M. R., Brown, K. A., Bruelheide, H., Brumnich, F., Bruun, H. H., Bruy, D., Buchanan, S. W., Bucher, S. F., Buchmann, N., Buitenwerf, R., Bunker, D. E., et al.: TRY plant trait database – enhanced coverage and open access, Glob. Change Biol., 26, 119–188, https://doi.org/10.1111/gcb.14904, 2020.

Kazmierczak, M., Wiegand, T., and Huth, A.: A neutral vs. non-neutral parametrizations of a physiological forest gap model, Ecol. Model., 288, 94–102, https://doi.org/10.1016/j.ecolmodel.2014.05.002, 2014.

Kearney, M. and Porter, W.: Mechanistic niche modelling: combining physiological and spatial data to predict species' ranges, Ecol. Lett., 12, 334–350, https://doi.org/10.1111/j.1461-0248.2008.01277.x, 2009.

Keenan, T., Sabate, S., and Gracia, C.: Soil water stress and coupled photosynthesis–conductance models: Bridging the gap between conflicting reports on the relative roles of stomatal, mesophyll conductance and biochemical limitations to photosynthesis, Agr. Forest Meteorol., 150, 443–453, https://doi.org/10.1016/j.agrformet.2010.01.008, 2010.

Kennedy, D., Swenson, S., Oleson, K. W., Lawrence, D. M., Fisher, R., Costa, A. C. L. da, and Gentine, P.: Implementing Plant Hydraulics in the Community Land Model, Version 5, J. Adv. Model. Earth Sy., 11, 485–513, https://doi.org/10.1029/2018MS001500, 2019.

Kenzo, T., Ichie, T., Hattori, D., Itioka, T., Handa, C., Ohkubo, T., Kendawang, J. J., Nakamura, M., Sakaguchi, M., Takahashi, N., Okamoto, M., Tanaka-Oda, A., Sakurai, K., and Ninomiya, I.: Development of allometric relationships for accurate estimation of above- and below-ground biomass in tropical secondary forests in Sarawak, Malaysia, J. Trop. Ecol., 25, 371–386, https://doi.org/10.1017/S0266467409006129, 2009.

Khan, S., Maréchaux, I., Vieilledent, G., Guitet, S., Brunaux, O., Ferry, B., Soulard, F., Stahl, C., Baraloto, C., Fortunel, C., and Freycon, V.: Regional Soil Profile Data Reveals the Predominant Role of Geomorphology and Geology in Accurately Deriving Digital Soil Texture Maps in a Tropical Area, SSRN [preprint], https://doi.org/10.2139/ssrn.4789279, 9 April 2024.

King, D. A., Davies, S. J., Tan, S., and Noor, N. S. Md.: The role of wood density and stem support costs in the growth and mortality of tropical trees, J. Ecol., 94, 670–680, https://doi.org/10.1111/j.1365-2745.2006.01112.x, 2006.

Kitajima, K., Mulkey, S., and Wright, S.: Decline of photosynthetic capacity with leaf age in relation to leaf longevities for five tropical canopy tree species, Am. J. Bot., 84, 702–702, 1997a.

Kitajima, K., Mulkey, S. S., and Wright, S. J.: Seasonal leaf phenotypes in the canopy of a tropical dry forest: photosynthetic characteristics and associated traits, Oecologia, 109, 490–498, https://doi.org/10.1007/s004420050109, 1997b.

Kitajima, K., Mulkey, S. S., Samaniego, M., and Wright, S. J.: Decline of photosynthetic capacity with leaf age and position in two tropical pioneer tree species, Am. J. Bot., 89, 1925–1932, https://doi.org/10.3732/ajb.89.12.1925, 2002.

Kitajima, K., Mulkey, S. S., and Wright, S. J.: Variation in crown light utilization characteristics among tropical canopy trees, Ann. Bot., 95, 535–547, https://doi.org/10.1093/aob/mci051, 2005.

Koch, A., Hubau, W., and Lewis, S. L.: Earth System Models Are Not Capturing Present-Day Tropical Forest Carbon Dynamics, Earth's Future, 9, e2020EF001874, https://doi.org/10.1029/2020EF001874, 2021.

Köhler, P. and Huth, A.: The effects of tree species grouping in tropical rainforest modelling: simulations with the individual-based model Formind, Ecol. Model., 109, 301–321, https://doi.org/10.1016/S0304-3800(98)00066-0, 1998.

Köhler, P., Ditzer, T., and Huth, A.: Concepts for the aggregation of tropical tree species into functional types and the application to Sabah's lowland rain forests, J. Trop. Ecol., 16, 591–602, https://doi.org/null, 2000.

König, L. A., Mohren, F., Schelhaas, M.-J., Bugmann, H., and Nabuurs, G.-J.: Tree regeneration in models of forest dynamics – Suitability to assess climate change impacts

on European forests, Forest Ecol. Manage., 520, 120390, https://doi.org/10.1016/j.foreco.2022.120390, 2022.

Körner, C.: Paradigm shift in plant growth control, Curr. Opin. Plant Biol., 25, 107–114, https://doi.org/10.1016/j.pbi.2015.05.003, 2015.

Koven, C. D., Knox, R. G., Fisher, R. A., Chambers, J. Q., Christoffersen, B. O., Davies, S. J., Detto, M., Dietze, M. C., Faybishenko, B., Holm, J., Huang, M., Kovenock, M., Kueppers, L. M., Lemieux, G., Massoud, E., McDowell, N. G., Muller-Landau, H. C., Needham, J. F., Norby, R. J., Powell, T., Rogers, A., Serbin, S. P., Shuman, J. K., Swann, A. L. S., Varadharajan, C., Walker, A. P., Wright, S. J., and Xu, C.: Benchmarking and parameter sensitivity of physiological and vegetation dynamics using the Functionally Assembled Terrestrial Ecosystem Simulator (FATES) at Barro Colorado Island, Panama, Biogeosciences, 17, 3017–3044, https://doi.org/10.5194/bg-17-3017-2020, 2020.

Kraft, N. J. B., Metz, M. R., Condit, R. S., and Chave, J.: The relationship between wood density and mortality in a global tropical forest data set, New Phytol., 188, 1124–1136, https://doi.org/10.1111/j.1469-8137.2010.03444.x, 2010.

Krinner, G., Viovy, N., de Noblet-Ducoudré, N., Ogée, J., Polcher, J., Friedlingstein, P., Ciais, P., Sitch, S., and Prentice, I. C.: A dynamic global vegetation model for studies of the coupled atmosphere-biosphere system, Global Biogeochem. Cy., 19, GB1015, https://doi.org/10.1029/2003GB002199, 2005.

Kume, A., Nasahara, K. N., Nagai, S., and Muraoka, H.: The ratio of transmitted near-infrared radiation to photosynthetically active radiation (PAR) increases in proportion to the adsorbed PAR in the canopy, J. Plant Res., 124, 99–106, https://doi.org/10.1007/s10265-010-0346-1, 2011.

Kupers, S. J., Engelbrecht, B. M. J., Hernández, A., Wright, S. J., Wirth, C., and Rüger, N.: Growth responses to soil water potential indirectly shape local species distributions of tropical forest seedlings, J. Ecol., 107, 860–874, https://doi.org/10.1111/1365-2745.13096, 2019.

Kursar, T. A., Engelbrecht, B. M. J., Burke, A., Tyree, M. T., EI Omari, B., and Giraldo, J. P.: Tolerance to low leaf water status of tropical tree seedlings is related to drought performance and distribution, Funct. Ecol., 23, 93–102, https://doi.org/10.1111/j.1365-2435.2008.01483.x, 2009.

Lagarrigues, G., Jabot, F., Lafond, V., and Courbaud, B.: Approximate Bayesian computation to recalibrate individual-based models with population data: illustration with a forest simulation model, Ecol. Model., 306, 278–286, https://doi.org/10.1016/j.ecolmodel.2014.09.023, 2015.

Laio, F., Porporato, A., Ridolfi, L., and Rodriguez-Iturbe, I.: Plants in water-controlled ecosystems: active role in hydrologic processes and response to water stress: II. Probabilistic soil moisture dynamics, Adv. Water Resour., 24, 707–723, https://doi.org/10.1016/S0309-1708(01)00005-7, 2001.

Lamour, J., Davidson, K. J., Ely, K. S., Le Moguédec, G., Leakey, A. D. B., Li, Q., Serbin, S. P., and Rogers, A.: An improved representation of the relationship between photosynthesis and stomatal conductance leads to more stable estimation of conductance parameters and improves the goodness-of-fit across diverse data sets, Glob. Change Biol., 28, 3537–3556, https://doi.org/10.1111/gcb.16103, 2022.

Lamour, J., Souza, D. C., Gimenez, B. O., Higuchi, N., Chave, J., Chambers, J., and Rogers, A.: Wood-density has no effect on stomatal control of leaf-level water use efficiency in an Amazonian forest, Plant Cell Environ., 46, 3806–3821, https://doi.org/10.1111/pce.14704, 2023.

Lamour, J., Davidson, K. J., Ely, K. S., Le Moguédec, G., Anderson, J. A., Li, Q., Calderón, O., Koven, C. D., Wright, S. J., Walker, A. P., Serbin, S. P., and Rogers, A.: The effect of the vertical gradients of photosynthetic parameters on the CO assimilation and transpiration of a Panamanian tropical forest, New Phytol., 238, 2345–2362, https://doi.org/10.1111/nph.18901, 2023a.

Lapola, D. M., Pinho, P., Barlow, J., Aragão, L. E. O. C., Berenguer, E., Carmenta, R., Liddy, H. M., Seixas, H., Silva, C. V. J., Silva-Junior, C. H. L., Alencar, A. A. C., Anderson, L. O., Armenteras, D., Brovkin, V., Calders, K., Chambers, J., Chini, L., Costa, M. H., Faria, B. L., Fearnside, P. M., Ferreira, J., Gatti, L., Gutierrez-Velez, V. H., Han, Z., Hibbard, K., Koven, C., Lawrence, P., Pongratz, J., Portela, B. T. T., Rounsevell, M., Ruane, A. C., Schaldach, R., da Silva, S. S., von Randow, C., and Walker, W. S.: The drivers and impacts of Amazon forest degradation, Science, 379, eabp8622, https://doi.org/10.1126/science.abp8622, 2023b.

Laurans, M., Munoz, F., Charles-Dominique, T., Heuret, P., Fortunel, C., Isnard, S., Sabatier, S.-A., Caraglio, Y., and Violle, C.: Why incorporate plant architecture into trait-based ecology?, Trend. Ecol. Evol., 39, 524–536, https://doi.org/10.1016/j.tree.2023.11.011, 2024.

LeBauer, D. S., Wang, D., Richter, K. T., Davidson, C. C., and Dietze, M. C.: Facilitating feedbacks between field measurements and ecosystem models, Ecol. Monogr., 83, 133–154, https://doi.org/10.1890/12-0137.1, 2013.

Ledo, A., Paul, K. I., Burslem, D. F. R. P., Ewel, J. J., Barton, C., Battaglia, M., Brooksbank, K., Carter, J., Eid, T. H., England, J. R., Fitzgerald, A., Jonson, J., Mencuccini, M., Montagu, K. D., Montero, G., Mugasha, W. A., Pinkard, E., Roxburgh, S., Ryan, C. M., Ruiz-Peinado, R., Sochacki, S., Specht, A., Wildy, D., Wirth, C., Zerihun, A., and Chave, J.: Tree size and climatic water deficit control root to shoot ratio in individual trees globally, New Phytol., 217, 8–11, https://doi.org/10.1111/nph.14863, 2018.

Leitold, V., Morton, D. C., Longo, M., dos-Santos, M. N., Keller, M., and Scaranello, M.: El Niño drought increased canopy turnover in Amazon forests, New Phytol., 219, 959–971, https://doi.org/10.1111/nph.15110, 2018.

Lenz, T. I., Wright, I. J., and Westoby, M.: Interrelations among pressure–volume curve traits across species and water availability gradients, Physiol. Plant., 127, 423–433, https://doi.org/10.1111/j.1399-3054.2006.00680.x, 2006.

Leuning, R., Kelliher, F. M., Pury, D. G. G., and Schulze, E. -d: Leaf nitrogen, photosynthesis, conductance and transpiration: scaling from leaves to canopies, Plant Cell Environ., 18, 1183–1200, https://doi.org/10.1111/j.1365-3040.1995.tb00628.x, 1995.

Leuning, R.: A critical appraisal of a combined stomatal-photosynthesis model for C3 plants, Plant Cell Environ., 18, 339–355, https://doi.org/10.1111/j.1365-3040.1995.tb00370.x, 1995.

Liang, J. and Picard, N.: Matrix Model of Forest Dynamics: An Overview and Outlook, Forest Sci., 59, 359–378, https://doi.org/10.5849/forsci.11-123, 2013.

Liang, X., Lettenmaier, D. P., Wood, E. F., and Burges, S. J.: A simple hydrologically based model of land surface water and en-

ergy fluxes for general circulation models, J. Geophys. Res., 99, 14415–14428, https://doi.org/10.1029/94JD00483, 1994.

Lin, Y.-S., Medlyn, B. E., Duursma, R. A., Prentice, I. C., Wang, H., Baig, S., Eamus, D., de Dios, V. R., Mitchell, P., Ellsworth, D. S., de Beeck, M. O., Wallin, G., Uddling, J., Tarvainen, L., Linderson, M.-L., Cernusak, L. A., Nippert, J. B., Ocheltree, T. W., Tissue, D. T., Martin-StPaul, N. K., Rogers, A., Warren, J. M., De Angelis, P., Hikosaka, K., Han, Q., Onoda, Y., Gimeno, T. E., Barton, C. V. M., Bennie, J., Bonal, D., Bosc, A., Löw, M., Macinins-Ng, C., Rey, A., Rowland, L., Setterfield, S. A., Tausz-Posch, S., Zaragoza-Castells, J., Broadmeadow, M. S. J., Drake, J. E., Freeman, M., Ghannoum, O., Hutley, L. B., Kelly, J. W., Kikuzawa, K., Kolari, P., Koyama, K., Limousin, J.-M., Meir, P., Lola da Costa, A. C., Mikkelsen, T. N., Salinas, N., Sun, W., and Wingate, L.: Optimal stomatal behaviour around the world, Nat. Clim. Change, 5, 459–464, https://doi.org/10.1038/nclimate2550, 2015.

Liu, Y., Parolari, A. J., Kumar, M., Huang, C.-W., Katul, G. G., and Porporato, A.: Increasing atmospheric humidity and CO_2 concentration alleviate forest mortality risk, P. Natl. Acad. Sci. USA, 114, 9918–9923, https://doi.org/10.1073/pnas.1704811114, 2017.

Lloyd, J., Patiño, S., Paiva, R. Q., Nardoto, G. B., Quesada, C. A., Santos, A. J. B., Baker, T. R., Brand, W. A., Hilke, I., Gielmann, H., Raessler, M., Luizão, F. J., Martinelli, L. A., and Mercado, L. M.: Optimisation of photosynthetic carbon gain and within-canopy gradients of associated foliar traits for Amazon forest trees, Biogeosciences, 7, 1833–1859, https://doi.org/10.5194/bg-7-1833-2010, 2010.

Long, S. P., Postl, W. F., and Bolhár-Nordenkampf, H. R.: Quantum yields for uptake of carbon dioxide in C3 vascular plants of contrasting habitats and taxonomic groupings, Planta, 189, 226–234, https://doi.org/10.1007/BF00195081, 1993.

Longo, M., Knox, R. G., Levine, N. M., Alves, L. F., Bonal, D., Camargo, P. B., Fitzjarrald, D. R., Hayek, M. N., Restrepo-Coupe, N., Saleska, S. R., Silva, R. da, Stark, S. C., Tapajós, R. P., Wiedemann, K. T., Zhang, K., Wofsy, S. C., and Moorcroft, P. R.: Ecosystem heterogeneity and diversity mitigate Amazon forest resilience to frequent extreme droughts, New Phytol., 914–931, https://doi.org/10.1111/nph.15185@10.1111/(ISSN)1469-8137.DroughtImpactsonTropicalForests, 2018.

Longo, M., Knox, R. G., Medvigy, D. M., Levine, N. M., Dietze, M. C., Kim, Y., Swann, A. L. S., Zhang, K., Rollinson, C. R., Bras, R. L., Wofsy, S. C., and Moorcroft, P. R.: The biophysics, ecology, and biogeochemistry of functionally diverse, vertically and horizontally heterogeneous ecosystems: the Ecosystem Demography model, version 2.2 – Part 1: Model description, Geosci. Model Dev., 12, 4309–4346, https://doi.org/10.5194/gmd-12-4309-2019, 2019.

Loubry, D.: La phénologie des arbres caducifoliés en forêt guyanaise (5° de latitude nord): illustration d'un déterminisme à composantes endogène et exogène, Can. J. Bot., 72, 1843–1857, https://doi.org/10.1139/b94-226, 1994.

Maclean, I. M. D. and Klinges, D. H.: Microclimc: A mechanistic model of above, below and within-canopy microclimate, Ecol. Model., 451, 109567, https://doi.org/10.1016/j.ecolmodel.2021.109567, 2021.

Mahnken, M., Cailleret, M., Collalti, A., Trotta, C., Biondo, C., D'Andrea, E., Dalmonech, D., Marano, G., Mäkelä, A., Minunno, F., Peltoniemi, M., Trotsiuk, V., Nadal-Sala, D., Sabaté, S., Vallet, P., Aussenac, R., Cameron, D. R., Bohn, F. J., Grote, R., Augustynczik, A. L. D., Yousefpour, R., Huber, N., Bugmann, H., Merganičová, K., Merganic, J., Valent, P., Lasch-Born, P., Hartig, F., Vega del Valle, I. D., Volkholz, J., Gutsch, M., Matteucci, G., Krejza, J., Ibrom, A., Meesenburg, H., Rötzer, T., van der Maaten-Theunissen, M., van der Maaten, E., and Reyer, C. P. O.: Accuracy, realism and general applicability of European forest models, Glob. Change Biol., 28, 6921–6943, https://doi.org/10.1111/gcb.16384, 2022.

Malhi, Y.: The productivity, metabolism and carbon cycle of tropical forest vegetation, J. Ecol., 100, 65–75, https://doi.org/10.1111/j.1365-2745.2011.01916.x, 2012.

Malhi, Y., Doughty, C., and Galbraith, D.: The allocation of ecosystem net primary productivity in tropical forests, Philos. T. Roy. Soc. Lond. B, 366, 3225–3245, https://doi.org/10.1098/rstb.2011.0062, 2011.

Manabe, S.: Climate and the ocean circulation: I. The atmospheric circulation and the hydrology of the earth's surface, Mon. Weather Rev., 97, 739–774, https://doi.org/10.1175/1520-0493(1969)097<0739:CATOC>2.3.CO;2, 1969.

Manoli, G., Ivanov, V. Y., and Fatichi, S.: Dry-Season Greening and Water Stress in Amazonia: The Role of Modeling Leaf Phenology, J. Geophys. Res.-Biogeo., 123, 1909–1926, https://doi.org/10.1029/2017JG004282, 2018.

Manzoni, S.: Integrating plant hydraulics and gas exchange along the drought-response trait spectrum, Tree Physiol., 34, 1031–1034, https://doi.org/10.1093/treephys/tpu088, 2014.

Manzoni, S., Vico, G., Katul, G., Fay, P. A., Polley, W., Palmroth, S., and Porporato, A.: Optimizing stomatal conductance for maximum carbon gain under water stress: a meta-analysis across plant functional types and climates, Funct. Ecol., 25, 456–467, https://doi.org/10.1111/j.1365-2435.2010.01822.x, 2011.

Maréchaux, I. and Chave, J.: An individual-based forest model to jointly simulate carbon and tree diversity in Amazonia: description and applications, Ecol. Monogr., 87, 632–664, https://doi.org/10.1002/ecm.1271, 2017.

Maréchaux, I., Bartlett, M. K., Sack, L., Baraloto, C., Engel, J., Joetzjer, E., and Chave, J.: Drought tolerance as predicted by leaf water potential at turgor loss point varies strongly across species within an Amazonian forest, Funct. Ecol., 29, 1268–1277, https://doi.org/10.1111/1365-2435.12452, 2015.

Maréchaux, I., Bartlett, M. K., Gaucher, P., Sack, L., and Chave, J.: Causes of variation in leaf-level drought tolerance within an Amazonian forest, J. Plant Hydraul., 3, e004, https://doi.org/10.20870/jph.2016.e004, 2016.

Maréchaux, I., Bonal, D., Bartlett, M. K., Burban, B., Coste, S., Courtois, E. A., Dulormne, M., Goret, J.-Y., Mira, E., Mirabel, A., Sack, L., Stahl, C., and Chave, J.: Dry-season decline in tree sapflux is correlated with leaf turgor loss point in a tropical rainforest, Funct. Ecol., 32, 2285–2297, https://doi.org/10.1111/1365-2435.13188, 2018.

Maréchaux, I., Saint-André, L., Bartlett, M. K., Sack, L., and Chave, J.: Leaf drought tolerance cannot be inferred from classic leaf traits in a tropical rainforest, J. Ecol., 108, 1030–1045, https://doi.org/10.1111/1365-2745.13321, 2020.

Maréchaux, I., Langerwisch, F., Huth, A., Bugmann, H., Morin, X., Reyer, C. P. O., Seidl, R., Collalti, A., Paula, M. D. de, Fischer, R., Gutsch, M., Lexer, M. J., Lischke, H., Rammig, A., Rödig,

E., Sakschewski, B., Taubert, F., Thonicke, K., Vacchiano, G., and Bohn, F. J.: Tackling unresolved questions in forest ecology: The past and future role of simulation models, Ecol. Evol., 11, 3746–3770, https://doi.org/10.1002/ece3.7391, 2021.

Maréchaux, I., Fischer, F. J., Schmitt, S., and Chave, J.: TROLL-code/TROLL: GMD preprint (4.0.0-GMD), Zenodo [code], https://doi.org/10.5281/zenodo.14013147, 2024.

Marthews, T. R., Malhi, Y., and Iwata, H.: Calculating downward longwave radiation under clear and cloudy conditions over a tropical lowland forest site: an evaluation of model schemes for hourly data, Theor. Appl. Climatol., 107, 461–477, https://doi.org/10.1007/s00704-011-0486-9, 2012.

Marthews, T. R., Quesada, C. A., Galbraith, D. R., Malhi, Y., Mullins, C. E., Hodnett, M. G., and Dharssi, I.: High-resolution hydraulic parameter maps for surface soils in tropical South America, Geosci. Model Dev., 7, 711–723, https://doi.org/10.5194/gmd-7-711-2014, 2014.

Martínez-Vilalta, J., Sala, A., Asensio, D., Galiano, L., Hoch, G., Palacio, S., Piper, F. I., and Lloret, F.: Dynamics of non-structural carbohydrates in terrestrial plants: a global synthesis, Ecol. Monogr., 86, 495–516, https://doi.org/10.1002/ecm.1231, 2016.

Martin-StPaul, N., Delzon, S., and Cochard, H.: Plant resistance to drought depends on timely stomatal closure, Ecol. Lett., 20, 1437–1447, https://doi.org/10.1111/ele.12851, 2017.

Massman, W. J.: A review of the molecular diffusivities of H_2O, CO_2, CH_4, CO, O_3, SO_2, NH_3, N_2O, NO, and NO_2 in air, O_2 and N_2 near STP, Atmos. Environ., 32, 1111–1127, https://doi.org/10.1016/S1352-2310(97)00391-9, 1998.

McDowell, N. G., Sapes, G., Pivovaroff, A., Adams, H. D., Allen, C. D., Anderegg, W. R. L., Arend, M., Breshears, D. D., Brodribb, T., Choat, B., Cochard, H., De Cáceres, M., De Kauwe, M. G., Grossiord, C., Hammond, W. M., Hartmann, H., Hoch, G., Kahmen, A., Klein, T., Mackay, D. S., Mantova, M., Martínez-Vilalta, J., Medlyn, B. E., Mencuccini, M., Nardini, A., Oliveira, R. S., Sala, A., Tissue, D. T., Torres-Ruiz, J. M., Trowbridge, A. M., Trugman, A. T., Wiley, E., and Xu, C.: Mechanisms of woody-plant mortality under rising drought, CO_2 and vapour pressure deficit, Nat. Rev. Earth Environ., 3, 294–308, https://doi.org/10.1038/s43017-022-00272-1, 2022.

McMahon, S. M., Harrison, S. P., Armbruster, W. S., Bartlein, P. J., Beale, C. M., Edwards, M. E., Kattge, J., Midgley, G., Morin, X., and Prentice, I. C.: Improving assessment and modelling of climate change impacts on global terrestrial biodiversity, Trend. Ecol. Evol., 26, 249–259, https://doi.org/10.1016/j.tree.2011.02.012, 2011.

Medlyn, B. E., Robinson, A. P., Clement, R., and McMurtrie, R. E.: On the validation of models of forest CO_2 exchange using eddy covariance data: some perils and pitfalls, Tree Physiol., 25, 839–857, https://doi.org/10.1093/treephys/25.7.839, 2005.

Medlyn, B. E., Pepper, D. A., O'Grady, A. P., and Keith, H.: Linking leaf and tree water use with an individual-tree model, Tree Physiol., 27, 1687–1699, https://doi.org/10.1093/treephys/27.12.1687, 2007.

Medlyn, B. E., Duursma, R. A., Eamus, D., Ellsworth, D. S., Prentice, I. C., Barton, C. V. M., Crous, K. Y., De Angelis, P., Freeman, M., and Wingate, L.: Reconciling the optimal and empirical approaches to modelling stomatal conductance, Glob. Change Biol., 17, 2134–2144, https://doi.org/10.1111/j.1365-2486.2010.02375.x, 2011.

Medlyn, B. E., Zaehle, S., De Kauwe, M. G., Walker, A. P., Dietze, M. C., Hanson, P. J., Hickler, T., Jain, A. K., Luo, Y., Parton, W., Prentice, I. C., Thornton, P. E., Wang, S., Wang, Y.-P., Weng, E., Iversen, C. M., McCarthy, H. R., Warren, J. M., Oren, R., and Norby, R. J.: Using ecosystem experiments to improve vegetation models, Nat. Clim. Change, 5, 528–534, https://doi.org/10.1038/nclimate2621, 2015.

Medlyn, B. E., De Kauwe, M. G., Zaehle, S., Walker, A. P., Duursma, R. A., Luus, K., Mishurov, M., Pak, B., Smith, B., Wang, Y.-P., Yang, X., Crous, K. Y., Drake, J. E., Gimeno, T. E., Macdonald, C. A., Norby, R. J., Power, S. A., Tjoelker, M. G., and Ellsworth, D. S.: Using models to guide field experiments: a priori predictions for the CO_2 response of a nutrient- and water-limited native Eucalypt woodland, Glob. Change Biol., 22, 2834–2851, https://doi.org/10.1111/gcb.13268, 2016.

Medvigy, D., Wofsy, S. C., Munger, J. W., Hollinger, D. Y., and Moorcroft, P. R.: Mechanistic scaling of ecosystem function and dynamics in space and time: Ecosystem Demography model version 2, J. Geophys. Res., 114, G01002, https://doi.org/10.1029/2008JG000812, 2009.

Meinzer, F. C., Andrade, J. L., Goldstein, G., Holbrook, N. M., Cavelier, J., and Jackson, P.: Control of transpiration from the upper canopy of a tropical forest: the role of stomatal, boundary layer and hydraulic architecture components, Plant Cell Environ., 20, 1242–1252, https://doi.org/10.1046/j.1365-3040.1997.d01-26.x, 1997.

Meinzer, F. C., Woodruff, D. R., Marias, D. E., Smith, D. D., McCulloh, K. A., Howard, A. R., and Magedman, A. L.: Mapping "hydroscapes" along the iso- to anisohydric continuum of stomatal regulation of plant water status, Ecol. Lett., 19, 1343–1352, https://doi.org/10.1111/ele.12670, 2016.

Meir, P. and Grace, J.: Scaling relationships for woody tissue respiration in two tropical rain forests, Plant Cell Environ., 25, 963–973, https://doi.org/10.1046/j.1365-3040.2002.00877.x, 2002.

Meir, P., Grace, J., and Miranda, A. C.: Leaf respiration in two tropical rainforests: constraints on physiology by phosphorus, nitrogen and temperature, Funct. Ecol., 15, 378–387, https://doi.org/10.1046/j.1365-2435.2001.00534.x, 2001.

Meir, P., Cox, P., and Grace, J.: The influence of terrestrial ecosystems on climate, Trend. Ecol. Evol., 21, 254–260, https://doi.org/10.1016/j.tree.2006.03.005, 2006.

Mencuccini, M., Martínez-Vilalta, J., Vanderklein, D., Hamid, H. A., Korakaki, E., Lee, S., and Michiels, B.: Size-mediated ageing reduces vigour in trees, Ecol. Lett., 8, 1183–1190, https://doi.org/10.1111/j.1461-0248.2005.00819.x, 2005.

Menezes, J., Garcia, S., Grandis, A., Nascimento, H., Domingues, T. F., Guedes, A. V., Aleixo, I., Camargo, P., Campos, J., Damasceno, A., Dias-Silva, R., Fleischer, K., Kruijt, B., Cordeiro, A. L., Martins, N. P., Meir, P., Norby, R. J., Pereira, I., Portela, B., Rammig, A., Ribeiro, A. G., Lapola, D. M., and Quesada, C. A.: Changes in leaf functional traits with leaf age: when do leaves decrease their photosynthetic capacity in Amazonian trees?, Tree Physiol., 42, 922–938, https://doi.org/10.1093/treephys/tpab042, 2021.

Mercado, L. M., Lloyd, J., Dolman, A. J., Sitch, S., and Patiño, S.: Modelling basin-wide variations in Amazon forest productivity – Part 1: Model calibration, evaluation and upscaling func-

tions for canopy photosynthesis, Biogeosciences, 6, 1247–1272, https://doi.org/10.5194/bg-6-1247-2009, 2009.

Mercado, L. M., Patiño, S., Domingues, T. F., Fyllas, N. M., Weedon, G. P., Sitch, S., Quesada, C. A., Phillips, O. L., Aragão, L. E. O. C., Malhi, Y., Dolman, A. J., Restrepo-Coupe, N., Saleska, S. R., Baker, T. R., Almeida, S., Higuchi, N., and Lloyd, J.: Variations in Amazon forest productivity correlated with foliar nutrients and modelled rates of photosynthetic carbon supply, Phil. Trans. R. Soc. B, 366, 3316–3329, https://doi.org/10.1098/rstb.2011.0045, 2011.

Merganičová, K., Merganič, J., Lehtonen, A., Vacchiano, G., Zorana, M., Ostrogović, S., Augustynczik, A. L. D., Grote, R., Kyselová, I., Mäkelä, A., Yousefpour, R., Krejza, J., Collalti, A., and Reyer, C.: Forest carbon allocation modelling under climate change, Tree Physiol., 39, 1937–1960, https://doi.org/10.1093/treephys/tpz105, 2019.

Merlin, O., Stefan, V. G., Amazirh, A., Chanzy, A., Ceschia, E., Er-Raki, S., Gentine, P., Tallec, T., Ezzahar, J., Bircher, S., Beringer, J., and Khabba, S.: Modeling soil evaporation efficiency in a range of soil and atmospheric conditions using a meta-analysis approach, Water Resour. Res., 52, 3663–3684, https://doi.org/10.1002/2015WR018233, 2016.

Metcalfe, D. B., Meir, P., Aragão, L. E. O. C., Costa, A. C. L. da, Braga, A. P., Gonçalves, P. H. L., Junior, J. de A. S., Almeida, S. S. de, Dawson, L. A., Malhi, Y., and Williams, M.: The effects of water availability on root growth and morphology in an Amazon rainforest, Plant Soil, 311, 189–199, https://doi.org/10.1007/s11104-008-9670-9, 2008.

Mokany, K., Ferrier, S., Connolly, S. R., Dunstan, P. K., Fulton, E. A., Harfoot, M. B., Harwood, T. D., Richardson, A. J., Roxburgh, S. H., Scharlemann, J. P. W., Tittensor, D. P., Westcott, D. A., and Wintle, B. A.: Integrating modelling of biodiversity composition and ecosystem function, Oikos, 125, 10–19, https://doi.org/10.1111/oik.02792, 2016.

Moles, A. T. and Westoby, M.: Seed size and plant strategy across the whole life cycle, Oikos, 113, 91–105, https://doi.org/10.1111/j.0030-1299.2006.14194.x, 2006.

Moles, A. T., Falster, D. S., Leishman, M. R., and Westoby, M.: Small-seeded species produce more seeds per square metre of canopy per year, but not per individual per lifetime, J. Ecol., 92, 384–396, https://doi.org/10.1111/j.0022-0477.2004.00880.x, 2004.

Moorcroft, P. R.: Recent advances in ecosystem-atmosphere interactions: an ecological perspective, Proc. Roy. Soc. Lond. B, 270, 1215–1227, https://doi.org/10.1098/rspb.2002.2251, 2003.

Moorcroft, P. R.: How close are we to a predictive science of the biosphere?, Trend. Ecol. Evol., 21, 400–407, https://doi.org/10.1016/j.tree.2006.04.009, 2006.

Moorcroft, P. R., Hurtt, G. C., and Pacala, S. W.: A method for scaling vegetation dynamics: the ecosystem demography model, Ecol. Monogr., 71, 557–586, https://doi.org/10.1890/0012-9615(2001)071[0557:AMFSVD]2.0.CO;2, 2001.

Morin, X. and Lechowicz, M. J.: Contemporary perspectives on the niche that can improve models of species range shifts under climate change, Biol. Lett., 4, 573–576, https://doi.org/10.1098/rsbl.2008.0181, 2008.

Morin, X. and Thuiller, W.: Comparing niche-and process-based models to reduce prediction uncertainty in species range shifts under climate change, Ecology, 90, 1301–1313, 2009.

Mualem, Y.: A new model for predicting the hydraulic conductivity of unsaturated porous media, Water Resour. Res., 12, 513–522, https://doi.org/10.1029/WR012i003p00513, 1976.

Muir, C. D.: Making pore choices: repeated regime shifts in stomatal ratio, Proc. Roy. Soc. B, 282, 20151498, https://doi.org/10.1098/rspb.2015.1498, 2015.

Muller, B., Pantin, F., Génard, M., Turc, O., Freixes, S., Piques, M., and Gibon, Y.: Water deficits uncouple growth from photosynthesis, increase C content, and modify the relationships between C and growth in sink organs, J. Exp. Bot., 62, 1715–1729, https://doi.org/10.1093/jxb/erq438, 2011.

Muller-Landau, H. C., Wright, S. J., Calderón, O., Condit, R., and Hubbell, S. P.: Interspecific variation in primary seed dispersal in a tropical forest, J. Ecol., 96, 653–667, https://doi.org/10.1111/j.1365-2745.2008.01399.x, 2008.

Muñoz-Sabater, J., Dutra, E., Agustí-Panareda, A., Albergel, C., Arduini, G., Balsamo, G., Boussetta, S., Choulga, M., Harrigan, S., Hersbach, H., Martens, B., Miralles, D. G., Piles, M., Rodríguez-Fernández, N. J., Zsoter, E., Buontempo, C., and Thépaut, J.-N.: ERA5-Land: a state-of-the-art global reanalysis dataset for land applications, Earth Syst. Sci. Data, 13, 4349–4383, https://doi.org/10.5194/essd-13-4349-2021, 2021.

Naudts, K., Ryder, J., McGrath, M. J., Otto, J., Chen, Y., Valade, A., Bellasen, V., Berhongaray, G., Bönisch, G., Campioli, M., Ghattas, J., De Groote, T., Haverd, V., Kattge, J., MacBean, N., Maignan, F., Merilä, P., Penuelas, J., Peylin, P., Pinty, B., Pretzsch, H., Schulze, E. D., Solyga, D., Vuichard, N., Yan, Y., and Luyssaert, S.: A vertically discretised canopy description for ORCHIDEE (SVN r2290) and the modifications to the energy, water and carbon fluxes, Geosci. Model Dev., 8, 2035–2065, https://doi.org/10.5194/gmd-8-2035-2015, 2015.

Nemetschek, D., Derroire, G., Marcon, E., Aubry-Kientz, M., Auer, J., Badouard, V., Baraloto, C., Bauman, D., Le Blaye, Q., Boisseaux, M., Bonal, D., Coste, S., Dardevet, E., Heuret, P., Hietz, P., Levionnois, S., Maréchaux, I., McMahon, S. M., Stahl, C., Vleminckx, J., Wanek, W., Ziegler, C., and Fortunel, C.: Climate anomalies and neighbourhood crowding interact in shaping tree growth in old-growth and selectively logged tropical forests, J. Ecol., 112, 590–612, https://doi.org/10.1111/1365-2745.14256, 2024.

Nemetschek, D., Fortunel, C., Marcon, E., Auer, J., Badouard, V., Baraloto, C., Boisseaux, M., Bonal, D., Coste, S., Dardevet, E., Heuret, P., Hietz, P., Levionnois, S., Maréchaux, I., Stahl, C., Vleminckx, J., Wanek, W., Ziegler, C., and Derroire, G.: Love Thy Neighbour? Tropical Tree Growth and Its Response to Climate Anomalies Is Mediated by Neighbourhood Hierarchy and Dissimilarity in Carbon- and Water-Related Traits, Ecol. Lett., 28, e70028, https://doi.org/10.1111/ele.70028, 2025.

Nepstad, D. C., de Carvalho, C. R., Davidson, E. A., Jipp, P. H., Lefebvre, P. A., Negreiros, G. H., da Silva, E. D., Stone, T. A., Trumbore, S. E., and Vieira, S.: The role of deep roots in the hydrological and carbon cycles of Amazonian forests and pastures, Nature, 372, 666–669, https://doi.org/10.1038/372666a0, 1994.

Newman, E. I.: Resistance to Water Flow in Soil and Plant. I. Soil Resistance in Relation to Amounts of Root: Theoretical Estimates, J. Appl. Ecol., 6, 1–12, https://doi.org/10.2307/2401297, 1969.

Nicolini, E., Beauchêne, J., de la Vallée, B. L., Ruelle, J., Mangenet, T., and Heuret, P.: Dating branch growth units in a tropical tree

using morphological and anatomical markers: the case of Parkia velutina Benoist (Mimosoïdeae), Ann. Forest Sci., 69, 543–555, https://doi.org/10.1007/s13595-011-0172-1, 2012.

Norby, R. J., De Kauwe, M. G., Domingues, T. F., Duursma, R. A., Ellsworth, D. S., Goll, D. S., Lapola, D. M., Luus, K. A., MacKenzie, A. R., Medlyn, B. E., Pavlick, R., Rammig, A., Smith, B., Thomas, R., Thonicke, K., Walker, A. P., Yang, X., and Zaehle, S.: Model–data synthesis for the next generation of forest free-air CO_2 enrichment (FACE) experiments, New Phytol., 209, 17–28, https://doi.org/10.1111/nph.13593, 2016.

Norden, N., Chave, J., Belbenoit, P., Caubère, A., Châtelet, P., Forget, P.-M., and Thébaud, C.: Mast fruiting is a frequent strategy in woody species of eastern South America, PLOS ONE, 2, e1079, https://doi.org/10.1371/journal.pone.0001079, 2007.

Novick, K. A., Ficklin, D. L., Stoy, P. C., Williams, C. A., Bohrer, G., Oishi, A. C., Papuga, S. A., Blanken, P. D., Noormets, A., Sulman, B. N., Scott, R. L., Wang, L., and Phillips, R. P.: The increasing importance of atmospheric demand for ecosystem water and carbon fluxes, Nat. Clim. Change, 6, 1023–1027, https://doi.org/10.1038/nclimate3114, 2016.

Novick, K. A., Ficklin, D. L., Baldocchi, D., Davis, K. J., Ghezzehei, T. A., Konings, A. G., MacBean, N., Raoult, N., Scott, R. L., Shi, Y., Sulman, B. N., and Wood, J. D.: Confronting the water potential information gap, Nat. Geosci., 15, 158–164, https://doi.org/10.1038/s41561-022-00909-2, 2022.

Nunes, M. H., Camargo, J. L. C., Vincent, G., Calders, K., Oliveira, R. S., Huete, A., Mendes de Moura, Y., Nelson, B., Smith, M. N., Stark, S. C., and Maeda, E. E.: Forest fragmentation impacts the seasonality of Amazonian evergreen canopies, Nat. Commun., 13, 917, https://doi.org/10.1038/s41467-022-28490-7, 2022.

Ogée, J., Brunet, Y., Loustau, D., Berbigier, P., and Delzon, S.: MuSICA, a CO_2, water and energy multilayer, multileaf pine forest model: evaluation from hourly to yearly time scales and sensitivity analysis, Glob. Change Biol., 9, 697–717, https://doi.org/10.1046/j.1365-2486.2003.00628.x, 2003.

Oleson, K. W., Niu, G.-Y., Yang, Z.-L., Lawrence, D. M., Thornton, P. E., Lawrence, P. J., Stöckli, R., Dickinson, R. E., Bonan, G. B., Levis, S., Dai, A., and Qian, T.: Improvements to the Community Land Model and their impact on the hydrological cycle, J. Geophys. Res., 113, G01021, https://doi.org/10.1029/2007JG000563, 2008.

Oliveira, R. S., Dawson, T. E., Burgess, S. S. O., and Nepstad, D. C.: Hydraulic redistribution in three Amazonian trees, Oecologia, 145, 354–363, https://doi.org/10.1007/s00442-005-0108-2, 2005.

Pacala, S. W. and Rees, M.: Models Suggesting Field Experiments to Test Two Hypotheses Explaining Successional Diversity, Am. Natural., 152, 729–737, https://doi.org/10.1086/286203, 1998.

Paine, C. E. T., Deasey, A., and Duthie, A. B.: Towards the general mechanistic prediction of community dynamics, Funct. Ecol., 32, 1681–1692, https://doi.org/10.1111/1365-2435.13096, 2018.

Pan, Y., Birdsey, R. A., Fang, J., Houghton, R., Kauppi, P. E., Kurz, W. A., Phillips, O. L., Shvidenko, A., Lewis, S. L., Canadell, J. G., Ciais, P., Jackson, R. B., Pacala, S. W., McGuire, A. D., Piao, S., Rautiainen, A., Sitch, S., and Hayes, D.: A Large and Persistent Carbon Sink in the World's Forests, Science, 333, 988–993, https://doi.org/10.1126/science.1201609, 2011.

Pantin, F., Simonneau, T., and Muller, B.: Coming of leaf age: control of growth by hydraulics and metabolics during leaf ontogeny, New Phytol., 196, 349–366, https://doi.org/10.1111/j.1469-8137.2012.04273.x, 2012.

Paschalis, A., Fatichi, S., Zscheischler, J., Ciais, P., Bahn, M., Boysen, L., Chang, J., De Kauwe, M., Estiarte, M., Goll, D., Hanson, P. J., Harper, A. B., Hou, E., Kigel, J., Knapp, A. K., Larsen, K. S., Li, W., Lienert, S., Luo, Y., Meir, P., Nabel, J. E. M. S., Ogaya, R., Parolari, A. J., Peng, C., Peñuelas, J., Pongratz, J., Rambal, S., Schmidt, I. K., Shi, H., Sternberg, M., Tian, H., Tschumi, E., Ukkola, A., Vicca, S., Viovy, N., Wang, Y.-P., Wang, Z., Williams, K., Wu, D., and Zhu, Q.: Rainfall manipulation experiments as simulated by terrestrial biosphere models: Where do we stand?, Glob. Change Biol., 26, 3336–3355, https://doi.org/10.1111/gcb.15024, 2020.

Paschalis, A., De Kauwe, M. G., Sabot, M., and Fatichi, S.: When do plant hydraulics matter in terrestrial biosphere modelling?, Glob. Change Biol., 30, e17022, https://doi.org/10.1111/gcb.17022, 2024.

Pavlick, R., Drewry, D. T., Bohn, K., Reu, B., and Kleidon, A.: The Jena Diversity-Dynamic Global Vegetation Model (JeDi-DGVM): a diverse approach to representing terrestrial biogeography and biogeochemistry based on plant functional trade-offs, Biogeosciences, 10, 4137–4177, https://doi.org/10.5194/bg-10-4137-2013, 2013.

Peñuelas, J., Poulter, B., Sardans, J., Ciais, P., van der Velde, M., Bopp, L., Boucher, O., Godderis, Y., Hinsinger, P., Llusia, J., Nardin, E., Vicca, S., Obersteiner, M., and Janssens, I. A.: Human-induced nitrogen–phosphorus imbalances alter natural and managed ecosystems across the globe, Nat. Commun., 4, 2934, https://doi.org/10.1038/ncomms3934, 2013.

Peters, R. L., Kaewmano, A., Fu, P.-L., Fan, Z.-X., Sterck, F., Steppe, K., and Zuidema, P. A.: High vapour pressure deficit enhances turgor limitation of stem growth in an Asian tropical rainforest tree, Plant Cell Environ., 46, 2747–2762, https://doi.org/10.1111/pce.14661, 2023.

Picard, N. and Franc, A.: Are ecological groups of species optimal for forest dynamics modelling?, Ecol. Model., 163, 175–186, https://doi.org/10.1016/S0304-3800(03)00010-3, 2003.

Picard, N., Köhler, P., Mortier, F., and Gourlet-Fleury, S.: A comparison of five classifications of species into functional groups in tropical forests of French Guiana, Ecol. Complex., 11, 75–83, https://doi.org/10.1016/j.ecocom.2012.03.003, 2012.

Pitman, A. J.: The evolution of, and revolution in, land surface schemes designed for climate models, Int. J. Climatol., 23, 479–510, https://doi.org/10.1002/joc.893, 2003.

Poggio, L., de Sousa, L. M., Batjes, N. H., Heuvelink, G. B. M., Kempen, B., Ribeiro, E., and Rossiter, D.: SoilGrids 2.0: producing soil information for the globe with quantified spatial uncertainty, SOIL, 7, 217–240, https://doi.org/10.5194/soil-7-217-2021, 2021.

Poorter, L., Bongers, L., and Bongers, F.: Architecture of 54 moist-forest tree species: traits, trade-offs, and functional groups, Ecology, 87, 1289–1301, https://doi.org/10.1890/0012-9658(2006)87[1289:AOMTST]2.0.CO;2, 2006.

Poorter, L., Wright, S. J., Paz, H., Ackerly, D. D., Condit, R., Ibarra-Manríquez, G., Harms, K. E., Licona, J. C., Martínez-Ramos, M., Mazer, S. J., Muller-Landau, H. C., Peña-Claros, M., Webb, C. O., and Wright, I. J.: Are functional traits good predictors of demographic rates? Evidence from five Neotropical forests, Ecology, 89, 1908–1920, https://doi.org/10.1890/07-0207.1, 2008.

Poorter, L., Oberbauer, S. F., and Clark, D. B.: Leaf optical properties along a vertical gradient in a tropical rain forest canopy in Costa Rica, Am. J. Bot., 82, 1257–1263, https://doi.org/10.2307/2446248, 1995.

Poorter, L., van der Sande, M. T., Thompson, J., Arets, E. J. M. M., Alarcón, A., Álvarez-Sánchez, J., Ascarrunz, N., Balvanera, P., Barajas-Guzmán, G., Boit, A., Bongers, F., Carvalho, F. A., Casanoves, F., Cornejo-Tenorio, G., Costa, F. R. C., de Castilho, C. V., Duivenvoorden, J. F., Dutrieux, L. P., Enquist, B. J., Fernández-Méndez, F., Finegan, B., Gormley, L. H. L., Healey, J. R., Hoosbeek, M. R., Ibarra-Manríquez, G., Junqueira, A. B., Levis, C., Licona, J. C., Lisboa, L. S., Magnusson, W. E., Martínez-Ramos, M., Martínez-Yrizar, A., Martorano, L. G., Maskell, L. C., Mazzei, L., Meave, J. A., Mora, F., Muñoz, R., Nytch, C., Pansonato, M. P., Parr, T. W., Paz, H., Pérez-García, E. A., Rentería, L. Y., Rodríguez-Velazquez, J., Rozendaal, D. M. A., Ruschel, A. R., Sakschewski, B., Salgado-Negret, B., Schietti, J., Simões, M., Sinclair, F. L., Souza, P. F., Souza, F. C., Stropp, J., ter Steege, H., Swenson, N. G., Thonicke, K., Toledo, M., Uriarte, M., van der Hout, P., Walker, P., Zamora, N., and Peña-Claros, M.: Diversity enhances carbon storage in tropical forests, Global Ecol. Biogeogr., 24, 1314–1328, https://doi.org/10.1111/geb.12364, 2015.

Poorter, L., Amissah, L., Bongers, F., Hordijk, I., Kok, J., Laurance, S. G. W., Lohbeck, M., Martínez-Ramos, M., Matsuo, T., Meave, J. A., Muñoz, R., Peña-Claros, M., and van der Sande, M. T.: Successional theories, Biol. Rev., 98, 2049–2077, https://doi.org/10.1111/brv.12995, 2023.

Porté, A. and Bartelink, H. H.: Modelling mixed forest growth: a review of models for forest management, Ecol. Model., 150, 141–188, https://doi.org/10.1016/S0304-3800(01)00476-8, 2002.

Poulter, B., Ciais, P., Hodson, E., Lischke, H., Maignan, F., Plummer, S., and Zimmermann, N. E.: Plant functional type mapping for earth system models, Geosci. Model Dev., 4, 993–1010, https://doi.org/10.5194/gmd-4-993-2011, 2011.

Powell, T. L., Galbraith, D. R., Christoffersen, B. O., Harper, A., Imbuzeiro, H. M. A., Rowland, L., Almeida, S., Brando, P. M., da Costa, A. C. L., Costa, M. H., Levine, N. M., Malhi, Y., Saleska, S. R., Sotta, E., Williams, M., Meir, P., and Moorcroft, P. R.: Confronting model predictions of carbon fluxes with measurements of Amazon forests subjected to experimental drought, New Phytol., 200, 350–365, https://doi.org/10.1111/nph.12390, 2013.

Powell, T. L., Wheeler, J. K., Oliveira, A. A. R. de, Costa, A. C. L. da, Saleska, S. R., Meir, P., and Moorcroft, P. R.: Differences in xylem and leaf hydraulic traits explain differences in drought tolerance among mature Amazon rainforest trees, Glob. Change Biol., 23, 4280–4293, https://doi.org/10.1111/gcb.13731, 2017.

Powell, T. L., Koven, C. D., Johnson, D. J., Faybishenko, B., Fisher, R. A., Knox, R. G., McDowell, N. G., Condit, R., Hubbell, S. P., Wright, S. J., Chambers, J. Q., and Kueppers, L. M.: Variation in hydroclimate sustains tropical forest biomass and promotes functional diversity, New Phytol., 219, 932–946, https://doi.org/10.1111/nph.15271, 2018.

Prentice, I. C., Bondeau, A., Cramer, W., Harrison, S. P., Hickler, T., Lucht, W., Sitch, S., Smith, B., and Sykes, M. T.: Dynamic Global Vegetation Modeling: Quantifying Terrestrial Ecosystem Responses to Large-Scale Environmental Change, in: Terrestrial ecosystems in a changing world, edited by: Canadell, J. G., Pataki, D. E., and Pitelka, L. F., Springer Berlin Heidelberg, 175–192, https://doi.org/10.1007/978-3-540-32730-1_15, 2007.

Prentice, I. C., Liang, X., Medlyn, B. E., and Wang, Y.-P.: Reliable, robust and realistic: the three R's of next-generation land-surface modelling, Atmos. Chem. Phys., 15, 5987–6005, https://doi.org/10.5194/acp-15-5987-2015, 2015.

Purves, D. and Pacala, S.: Predictive models of forest dynamics, Science, 320, 1452–1453, https://doi.org/10.1126/science.1155359, 2008.

Qie, L., Lewis, S. L., Sullivan, M. J. P., Lopez-Gonzalez, G., Pickavance, G. C., Sunderland, T., Ashton, P., Hubau, W., Salim, K. A., Aiba, S.-I., Banin, L. F., Berry, N., Brearley, F. Q., Burslem, D. F. R. P., Dančák, M., Davies, S. J., Fredriksson, G., Hamer, K. C., Hédl, R., Kho, L. K., Kitayama, K., Krisnawati, H., Lhota, S., Malhi, Y., Maycock, C., Metali, F., Mirmanto, E., Nagy, L., Nilus, R., Ong, R., Pendry, C. A., Poulsen, A. D., Primack, R. B., Rutishauser, E., Samsoedin, I., Saragih, B., Sist, P., Slik, J. W. F., Sukri, R. S., Svátek, M., Tan, S., Tjoa, A., Nieuwstadt, M. van, Vernimmen, R. R. E., Yassir, I., Kidd, P. S., Fitriadi, M., Ideris, N. K. H., Serudin, R. M., Lim, L. S. A., Saparudin, M. S., and Phillips, O. L.: Long-term carbon sink in Borneo's forests halted by drought and vulnerable to edge effects, Nat. Commun., 8, 1966, https://doi.org/10.1038/s41467-017-01997-0, 2017.

Rau, E.-P., Fischer, F., Joetzjer, É., Maréchaux, I., Sun, I. F., and Chave, J.: Transferability of an individual- and trait-based forest dynamics model: A test case across the tropics, Ecol. Model., 463, 109801, https://doi.org/10.1016/j.ecolmodel.2021.109801, 2022a.

Rau, E.-P., Gardiner, B. A., Fischer, F. J., Maréchaux, I., Joetzjer, E., Sun, I.-F., and Chave, J.: Wind Speed Controls Forest Structure in a Subtropical Forest Exposed to Cyclones: A Case Study Using an Individual-Based Model, Front. Forests Global Change, 5, https://doi.org/10.3389/ffgc.2022.753100, 2022b.

Raupach, M. R., Finnigan, J. J., and Brunet, Y.: Coherent Eddies and Turbulence in Vegetation Canopies: The Mixing-Layer Analogy, Bound.-Lay. Meteorol., 78, 351–382, https://doi.org/10.1007/978-94-017-0944-6_15, 1996.

Restrepo-Coupe, N., da Rocha, H. R., Hutyra, L. R., da Araujo, A. C., Borma, L. S., Christoffersen, B., Cabral, O. M. R., de Camargo, P. B., Cardoso, F. L., da Costa, A. C. L., Fitzjarrald, D. R., Goulden, M. L., Kruijt, B., Maia, J. M. F., Malhi, Y. S., Manzi, A. O., Miller, S. D., Nobre, A. D., von Randow, C., Sá, L. D. A., Sakai, R. K., Tota, J., Wofsy, S. C., Zanchi, F. B., and Saleska, S. R.: What drives the seasonality of photosynthesis across the Amazon basin? A cross-site analysis of eddy flux tower measurements from the Brasil flux network, Agr. Forest Meteorol., 182–183, 128–144, https://doi.org/10.1016/j.agrformet.2013.04.031, 2013.

Restrepo-Coupe, N., Levine, N. M., Christoffersen, B. O., Albert, L. P., Wu, J., Costa, M. H., Galbraith, D., Imbuzeiro, H., Martins, G., da Araujo, A. C., Malhi, Y. S., Zeng, X., Moorcroft, P., and Saleska, S. R.: Do dynamic global vegetation models capture the seasonality of carbon fluxes in the Amazon basin? A data-model intercomparison, Glob. Change Biol., 23, 191–208, https://doi.org/10.1111/gcb.13442, 2017.

Richards, L. A.: Capillary conduction of liquids through porous mediums, Physics, 1, 318–333, https://doi.org/10.1063/1.1745010, 1931.

Riva, F. and Fahrig, L.: Landscape-scale habitat fragmentation is positively related to biodiversity, despite patch-scale ecosystem decay, Ecol. Lett., 26, 268–277, https://doi.org/10.1111/ele.14145, 2023.

Rödig, E., Cuntz, M., Heinke, J., Rammig, A., and Huth, A.: Spatial heterogeneity of biomass and forest structure of the Amazon rain forest: Linking remote sensing, forest modelling and field inventory, Global Ecol. Biogeogr., 26, 1292–1302, https://doi.org/10.1111/geb.12639, 2017.

Rodriguez-Dominguez, C. M., Buckley, T. N., Egea, G., de Cires, A., Hernandez-Santana, V., Martorell, S., and Diaz-Espejo, A.: Most stomatal closure in woody species under moderate drought can be explained by stomatal responses to leaf turgor, Plant Cell Environ., 39, 2014–2026, https://doi.org/10.1111/pce.12774, 2016.

Rodriguez-Iturbe, I., Porporato, A., Ridolfi, L., Isham, V., and Coxi, D. R.: Probabilistic modelling of water balance at a point: the role of climate, soil and vegetation, P. Roy. Soc. Lond. A, 455, 3789–3805, https://doi.org/10.1098/rspa.1999.0477, 1999.

Rogers, A., Medlyn, B. E., Dukes, J. S., Bonan, G., von Caemmerer, S., Dietze, M. C., Kattge, J., Leakey, A. D. B., Mercado, L. M., Niinemets, Ü., Prentice, I. C., Serbin, S. P., Sitch, S., Way, D. A., and Zaehle, S.: A roadmap for improving the representation of photosynthesis in Earth system models, New Phytol., 213, 22–42, https://doi.org/10.1111/nph.14283, 2017.

Rosas, T., Mencuccini, M., Barba, J., Cochard, H., Saura-Mas, S., and Martínez-Vilalta, J.: Adjustments and coordination of hydraulic, leaf and stem traits along a water availability gradient, New Phytol., 223, 632–646, https://doi.org/10.1111/nph.15684, 2019.

Ross, J.: The radiation regime and architecture of plant stands, The Hague, The Netherlands, 1981.

Rowland, L., Lobo-do-Vale, R. L., Christoffersen, B. O., Melém, E. A., Kruijt, B., Vasconcelos, S. S., Domingues, T., Binks, O. J., Oliveira, A. A. R., Metcalfe, D., da Costa, A. C. L., Mencuccini, M., and Meir, P.: After more than a decade of soil moisture deficit, tropical rainforest trees maintain photosynthetic capacity, despite increased leaf respiration, Glob. Change Biol., 21, 4662–4672, https://doi.org/10.1111/gcb.13035, 2015.

Rowland, L., Costa, A. C. L. da, Oliveira, A. A. R., Oliveira, R. S., Bittencourt, P. L., Costa, P. B., Giles, A. L., Sosa, A. I., Coughlin, I., Godlee, J. L., Vasconcelos, S. S., Junior, J. A. S., Ferreira, L. V., Mencuccini, M., and Meir, P.: Drought stress and tree size determine stem CO_2 efflux in a tropical forest, New Phytol., 218, 1393–1405, https://doi.org/10.1111/nph.15024, 2018.

Rowland, L., Ramírez-Valiente, J.-A., Hartley, I. P., and Mencuccini, M.: How woody plants adjust above- and below-ground traits in response to sustained drought, New Phytol., 239, 1173–1189, https://doi.org/10.1111/nph.19000, 2023.

Rutter, A. J. and Morton, A. J.: A Predictive Model of Rainfall Interception in Forests. III. Sensitivity of The Model to Stand Parameters and Meteorological Variables, J. Appl. Ecol., 14, 567–588, https://doi.org/10.2307/2402568, 1977.

Ryan, M. G., Hubbard, R. M., Clark, D. A., and Jr, R. L. S.: Woody-tissue respiration for Simarouba amara and Minquartia guianensis, two tropical wet forest trees with different growth habits, Oecologia, 100, 213–220, https://doi.org/10.1007/BF00316947, 1994.

Ryan, M. G., Binkley, D., and Fownes, J. H.: Age-related decline in forest productivity, Adv. Ecol. Res., 27, 213–262, 1997.

Sabot, M. E. B., Kauwe, M. G. D., Pitman, A. J., Medlyn, B. E., Verhoef, A., Ukkola, A. M., and Abramowitz, G.: Plant profit maximization improves predictions of European forest responses to drought, New Phytol., 226, 1638–1655, https://doi.org/10.1111/nph.16376, 2020.

Sabot, M. E. B., De Kauwe, M. G., Pitman, A. J., Medlyn, B. E., Ellsworth, D. S., Martin-StPaul, N. K., Wu, J., Choat, B., Limousin, J.-M., Mitchell, P. J., Rogers, A., and Serbin, S. P.: One Stomatal Model to Rule Them All? Toward Improved Representation of Carbon and Water Exchange in Global Models, J. Adv. Model. Earth Sy., 14, e2021MS002761, https://doi.org/10.1029/2021MS002761, 2022.

Sakschewski, B., von Bloh, W., Boit, A., Rammig, A., Kattge, J., Poorter, L., Peñuelas, J., and Thonicke, K.: Leaf and stem economics spectra drive diversity of functional plant traits in a dynamic global vegetation model, Glob. Change Biol., 21, 2711–2725, https://doi.org/10.1111/gcb.12870, 2015.

Sakschewski, B., von Bloh, W., Boit, A., Poorter, L., Peña-Claros, M., Heinke, J., Joshi, J., and Thonicke, K.: Resilience of Amazon forests emerges from plant trait diversity, Nat. Clim. Change, 6, 1032–1036, https://doi.org/10.1038/nclimate3109, 2016.

Sakschewski, B., von Bloh, W., Drüke, M., Sörensson, A. A., Ruscica, R., Langerwisch, F., Billing, M., Bereswill, S., Hirota, M., Oliveira, R. S., Heinke, J., and Thonicke, K.: Variable tree rooting strategies are key for modelling the distribution, productivity and evapotranspiration of tropical evergreen forests, Biogeosciences, 18, 4091–4116, https://doi.org/10.5194/bg-18-4091-2021, 2021.

Sander, H.: The porosity of tropical soils and implications for geomorphological and pedogenetic processes and the movement of solutions within the weathering cover, CATENA, 49, 129–137, https://doi.org/10.1016/S0341-8162(02)00021-8, 2002.

Santos, V. A. H. F. dos, Ferreira, M. J., Rodrigues, J. V. F. C., Garcia, M. N., Ceron, J. V. B., Nelson, B. W., and Saleska, S. R.: Causes of reduced leaf-level photosynthesis during strong El Niño drought in a Central Amazon forest, Glob. Change Biol., 24, 4266–4279, https://doi.org/10.1111/gcb.14293, 2018.

Sato, H., Itoh, A., and Kohyama, T.: SEIB-DGVM: a new dynamic global vegetation model using a spatially explicit individual-based approach, Ecol. Model., 200, 279–307, https://doi.org/10.1016/j.ecolmodel.2006.09.006, 2007.

Schaphoff, S., von Bloh, W., Rammig, A., Thonicke, K., Biemans, H., Forkel, M., Gerten, D., Heinke, J., Jägermeyr, J., Knauer, J., Langerwisch, F., Lucht, W., Müller, C., Rolinski, S., and Waha, K.: LPJmL4 – a dynamic global vegetation model with managed land – Part 1: Model description, Geosci. Model Dev., 11, 1343–1375, https://doi.org/10.5194/gmd-11-1343-2018, 2018.

Scheiter, S., Langan, L., and Higgins, S. I.: Next-generation dynamic global vegetation models: learning from community ecology, New Phytol., 198, 957–969, https://doi.org/10.1111/nph.12210, 2013.

Schenk, H. J. and Jackson, R. B.: Rooting depths, lateral root spreads and below-ground/above-ground allometries of plants in water-limited ecosystems, J. Ecol., 90, 480–494, https://doi.org/10.1046/j.1365-2745.2002.00682.x, 2002.

Schimel, D., Pavlick, R., Fisher, J. B., Asner, G. P., Saatchi, S., Townsend, P., Miller, C., Frankenberg, C., Hibbard, K.,

and Cox, P.: Observing terrestrial ecosystems and the carbon cycle from space, Glob. Change Biol., 21, 1762–1776, https://doi.org/10.1111/gcb.12822, 2015.

Schippers, P., Vlam, M., Zuidema, P. A., and Sterck, F.: Sapwood allocation in tropical trees: a test of hypotheses, Funct. Plant Biol., 42, 697–709, https://doi.org/10.1071/FP14127, 2015.

Schmidhalter, U.: The gradient between pre-dawn rhizoplane and bulk soil matric potentials, and its relation to the pre-dawn root and leaf water potentials of four species, Plant Cell Environ., 20, 953–960, https://doi.org/10.1046/j.1365-3040.1997.d01-136.x, 1997.

Schmitt, S., Maréchaux, I., Chave, J., Fischer, F. J., Piponiot, C., Traissac, S., and Hérault, B.: Functional diversity improves tropical forest resilience: Insights from a long-term virtual experiment, J. Ecol., 108, 831–843, https://doi.org/10.1111/1365-2745.13320, 2020.

Schmitt, S.: Rôle de la biodiversité dans la résilience des écosystèmes forestiers tropicaux après perturbations, AgroParisTech, Université de Montpellier, Kourou, https://sylvainschmitt.github.io/master-thesis/ (last access: 24 July 2025), 2017.

Schmitt, S., Salzet, G., Fischer, F. J., Maréchaux, I., and Chave, J.: rcontroll: An R interface for the individual-based forest dynamics simulator TROLL, Meth. Ecol. Evol., 14, 2749–2757, https://doi.org/10.1111/2041-210X.14215, 2023.

Schmitt, S., Salzet, G., Fischer, F. J., Maréchaux, I., and Chave, J.: sylvainschmitt/rcontroll: GMD preprint (v0.2.0), Zenodo [code], https://doi.org/10.5281/zenodo.14012116, 2024.

Schmitt, S., Fischer, F., Ball, J. G. C., Barbier, N., Boisseaux, M., Bonal, D., Burban, B., Chen, X., Derroire, G., Lichstein, J. W., Nemetschek, D., Restrepo-Coupe, N., Saleska, S., Sellan, G., Verley, P., Vincent, G., Ziegler, C., Chave, J., and Maréchaux, I.: TROLL 4.0: representing water and carbon fluxes, leaf phenology, and intraspecific trait variation in a mixed-species individual-based forest dynamics model – Part 2: Model evaluation for two Amazonian sites, Geosci. Model Dev., 18, 5205–5243, https://doi.org/10.5194/gmd-18-5205-2025, 2025.

Schnabel, F., Schwarz, J. A., Dănescu, A., Fichtner, A., Nock, C. A., Bauhus, J., and Potvin, C.: Drivers of productivity and its temporal stability in a tropical tree diversity experiment, Glob. Change Biol., 25, 4257–4272, https://doi.org/10.1111/gcb.14792, 2019.

Schnitzer, S. A. and Carson, W. P.: Would Ecology Fail the Repeatability Test?, BioScience, 66, 98–99, https://doi.org/10.1093/biosci/biv176, 2016.

Seidl, R., Rammer, W., and Blennow, K.: Simulating wind disturbance impacts on forest landscapes: Tree-level heterogeneity matters, Environ. Model. Softw., 51, 1–11, https://doi.org/10.1016/j.envsoft.2013.09.018, 2014.

Seidler, T. G. and Plotkin, J. B.: Seed Dispersal and Spatial Pattern in Tropical Trees, PLOS Biology, 4, e344, https://doi.org/10.1371/journal.pbio.0040344, 2006.

Sellers, P. J., Mintz, Y., Sud, Y. C., and Dalcher, A.: A Simple Biosphere Model (SIB) for Use within General Circulation Models, J. Atmos. Sci., 43, 505–531, https://doi.org/10.1175/1520-0469(1986)043<0505:ASBMFU> 2.0.CO;2, 1986.

Sellers, P. J., Heiser, M. D., and Hall, F. G.: Relations between surface conductance and spectral vegetation indices at intermediate (100 m^2 to 15 km^2) length scales, J. Geophys. Res.-Atmos., 97, 19033–19059, https://doi.org/10.1029/92JD01096, 1992.

Sellers, P. J., Dickinson, R. E., Randall, D. A., Betts, A. K., Hall, F. G., Berry, J. A., Collatz, G. J., Denning, A. S., Mooney, H. A., Nobre, C. A., Sato, N., Field, C. B., and Henderson-Sellers, A.: Modeling the Exchanges of Energy, Water, and Carbon Between Continents and the Atmosphere, Science, 275, 502–509, https://doi.org/10.1126/science.275.5299.502, 1997.

Sergent, A. S., Varela, S. A., Barigah, T. S., Badel, E., Cochard, H., Dalla-Salda, G., Delzon, S., Fernández, M. E., Guillemot, J., Gyenge, J., Lamarque, L. J., Martinez-Meier, A., Rozenberg, P., Torres-Ruiz, J. M., and Martin-StPaul, N. K.: A comparison of five methods to assess embolism resistance in trees, Forest Ecol. Manage., 468, 118175, https://doi.org/10.1016/j.foreco.2020.118175, 2020.

Sevanto, S., Mcdowell, N. G., Dickman, L. T., Pangle, R., and Pockman, W. T.: How do trees die? A test of the hydraulic failure and carbon starvation hypotheses, Plant Cell Environ., 37, 153–161, https://doi.org/10.1111/pce.12141, 2014.

Sheil, D., Burslem, D. F. R. P., and Alder, D.: The interpretation and misinterpretation of mortality rate measures, J. Ecol., 83, 331–333, https://doi.org/10.2307/2261571, 1995.

Shugart, H. H., Asner, G. P., Fischer, R., Huth, A., Knapp, N., Le Toan, T., and Shuman, J. K.: Computer and remote-sensing infrastructure to enhance large-scale testing of individual-based forest models, Front. Ecol. Environ., 13, 503–511, 2015.

Shugart, H. H., Wang, B., Fischer, R., Ma, J., Fang, J., Yan, X., Huth, A., and Armstrong, A. H.: Gap models and their individual-based relatives in the assessment of the consequences of global change, Environ. Res. Lett., 13, 033001, https://doi.org/10.1088/1748-9326/aaaacc, 2018.

Shugart, H. H., Foster, A., Wang, B., Druckenbrod, D., Ma, J., Lerdau, M., Saatchi, S., Yang, X., and Yan, X.: Gap models across micro- to mega-scales of time and space: examples of Tansley's ecosystem concept, For. Ecosyst., 7, 14, https://doi.org/10.1186/s40663-020-00225-4, 2020.

Shuttleworth, W. J.: Daily variations of temperature and humidity within and above Amazonian forest, Weather, 40, 102–108, https://doi.org/10.1002/j.1477-8696.1985.tb07489.x, 1985.

Shuttleworth, W. J., Leuning, R., Black, T. A., Grace, J., Jarvis, P. G., Roberts, J., and Jones, H. G.: Micrometeorology of temperate and tropical forest, Philos. T. Roy. Soc. Lond. B, 324, 299–334, https://doi.org/10.1098/rstb.1989.0050, 1989.

Signori-Müller, C., Oliveira, R. S., Valentim Tavares, J., Carvalho Diniz, F., Gilpin, M., de V. Barros, F., Marca Zevallos, M. J., Salas Yupayccana, C. A., Nina, A., Brum, M., Baker, T. R., Cosio, E. G., Malhi, Y., Monteagudo Mendoza, A., Phillips, O. L., Rowland, L., Salinas, N., Vasquez, R., Mencuccini, M., and Galbraith, D.: Variation of non-structural carbohydrates across the fast–slow continuum in Amazon Forest canopy trees, Funct. Ecol., 36, 341–355, https://doi.org/10.1111/1365-2435.13971, 2022.

Sitch, S., Smith, B., Prentice, I. C., Arneth, A., Bondeau, A., Cramer, W., Kaplan, J. O., Levis, S., Lucht, W., Sykes, M. T., Thonicke, K., and Venevsky, S.: Evaluation of ecosystem dynamics, plant geography and terrestrial carbon cycling in the LPJ dynamic global vegetation model, Glob. Change Biol., 9, 161–185, https://doi.org/10.1046/j.1365-2486.2003.00569.x, 2003.

Slik, J. W. F.: El Niño droughts and their effects on tree species composition and diversity in tropical rain forests, Oecologia, 141, 114–120, https://doi.org/10.1007/s00442-004-1635-y, 2004.

Slot, M., Wright, S. J., and Kitajima, K.: Foliar respiration and its temperature sensitivity in trees and lianas: in situ measurements in the upper canopy of a tropical forest, Tree Physiol., 33, 505–515, https://doi.org/10.1093/treephys/tpt026, 2013.

Slot, M., Nardwattanawong, T., Hernández, G. G., Bueno, A., Riederer, M., and Winter, K.: Large differences in leaf cuticle conductance and its temperature response among 24 tropical tree species from across a rainfall gradient, New Phytol., 232, 1618–1631, https://doi.org/10.1111/nph.17626, 2021.

Smith, B., Prentice, I. C., and Sykes, M. T.: Representation of vegetation dynamics in the modelling of terrestrial ecosystems: comparing two contrasting approaches within European climate space, Global Ecol. Biogeogr., 10, 621–637, https://doi.org/10.1046/j.1466-822X.2001.t01-1-00256.x, 2001.

Smith, N. G. and Dukes, J. S.: Plant respiration and photosynthesis in global-scale models: incorporating acclimation to temperature and CO_2, Glob. Change Biol., 19, 45–63, https://doi.org/10.1111/j.1365-2486.2012.02797.x, 2013.

Smith-Martin, C. M., Xu, X., Medvigy, D., Schnitzer, S. A., and Powers, J. S.: Allometric scaling laws linking biomass and rooting depth vary across ontogeny and functional groups in tropical dry forest lianas and trees, New Phytol., 226, 714–726, https://doi.org/10.1111/nph.16275, 2020.

Soberón, J.: Grinnellian and Eltonian niches and geographic distributions of species, Ecol. Lett., 10, 1115–1123, https://doi.org/10.1111/j.1461-0248.2007.01107.x, 2007.

Sobrado, M. A.: Aspects of tissue water relations and seasonal changes of leaf water potential components of evergreen and deciduous species coexisting in tropical dry forests, Oecologia, 68, 413–416, https://doi.org/10.1007/BF01036748, 1986.

Song, X., Wang, D.-Y., Li, F., and Zeng, X.-D.: Evaluating the performance of CMIP6 Earth system models in simulating global vegetation structure and distribution, Adv. Clim. Change Res., 12, 584–595, https://doi.org/10.1016/j.accre.2021.06.008, 2021.

Sousa, T. R., Schietti, J., Ribeiro, I. O., Emílio, T., Fernández, R. H., ter Steege, H., Castilho, C. V., Esquivel-Muelbert, A., Baker, T., Pontes-Lopes, A., Silva, C. V. J., Silveira, J. M., Derroire, G., Castro, W., Mendoza, A. M., Ruschel, A., Prieto, A., Lima, A. J. N., Rudas, A., Araujo-Murakami, A., Gutierrez, A. P., Andrade, A., Roopsind, A., Manzatto, A. G., Di Fiore, A., Torres-Lezama, A., Dourdain, A., Marimon, B., Marimon, B. H., Burban, B., van Ulft, B., Herault, B., Quesada, C., Mendoza, C., Stahl, C., Bonal, D., Galbraith, D., Neill, D., de Oliveira, E. A., Hase, E., Jimenez-Rojas, E., Vilanova, E., Arets, E., Berenguer, E., Alvarez-Davila, E., Honorio Coronado, E. N., Almeida, E., Coelho, F., Valverde, F. C., Elias, F., Brown, F., Bongers, F., Arevalo, F. R., Lopez-Gonzalez, G., van der Heijden, G., Aymard C., G. A., Llampazo, G. F., Pardo, G., Ramírez-Angulo, H., do Amaral, I. L., Vieira, I. C. G., Huamantupa-Chuquimaco, I., Comiskey, J. A., Singh, J., Espejo, J. S., del Aguila-Pasquel, J., Zwerts, J. A., Talbot, J., Terborgh, J., Ferreira, J., Barroso, J. G., Barlow, J., Camargo, J. L., Stropp, J., Peacock, J., Serrano, J., Melgaço, K., Ferreira, L. V., Blanc, L., Poorter, L., Gamarra, L. V., Aragão, L., Arroyo, L., Silveira, M., Peñuela-Mora, M. C., Vargas, M. P. N., Toledo, M., Disney, M., Réjou-Méchain, M., Baisie, M., Kalamandeen, M., Camacho, N. P., Cardozo, N. D., Silva, N., Pitman, N., Higuchi, N., Banki, O., Loayza, P. A., Graça, P. M. L. A., Morandi, P. S., van der Meer, P. J., van der Hout, P., Naisso, P., Barbosa Camargo, P., Salomão, R., Thomas, R., Boot, R., Keichi Umetsu, R., da Costa Silva, R., Burnham, R., Zagt, R., Vasquez Martinez, R., Brienen, R., Cerruto Ribeiro, S., Lewis, S. L., Aparecida Vieira, S., Reis, S. M. A., Fauset, S., Laurance, S., Feldpausch, T., Erwin, T., Killeen, T., Wortel, V., Chama Moscoso, V., Vos, V., Huaraca Huasco, W., Laurance, W., Malhi, Y., Magnusson, W. E., Phillips, O. L., and Costa, F. R. C.: Water table depth modulates productivity and biomass across Amazonian forests, Global Ecol. Biogeogr., 31, 1571–1588, https://doi.org/10.1111/geb.13531, 2022.

Sperry, J. S., Hacke, U. G., Oren, R., and Comstock, J. P.: Water deficits and hydraulic limits to leaf water supply, Plant Cell Environ., 25, 251–263, 2002.

Sperry, J. S., Venturas, M. D., Anderegg, W. R. L., Mencuccini, M., Mackay, D. S., Wang, Y., and Love, D. M.: Predicting stomatal responses to the environment from the optimization of photosynthetic gain and hydraulic cost, Plant Cell Environ., 40, 816–830, https://doi.org/10.1111/pce.12852, 2017.

Stahl, C., Burban, B., Goret, J.-Y., and Bonal, D.: Seasonal variations in stem CO_2 efflux in the Neotropical rainforest of French Guiana, Ann. Forest Sci., 68, 771–782, https://doi.org/10.1007/s13595-011-0074-2, 2011.

Stahl, C., Herault, B., Rossi, V., Burban, B., Brechet, C., and Bonal, D.: Depth of soil water uptake by tropical rainforest trees during dry periods: does tree dimension matter?, Oecologia, 173, 1191–1201, https://doi.org/10.1007/s00442-013-2724-6, 2013a.

Stahl, C., Burban, B., Wagner, F., Goret, J.-Y., Bompy, F., and Bonal, D.: Influence of seasonal variations in soil water availability on gas exchange of tropical canopy trees, Biotropica, 45, 155–164, https://doi.org/10.1111/j.1744-7429.2012.00902.x, 2013b.

Stephenson, N. L., Das, A. J., Condit, R., Russo, S. E., Baker, P. J., Beckman, N. G., Coomes, D. A., Lines, E. R., Morris, W. K., Rüger, N., Álvarez, E., Blundo, C., Bunyavejchewin, S., Chuyong, G., Davies, S. J., Duque, Á., Ewango, C. N., Flores, O., Franklin, J. F., Grau, H. R., Hao, Z., Harmon, M. E., Hubbell, S. P., Kenfack, D., Lin, Y., Makana, J.-R., Malizia, A., Malizia, L. R., Pabst, R. J., Pongpattananurak, N., Su, S.-H., Sun, I.-F., Tan, S., Thomas, D., van Mantgem, P. J., Wang, X., Wiser, S. K., and Zavala, M. A.: Rate of tree carbon accumulation increases continuously with tree size, Nature, 507, 90–93, https://doi.org/10.1038/nature12914, 2014.

Strigul, N., Pristinski, D., Purves, D., Dushoff, J., and Pacala, S.: Scaling from trees to forests: tractable macroscopic equations for forest dynamics, Ecol. Monogr., 78, 523–545, https://doi.org/10.1890/08-0082.1, 2008.

Sun, S., Jung, E.-Y., Gaviria, J., and Engelbrecht, B. M. J.: Drought survival is positively associated with high turgor loss points in temperate perennial grassland species, Funct. Ecol., 34, 788–798, https://doi.org/10.1111/1365-2435.13522, 2020.

Swaine, M. D. and Whitmore, T. C.: On the definition of ecological species groups in tropical rain forests, Vegetatio, 75, 81–86, https://doi.org/10.1007/BF00044629, 1988.

Tamme, R., Götzenberger, L., Zobel, M., Bullock, J. M., Hooftman, D. A. P., Kaasik, A., and Pärtel, M.: Predicting species' maximum dispersal distances from simple plant traits, Ecology, 95, 505–513, https://doi.org/10.1890/13-1000.1, 2014.

Thornley, J. H. M. and Cannell, M. G. R.: Modelling the components of plant respiration: representation and realism, Ann. Bot., 85, 55–67, https://doi.org/10.1006/anbo.1999.0997, 2000.

Thuiller, W., Albert, C., Araújo, M. B., Berry, P. M., Cabeza, M., Guisan, A., Hickler, T., Midgley, G. F., Paterson, J., Schurr, F. M., Sykes, M. T., and Zimmermann, N. E.: Predicting global change impacts on plant species' distributions: Future challenges, Perspect. Plant Ecol. Evol. Sys., 9, 137–152, https://doi.org/10.1016/j.ppees.2007.09.004, 2008.

Tomasella, J. and Hodnett, M. G.: Estimating soil water retention characteristics from limited data in Brazilian Amazonia, Soil Sci., 163, 190–202, 1998.

Trueba, S., Pan, R., Scoffoni, C., John, G. P., Davis, S. D., and Sack, L.: Thresholds for leaf damage due to dehydration: declines of hydraulic function, stomatal conductance and cellular integrity precede those for photochemistry, New Phytol., 223, 134–149, https://doi.org/10.1111/nph.15779, 2019.

Trugman, A. T., Medvigy, D., Mankin, J. S., and Anderegg, W. R. L.: Soil Moisture Stress as a Major Driver of Carbon Cycle Uncertainty, Geophys. Res. Lett., 45, 6495–6503, https://doi.org/10.1029/2018GL078131, 2018.

Turner, B. L., Brenes-Arguedas, T., and Condit, R.: Pervasive phosphorus limitation of tree species but not communities in tropical forests, Nature, 555, 367–370, https://doi.org/10.1038/nature25789, 2018.

Tuzet, A., Perrier, A., and Leuning, R.: A coupled model of stomatal conductance, photosynthesis and transpiration, Plant Cell Environ., 26, 1097–1116, https://doi.org/10.1046/j.1365-3040.2003.01035.x, 2003.

Tymen, B., Vincent, G., Courtois, E. A., Heurtebize, J., Dauzat, J., Marechaux, I., and Chave, J.: Quantifying micro-environmental variation in tropical rainforest understory at landscape scale by combining airborne LiDAR scanning and a sensor network, Ann. Forest Sci., 74, 32, https://doi.org/10.1007/s13595-017-0628-z, 2017.

Urbina, I., Grau, O., Sardans, J., Margalef, O., Peguero, G., Asensio, D., LLusià, J., Ogaya, R., Gargallo-Garriga, A., Van Langenhove, L., Verryckt, L. T., Courtois, E. A., Stahl, C., Soong, J. L., Chave, J., Hérault, B., Janssens, I. A., Sayer, E., and Peñuelas, J.: High foliar K and P resorption efficiencies in old-growth tropical forests growing on nutrient-poor soils, Ecol. Evol., 11, 8969–8982, https://doi.org/10.1002/ece3.7734, 2021.

Vacchiano, G., Ascoli, D., Berzaghi, F., Lucas-Borja, M. E., Caignard, T., Collalti, A., Mairota, P., Palaghianu, C., Reyer, C. P. O., Sanders, T. G. M., Schermer, E., Wohlgemuth, T., and Hacket-Pain, A.: Reproducing reproduction: How to simulate mast seeding in forest models, Ecol. Model., 376, 40–53, https://doi.org/10.1016/j.ecolmodel.2018.03.004, 2018.

Van Bodegom, P. M., Douma, J. C., and Verheijen, L. M.: A fully traits-based approach to modeling global vegetation distribution, P. Natl. Acad. Sci. USA, 111, 13733–13738, https://doi.org/10.1073/pnas.1304551110, 2014.

Van Nes, E. H. and Scheffer, M.: A strategy to improve the contribution of complex simulation models to ecological theory, Ecol. Model., 185, 153–164, https://doi.org/10.1016/j.ecolmodel.2004.12.001, 2005.

Vanclay, J. K.: Aggregating tree species to develop diameter increment equations for tropical rainforests, Forest Ecol. Manage., 42, 143–168, https://doi.org/10.1016/0378-1127(91)90022-N, 1991.

Vanclay, J. K.: Modelling forest growth and yield: applications to mixed tropical forests, CAB INternational, Wallingford, 312 pp., ISBN 0-85198-913-6, 1994.

van der Meer, P. J. and Bongers, F.: Patterns of tree-fall and branch-fall in a tropical rain forest in French Guiana, J. Ecol., 84, 19–29, https://doi.org/10.2307/2261696, 1996.

van Genuchten, M. Th.: A Closed-form Equation for Predicting the Hydraulic Conductivity of Unsaturated Soils1, Soil Sci. Soc. Am. J., 44, 892–898, https://doi.org/10.2136/sssaj1980.03615995004400050002x, 1980.

Vargas Godoy, M. R., Markonis, Y., Hanel, M., Kyselý, J., and Papalexiou, S. M.: The Global Water Cycle Budget: A Chronological Review, Surv. Geophys., 42, 1075–1107, https://doi.org/10.1007/s10712-021-09652-6, 2021.

Verbeeck, H., Peylin, P., Bacour, C., Bonal, D., Steppe, K., and Ciais, P.: Seasonal patterns of CO_2 fluxes in Amazon forests: Fusion of eddy covariance data and the ORCHIDEE model, J. Geophys. Res.-Biogeo., 116, https://doi.org/10.1029/2010JG001544, 2011.

Verheijen, L. M., Aerts, R., Brovkin, V., Cavender-Bares, J., Cornelissen, J. H. C., Kattge, J., and van Bodegom, P. M.: Inclusion of ecologically based trait variation in plant functional types reduces the projected land carbon sink in an earth system model, Glob. Change Biol., 21, 3074–3086, https://doi.org/10.1111/gcb.12871, 2015.

Verhoef, A. and Egea, G.: Modeling plant transpiration under limited soil water: Comparison of different plant and soil hydraulic parameterizations and preliminary implications for their use in land surface models, Agr. Forest Meteorol., 191, 22–32, https://doi.org/10.1016/j.agrformet.2014.02.009, 2014.

Vezy, R., Christina, M., Roupsard, O., Nouvellon, Y., Duursma, R., Medlyn, B., Soma, M., Charbonnier, F., Blitz-Frayret, C., Stape, J.-L., Laclau, J.-P., de Melo Virginio Filho, E., Bonnefond, J.-M., Rapidel, B., Do, F. C., Rocheteau, A., Picart, D., Borgonovo, C., Loustau, D., and le Maire, G.: Measuring and modelling energy partitioning in canopies of varying complexity using MAESPA model, Agr. Forest Meteorol., 253–254, 203–217, https://doi.org/10.1016/j.agrformet.2018.02.005, 2018.

Vico, G., Manzoni, S., Palmroth, S., Weih, M., and Katul, G.: A perspective on optimal leaf stomatal conductance under CO_2 and light co-limitations, Agr. Forest Meteorol., 182–183, 191–199, https://doi.org/10.1016/j.agrformet.2013.07.005, 2013.

Villar, R., Held, A. A., and Merino, J.: Dark Leaf Respiration in Light and Darkness of an Evergreen and a Deciduous Plant Species, Plant Physiol., 107, 421–427, https://doi.org/10.1104/pp.107.2.421, 1995.

Visser, M. D., Bruijning, M., Wright, S. J., Muller-Landau, H. C., Jongejans, E., Comita, L. S., and de Kroon, H.: Functional traits as predictors of vital rates across the life cycle of tropical trees, Funct. Ecol., 30, 168–180, https://doi.org/10.1111/1365-2435.12621, 2016.

Vleminckx, J., Fortunel, C., Valverde-Barrantes, O., Timothy Paine, C. E., Engel, J., Petronelli, P., Dourdain, A. K., Guevara, J., Béroujon, S., and Baraloto, C.: Resolving whole-plant economics from leaf, stem and root traits of 1467 Amazonian tree species, Oikos, 130, 1193–1208, https://doi.org/10.1111/oik.08284, 2021.

von Caemmerer, S.: Biochemical models of leaf photosynthesis, Csiro Publishing, 184 pp., https://doi.org/10.1071/9780643103405, 2000.

von Humboldt, A.: Aspects of nature, in different lands and different climates; with scientific elucidations, Lea and Blanchard, 512 pp., https://doi.org/10.5962/bhl.title.45601, 1849.

Wagner, F. H., Hérault, B., Bonal, D., Stahl, C., Anderson, L. O., Baker, T. R., Becker, G. S., Beeckman, H., Boanerges Souza, D., Botosso, P. C., Bowman, D. M. J. S., Bräuning, A., Brede, B., Brown, F. I., Camarero, J. J., Camargo, P. B., Cardoso, F. C. G., Carvalho, F. A., Castro, W., Chagas, R. K., Chave, J., Chidumayo, E. N., Clark, D. A., Costa, F. R. C., Couralet, C., da Silva Mauricio, P. H., Dalitz, H., de Castro, V. R., de Freitas Milani, J. E., de Oliveira, E. C., de Souza Arruda, L., Devineau, J.-L., Drew, D. M., Dünisch, O., Durigan, G., Elifuraha, E., Fedele, M., Ferreira Fedele, L., Figueiredo Filho, A., Finger, C. A. G., Franco, A. C., Freitas Júnior, J. L., Galvão, F., Gebrekirstos, A., Gliniars, R., Graça, P. M. L. D. A., Griffiths, A. D., Grogan, J., Guan, K., Homeier, J., Kanieski, M. R., Kho, L. K., Koenig, J., Kohler, S. V., Krepkowski, J., Lemos-Filho, J. P., Lieberman, D., Lieberman, M. E., Lisi, C. S., Longhi Santos, T., López Ayala, J. L., Maeda, E. E., Malhi, Y., Maria, V. R. B., Marques, M. C. M., Marques, R., Maza Chamba, H., Mbwambo, L., Melgaço, K. L. L., Mendivelso, H. A., Murphy, B. P., O'Brien, J. J., Oberbauer, S. F., Okada, N., Pélissier, R., Prior, L. D., Roig, F. A., Ross, M., Rossatto, D. R., Rossi, V., Rowland, L., Rutishauser, E., Santana, H., Schulze, M., Selhorst, D., Silva, W. R., Silveira, M., Spannl, S., Swaine, M. D., Toledo, J. J., Toledo, M. M., Toledo, M., Toma, T., Tomazello Filho, M., Valdez Hernández, J. I., Verbesselt, J., Vieira, S. A., Vincent, G., Volkmer de Castilho, C., Volland, F., Worbes, M., Zanon, M. L. B., and Aragão, L. E. O. C.: Climate seasonality limits leaf carbon assimilation and wood productivity in tropical forests, Biogeosciences, 13, 2537–2562, https://doi.org/10.5194/bg-13-2537-2016, 2016.

Walker, A. P., Beckerman, A. P., Gu, L., Kattge, J., Cernusak, L. A., Domingues, T. F., Scales, J. C., Wohlfahrt, G., Wullschleger, S. D., and Woodward, F. I.: The relationship of leaf photosynthetic traits – Vcmax and Jmax – to leaf nitrogen, leaf phosphorus, and specific leaf area: a meta-analysis and modeling study, Ecol. Evol., 4, 3218–3235, https://doi.org/10.1002/ece3.1173, 2014.

Wang, Y. P. and Jarvis, P. G.: Description and validation of an array model – MAESTRO, Agr. Forest Meteorol., 51, 257–280, https://doi.org/10.1016/0168-1923(90)90112-J, 1990.

Wang, Y.-P. and Leuning, R.: A two-leaf model for canopy conductance, photosynthesis and partitioning of available energy I, Agr. Forest Meteorol., 91, 89–111, https://doi.org/10.1016/S0168-1923(98)00061-6, 1998.

Wang, Y. P., Kowalczyk, E., Leuning, R., Abramowitz, G., Raupach, M. R., Pak, B., Gorsel, E. van, and Luhar, A.: Diagnosing errors in a land surface model (CABLE) in the time and frequency domains, J. Geophys. Res.-Biogeo., 116, G01034, https://doi.org/10.1029/2010JG001385, 2011.

Warneke, C. R., Caughlin, T. T., Damschen, E. I., Haddad, N. M., Levey, D. J., and Brudvig, L. A.: Habitat fragmentation alters the distance of abiotic seed dispersal through edge effects and direction of dispersal, Ecology, 103, e03586, https://doi.org/10.1002/ecy.3586, 2022.

Watt, A. S.: Pattern and Process in the Plant Community, J. Ecol., 35, 1–22, https://doi.org/10.2307/2256497, 1947.

Weemstra, M., Mommer, L., Visser, E. J. W., van Ruijven, J., Kuyper, T. W., Mohren, G. M. J., and Sterck, F. J.: Towards a multidimensional root trait framework: a tree root review, New Phytol., 211, 1159–1169, https://doi.org/10.1111/nph.14003, 2016.

Weerasinghe, L. K., Creek, D., Crous, K. Y., Xiang, S., Liddell, M. J., Turnbull, M. H., and Atkin, O. K.: Canopy position affects the relationships between leaf respiration and associated traits in a tropical rainforest in Far North Queensland, Tree Physiol., 34, 564–584, https://doi.org/10.1093/treephys/tpu016, 2014.

Williams, M., Rastetter, E. B., Fernandes, D. N., Goulden, M. L., Wofsy, S. C., Shaver, G. R., Melillo, J. M., Munger, J. W., Fan, S.-M., and Nadelhoffer, K. J.: Modelling the soil-plant-atmosphere continuum in a Quercus–Acer stand at Harvard Forest: the regulation of stomatal conductance by light, nitrogen and soil/plant hydraulic properties, Plant Cell Environ., 19, 911–927, https://doi.org/10.1111/j.1365-3040.1996.tb00456.x, 1996.

Williams, M., Law, B. E., Anthoni, P. M., and Unsworth, M. H.: Use of a simulation model and ecosystem flux data to examine carbon–water interactions in ponderosa pine, Tree Physiol., 21, 287–298, https://doi.org/10.1093/treephys/21.5.287, 2001.

Wilson, J. B., Peet, R. K., Dengler, J., and Pärtel, M.: Plant species richness: the world records, J. Veg. Sci., 23, 796–802, https://doi.org/10.1111/j.1654-1103.2012.01400.x, 2012.

Wolf, A., Anderegg, W. R. L., and Pacala, S. W.: Optimal stomatal behavior with competition for water and risk of hydraulic impairment, P. Natl. Acad. Sci. USA, 113, E7222–E7230, https://doi.org/10.1073/pnas.1615144113, 2016.

Wolz, K. J., Wertin, T. M., Abordo, M., Wang, D., and Leakey, A. D. B.: Diversity in stomatal function is integral to modelling plant carbon and water fluxes, Nat. Ecol. Evol., 1, 1292–1298, https://doi.org/10.1038/s41559-017-0238-z, 2017.

Woodruff, D. R. and Meinzer, F. C.: Water stress, shoot growth and storage of non-structural carbohydrates along a tree height gradient in a tall conifer, Plant Cell Environ., 34, 1920–1930, https://doi.org/10.1111/j.1365-3040.2011.02388.x, 2011.

Wright, S. J., Kitajima, K., Kraft, N. J. B., Reich, P. B., Wright, I. J., Bunker, D. E., Condit, R., Dalling, J. W., Davies, S. J., Díaz, S., Engelbrecht, B. M. J., Harms, K. E., Hubbell, S. P., Marks, C. O., Ruiz-Jaen, M. C., Salvador, C. M., and Zanne, A. E.: Functional traits and the growth–mortality trade-off in tropical trees, Ecology, 91, 3664–3674, https://doi.org/10.1890/09-2335.1, 2010.

Wu, J., Albert, L. P., Lopes, A. P., Restrepo-Coupe, N., Hayek, M., Wiedemann, K. T., Guan, K., Stark, S. C., Christoffersen, B., Prohaska, N., Tavares, J. V., Marostica, S., Kobayashi, H., Ferreira, M. L., Campos, K. S., Silva, R. da, Brando, P. M., Dye, D. G., Huxman, T. E., Huete, A. R., Nelson, B. W., and Saleska, S. R.: Leaf development and demography explain photosynthetic seasonality in Amazon evergreen forests, Science, 351, 972–976, https://doi.org/10.1126/science.aad5068, 2016.

Wu, J., Serbin, S. P., Xu, X., Albert, L. P., Chen, M., Meng, R., Saleska, S. R., and Rogers, A.: The phenology of leaf quality and its within-canopy variation is essential for accurate modeling of photosynthesis in tropical evergreen forests, Glob. Change Biol., 23, 4814–4827, https://doi.org/10.1111/gcb.13725, 2017.

Wu, J., Serbin, S. P., Ely, K. S., Wolfe, B. T., Dickman, L. T., Grossiord, C., Michaletz, S. T., Collins, A. D., Detto, M., McDowell, N. G., Wright, S. J., and Rogers, A.: The response of stomatal conductance to seasonal drought in tropical forests, Glob. Change Biol., 26, 823–839, https://doi.org/10.1111/gcb.14820, 2020.

Xu, X., Medvigy, D., Powers, J. S., Becknell, J. M., and Guan, K.: Diversity in plant hydraulic traits explains seasonal and inter-annual variations of vegetation dynamics in seasonally dry tropical forests, New Phytol., 212, 80–95, https://doi.org/10.1111/nph.14009, 2016.

Xu, X. and Trugman, A. T.: Trait-Based Modeling of Terrestrial Ecosystems: Advances and Challenges Under Global Change, Curr. Clim. Change Rep., 7, 1–13, https://doi.org/10.1007/s40641-020-00168-6, 2021.

Xu, X., Konings, A. G., Longo, M., Feldman, A., Xu, L., Saatchi, S., Wu, D., Wu, J., and Moorcroft, P.: Leaf surface water, not plant water stress, drives diurnal variation in tropical forest canopy water content, New Phytol., 231, 122–136, https://doi.org/10.1111/nph.17254, 2021.

Yang, X., Wu, J., Chen, X., Ciais, P., Maignan, F., Yuan, W., Piao, S., Yang, S., Gong, F., Su, Y., Dai, Y., Liu, L., Zhang, H., Bonal, D., Liu, H., Chen, G., Lu, H., Wu, S., Fan, L., Gentine, P., and Wright, S. J.: A comprehensive framework for seasonal controls of leaf abscission and productivity in evergreen broadleaved tropical and subtropical forests, The Innovation, 2, 100154, https://doi.org/10.1016/j.xinn.2021.100154, 2021.

Yao, Y., Joetzjer, E., Ciais, P., Viovy, N., Cresto Aleina, F., Chave, J., Sack, L., Bartlett, M., Meir, P., Fisher, R., and Luyssaert, S.: Forest fluxes and mortality response to drought: model description (ORCHIDEE-CAN-NHA r7236) and evaluation at the Caxiuanã drought experiment, Geosci. Model Dev., 15, 7809–7833, https://doi.org/10.5194/gmd-15-7809-2022, 2022.

Yao, Y., Ciais, P., Viovy, N., Joetzjer, E., and Chave, J.: How drought events during the last century have impacted biomass carbon in Amazonian rainforests, Glob. Change Biol., 29, 747–762, https://doi.org/10.1111/gcb.16504, 2023.

Yao, Y., Ciais, P., Joetzjer, E., Li, W., Zhu, L., Wang, Y., Frankenberg, C., and Viovy, N.: The impacts of elevated CO_2 on forest growth, mortality, and recovery in the Amazon rainforest, Earth Syst. Dynam., 15, 763–778, https://doi.org/10.5194/esd-15-763-2024, 2024.

Yoda, K., Shinozaki, K., Ogawa, H., Hozumi, K., and Kira, T.: Estimation of the total amount of respiration in woody organs of trees and forest communities., J. Biol. Osaka City Univ., 16, 15–26, 1965.

Yu, W., Albert, G., Rosenbaum, B., Schnabel, F., Bruelheide, H., Connolly, J., Härdtle, W., von Oheimb, G., Trogisch, S., Rüger, N., and Brose, U.: Systematic distributions of interaction strengths across tree interaction networks yield positive diversity–productivity relationships, Ecol. Lett., 27, e14338, https://doi.org/10.1111/ele.14338, 2024.

Zaehle, S., Sitch, S., Smith, B., and Hatterman, F.: Effects of parameter uncertainties on the modeling of terrestrial biosphere dynamics, Global Biogeochem. Cy., 19, GB3020, https://doi.org/10.1029/2004GB002395, 2005.

Zellweger, F., Frenne, P. D., Lenoir, J., Rocchini, D., and Coomes, D.: Advances in Microclimate Ecology Arising from Remote Sensing, Trend. Ecol. Evol., 34, 327–341, https://doi.org/10.1016/j.tree.2018.12.012, 2019.

Zhou, S., Duursma, R. A., Medlyn, B. E., Kelly, J. W. G., and Prentice, I. C.: How should we model plant responses to drought? An analysis of stomatal and non-stomatal responses to water stress, Agr. Forest Meteorol., 182, 204–214, https://doi.org/10.1016/j.agrformet.2013.05.009, 2013.

Zhou, S., Medlyn, B., Sabaté, S., Sperlich, D., Prentice, I. C., and others: Short-term water stress impacts on stomatal, mesophyll and biochemical limitations to photosynthesis differ consistently among tree species from contrasting climates, Tree Physio.y, 34, 1035–46, 2014.

Ziegler, C., Coste, S., Stahl, C., Delzon, S., Levionnois, S., Cazal, J., Cochard, H., Esquivel-Muelbert, A., Goret, J.-Y., Heuret, P., Jaouen, G., Santiago, L. S., and Bonal, D.: Large hydraulic safety margins protect Neotropical canopy rainforest tree species against hydraulic failure during drought, Ann. Forest Sci., 76, 115, https://doi.org/10.1007/s13595-019-0905-0, 2019.